03

E79-10102
CR-158058

(E79-10102) APPLICATION OF LANDSAT DATA AND DIGITAL IMAGE PROCESSING Technical Report, 1975 - 1978 (Zentralstelle fuer Geo-Photogrammetrie) 169 p HC A08/MF A01 CSCL 05B G3/43

N79-17291

Unclas
00102

28380

ZGF - ZENTRALSTELLE FUR GEO-PHOTOGRAMMETRIE UND FERNERKUNDUNG (DFG)

am Institut fur allgemeine und angewandte Geologie der Universitat, Luisenstr 37, D-8 Munchen 2

1. SR No. 2838o	2. Type of Report III	3. Recipient's Catalog No.
4. Title: Application of LANDSAT-data and digital image processing.		5. Report Data May 1978
7. Principal Investigator Prof. Dr. J. Bodechtel		6. Period Covered 1975 - 1978
9. Name and Address of Principal Investigators Organization Zentralstelle für Geo-Photogrammetrie und Fernerkundung		8. Number of Pages: 164 1o. Principal Investig. Rept.No.
12. Sponsoring Agency and Address Deutsche Forschungsgemeinschaft Kennedyallee 4o 53oo Bonn - Bad Godesberg 1		11. GSFC Technical Monitor James Broderick 13. Key words (selected by PI) Geology, Landuse, Landsat-application, data and image processing

Supplementary notes

This report consists of the results of research work carried out at the Zentralstelle für Geo-Photogrammetrie und Fernerkundung der Deutschen Forschungsgemeinschaft (Central Laboratory of geophotogrammetry and remote sensing of the German Research Council)

Summary:
On the basis of Landsat-1 and -2 data, part I of the following report demonstrates applications in the fields of coal mining, lignite exploration, and thematic mapping in geology. Section II describes the hybrid image processing system of the ZGF, its software and its utilization for educational purposes.
In Part III a proposal for a pre-operational European satellite which has been prepared in cooperation with Messerschmitt-Bölkow-Blohm is being discussed.

I

Content page

Introduction

With respect to several discussions with the Mission Utilization Office, the following Landsat-2 final report covers a wider field of activities based on the availability of Landsat data through the PI-contract with NASA and through the receiving capabilities of Fuccino.
The generous data contribution by NASA has initiated a tremendous increase in carrying out more application oriented investigations also by user groups which have not been involved at all by Landsat-1 investigations.
Besides a constantly increasing user community and improved capabilities of handling remote sensing data, the potential of space borne remote sensing has become evident, even though it can be stated , that Landsat-2 does not provide an optimum data base for all relevant European key applications.
Encouraged by the increased interest in Landsat data, we have put effort in providing the user community with sophisticated data processing techniques and in discussing the specific user requirements towards operatinal remote sensing systems.
With respect to Landsat investigations carried out and to above mentioned activities the submitted final Landsat-2 report consists of 3 parts:

Part 1 describes various applications of Landsat data and in accordance with the Mission Utilization Office also the use of aircraft data, within several projects. These studies involved the application of conventional photo interpretation techniques and digital data processing.

Part 2 describes in detail technical aspects of the hybrid image processing system and discusses how we are using our technical capabilities in order to approach the potential user community.

Part 3 summarizes our experience gained by discussing the needs for remote sensing with several user groups. These results in combination with the technical design considerations by MBB on the basis of an experimental CCD scanner has led to a proposal for an european earth resources satellite.

PART I

EVALUATION OF LANDSAT DATA BY CONVENTIONAL INTERPRETATION TECHNIQUES AND BY DIGITAL IMAGE PROCESSING

With respect to the sophisticated image data processing techniques available today, the visual interpretation of Landsat images with an eye to linear features seems not anymore to be of specific interest. Furthermore, methodological aspects of extracting photolineations from space borne images have been described by many authors and have also been discussed in our Landsat-1 final report.

Nevertheless, we continued to apply above methods of lineament interpretation and have decided to adapt these activities in the final report, because we strongly feel, that the interpretation and evaluation of linear features is still of basic interest and often provides significant information not only under scientific aspects but also for direct application.

A Satellite Lineations in Comparison with Structural Field Measurements

- A Tectonical Model of the Northern Apennines

Since 1970 the Photogeologic Department of the University of Munich has participated in a research project "Geodynamics" of the German Research Council. The research work within this program has been based on the combination of satellite and aircraft data interpretation and structural field measurements. The first interpretation phase (since 1973) showed already reasonable results, which have been published in GEOFORUM (1974), and will be briefly reviewed here (fig. 1).

1. The evaluation of Landsat-1 images suggests two large horizontal fault zones within the Northern Apennines:
   - the first zone (80° striking) follows the Arno Valley resp. its eastern prolongation
   - the second zone (0 - 10° striking) is well known as the "Ancona-Anzio-Line".

   The sense of movement derived by photointerpretation techniques is sinistral for both the Arno fault and the Ancona-Anzio Line. The result of these opposite movements is a clockwise rotation of the block bounded by the two faults.

2. This rotation is confirmed by joint-plane-measurements in an area SE Siena (Tuscany), which indicates the existence of two different fabric systems. The b-axis of the older system strikes about 160° (NNW), the b-axis of the younger system strikes about 140° (NW), and corresponds to the main fold axes of the region.

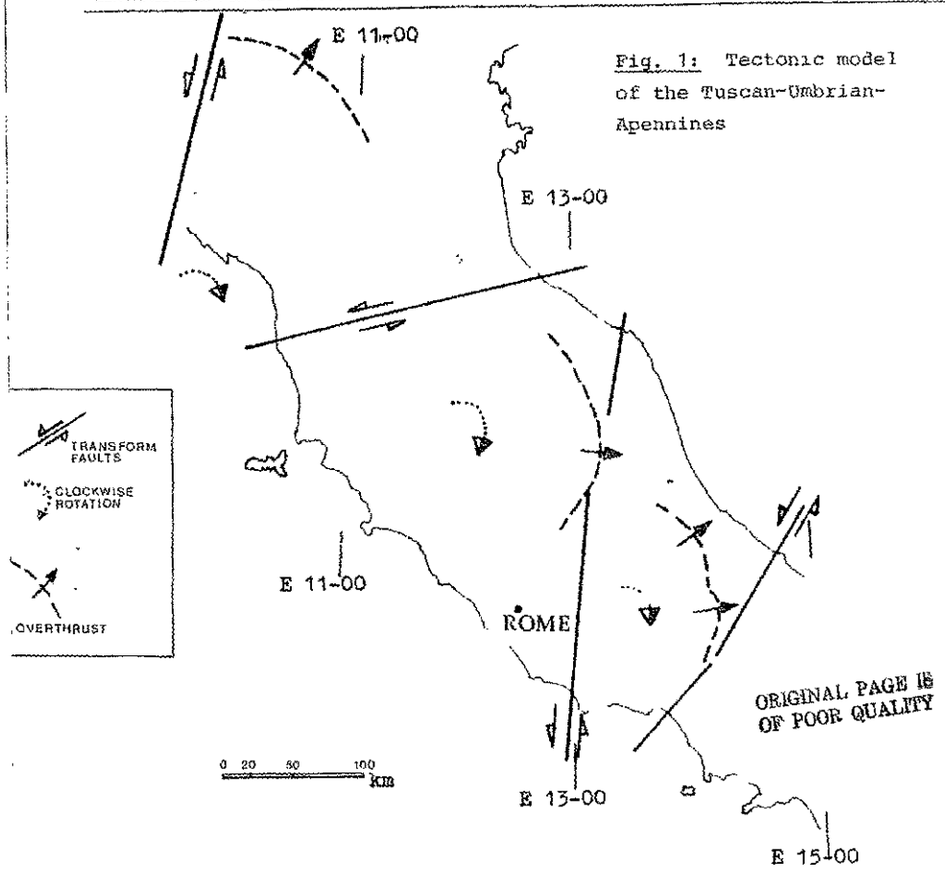

Fig. 1: Tectonic model of the Tuscan-Umbrian-Apennines

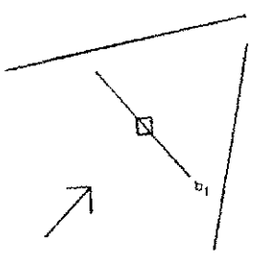

stress direction SW-NE
primary fracture system
b_1 140°

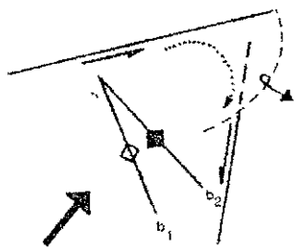

Same stress direction
clockwise rotation by movements along the great transform faults
b_1 160° b_2 140°
vertical movements parallel to b_2 overthrusts the north.

3. The statistical analysis of lineament directions visible on satellite images and aerial photographs (BODECHTEL 1969) confirm the two "axis systems" for wide parts of the Southern Tuscany.

Based on these results and the work done by the research team of the FU Berlin (especially in the region of the Prato-Sillaro-Line) and, before all, the almost totally lacking information on joint configurations in the entire Northern Apennines, a final working program was started. It includes the following objects:

1. Tectonic field measurements along two traverses through the Northern Apennines.* The position of the two sections was chosen with respect to the previous described results based on the evaluation of satellite imagery. The position of profiles is indicated by fig. 2.
   The southern profile (measurement points 1 through 10 - fig. 2) was selected in order to classify the problem of the clockwise rotation of the Tuscan-Umbrian Apennines.
   Furthermore, the influence of a fault zone in the eastern part of the section should be tested. The northern section (measurement points 11 through 16) should serve for clearing the structural implications of the Prato-Sillaro-Line.

2. Detailed evaluation, especially lineament analysis, of satellite images covering the Northern Apennines. The additional use of SKYLAB data has also been incorporated.

---

* A description of the relationship between in situ point measurements and their statistical evaluation is given in the Landsat-1 final report.

FOLDOUT FRAME

1 Mti.dell' Uccellina
2 Scansano
3 Poggio il Sasso
4 Castell'Azzara
5 Mte.Cetona
6 Trasumeno Sud
7 Mte.Malbe
8 Gualdo Tadino-Fabriano
9 Mte. S.Vicino
10 Mte.Conero
11 Mte. Albano South
12 Mte.Albano North
13 La Querce-Filettole
14 Montepiano-Vernio
15 Valle Santerno

A Line Sestri-Voltaggio
B Line Prato-Sillaro
C Cervarola-Overthrust
D Line Ancona-Anzio

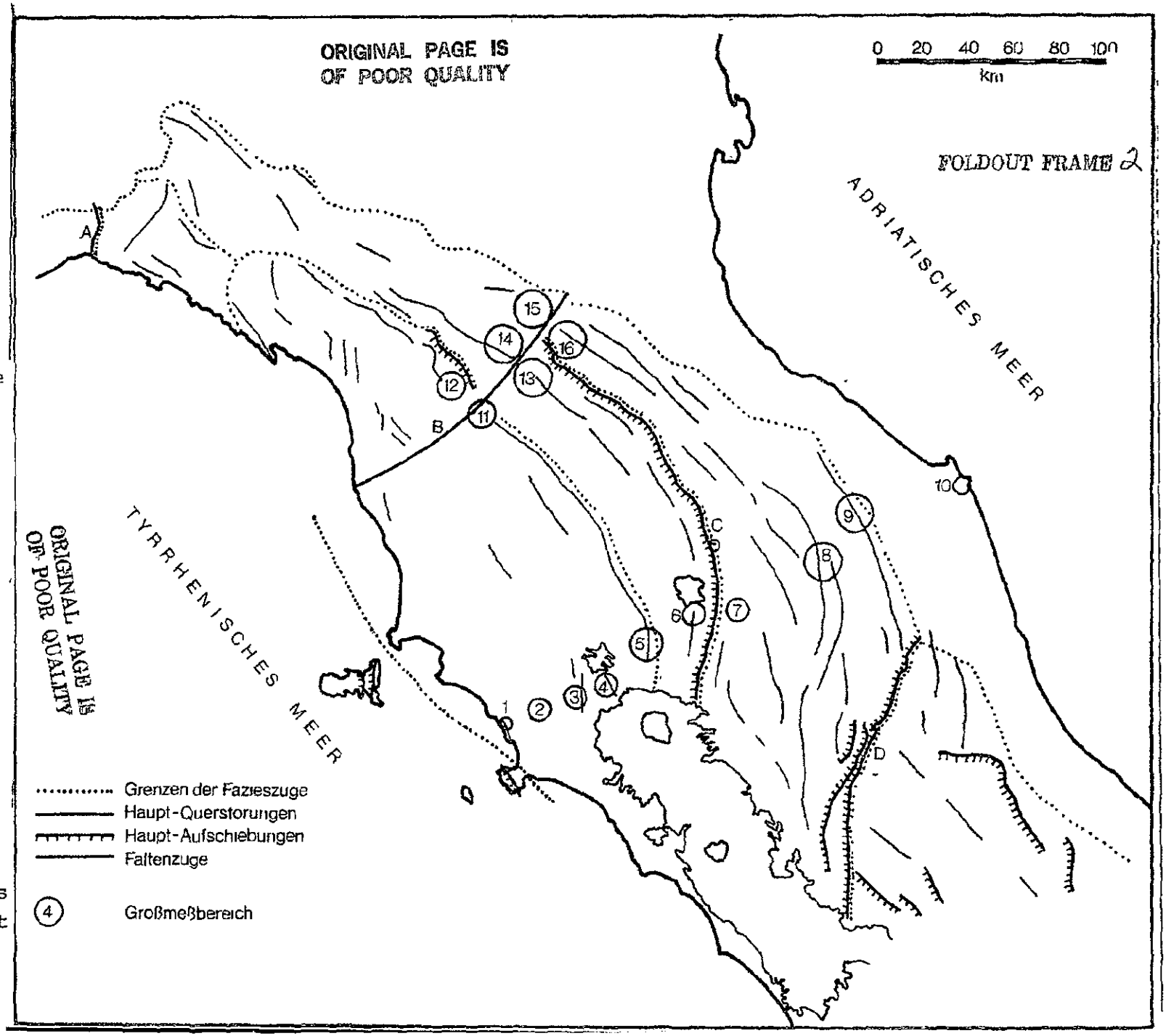

Fig.2: Position of in situ measurements (map after ABBATE et al. 1970)

1. Field Measurements

About 15.ooo joint planes were measured along the two profiles, the largest part by use of terrestrial-photogrammetric techniques. These techniques give an optimum base for digital processing of the data. In the southern part the measurements were concentrated on the several "horst"-zones in which the Tuscan-Umbrian-Apennines are arranged from West to East. The analysis of the joint-pole configurations on an equal-area-net led to the following results.

1. The existence of two (or more) fabric systems has been confirmed for all sites but two: Nearly at all the localities the striking of the b-axes of the two systems is significantly different (see fig. 3).

2. The differences of the axis-trends vary uniformly between +1o° and +25° in the southern section. The amount does not depend on the age of the measured rock formation. Only on the limbs of overturned or upright folds (Mte. Cetona, Umbrian Apennines) higher differences up to 4o - 6o° can be observed. This phenomenon has to be explained by the fact that on the outer arc of a fold formed by buckling the original angle between rotated linears (b_1-axis) and fold axis (b_2-axis) is increased. An exact re-orientation of the upfolded linears is not possible without knowledge of the state of strain (RAMSAY 1966). Data for defining this state of strain cannot be obtained in this region.
In the northern section the pattern exhibited by the axis differences is not uniform. This is caused by the influence of the Prato-Sillaro-Line. The following angle differences could be derived:

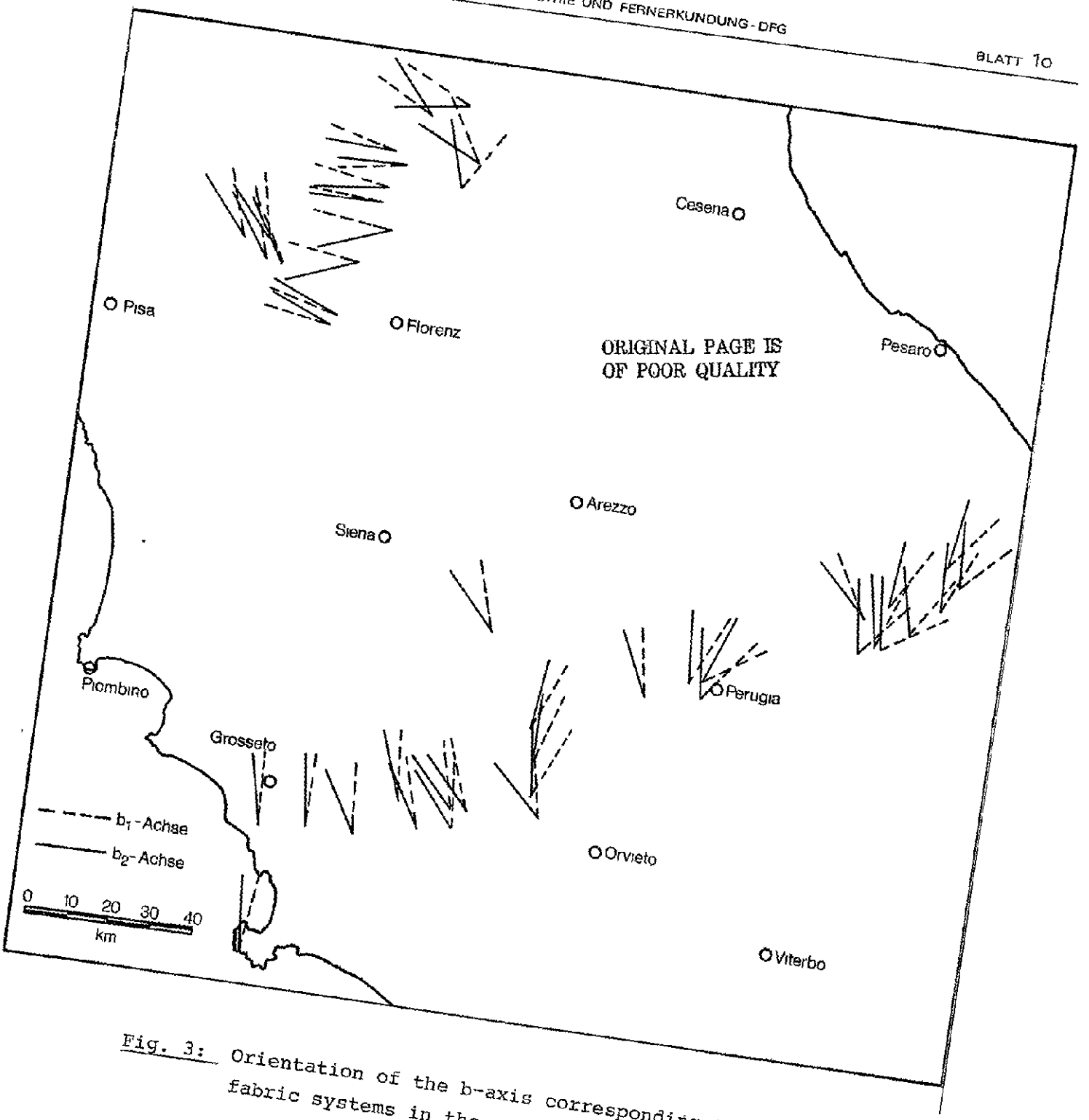

Fig. 3: Orientation of the b-axis corresponding to fabric systems in the northern Apennin.

For the Marnoso-Arenacea-formation (South of Prato-Sillaro-Line) $+25^{\circ}$; (-15°)-(-45°) for the Cervarola-Sandstone (North of Prato-Sillaro-Line); $(+35)$ - $(+50^{\circ})$ for the Morello-Alberese (immediately in the Prato-Sillaro-Line-Zone), and $\pm$ 0 for the Macigno of the Mte. Albano (southern prolongation of the Prato-Sillaro-Line?) (see fig. 1). Only at the Passo Giogo the situation is veiled by the main overthrust of the Cervarola-Sandstone.

3. At the localities situated near large faults or fault zones the b_2-axis do not follow the general striking of the main fold structures (fig.4). These deviations can be considered as drag effects indicating the sense of movement occurred on the fault. For example, near the fault marked by the Esino Valley (Gola della Rossa) and its prolongation to the W the axis deflection suggests a dextral movement. In the same way the axis deviations in the Cervarola-Sandstone and the Morello-Alberese near the Prato-Sillaro-Line indicate a sinistral sense of movement. The same movement was postulated by BORTOLOTTI (1968) based on rather intuitive arguments. It has to be mentioned that also at the southern end of the Mte. Albano a similar axis deviation can be observed.

4. Concerning the fact, that the Marnoso-Arenacea-formation cannot be observed in the North of the Prato-Sillaro-Line, bedding plane measurements indicate its plunging with 15° to NW.

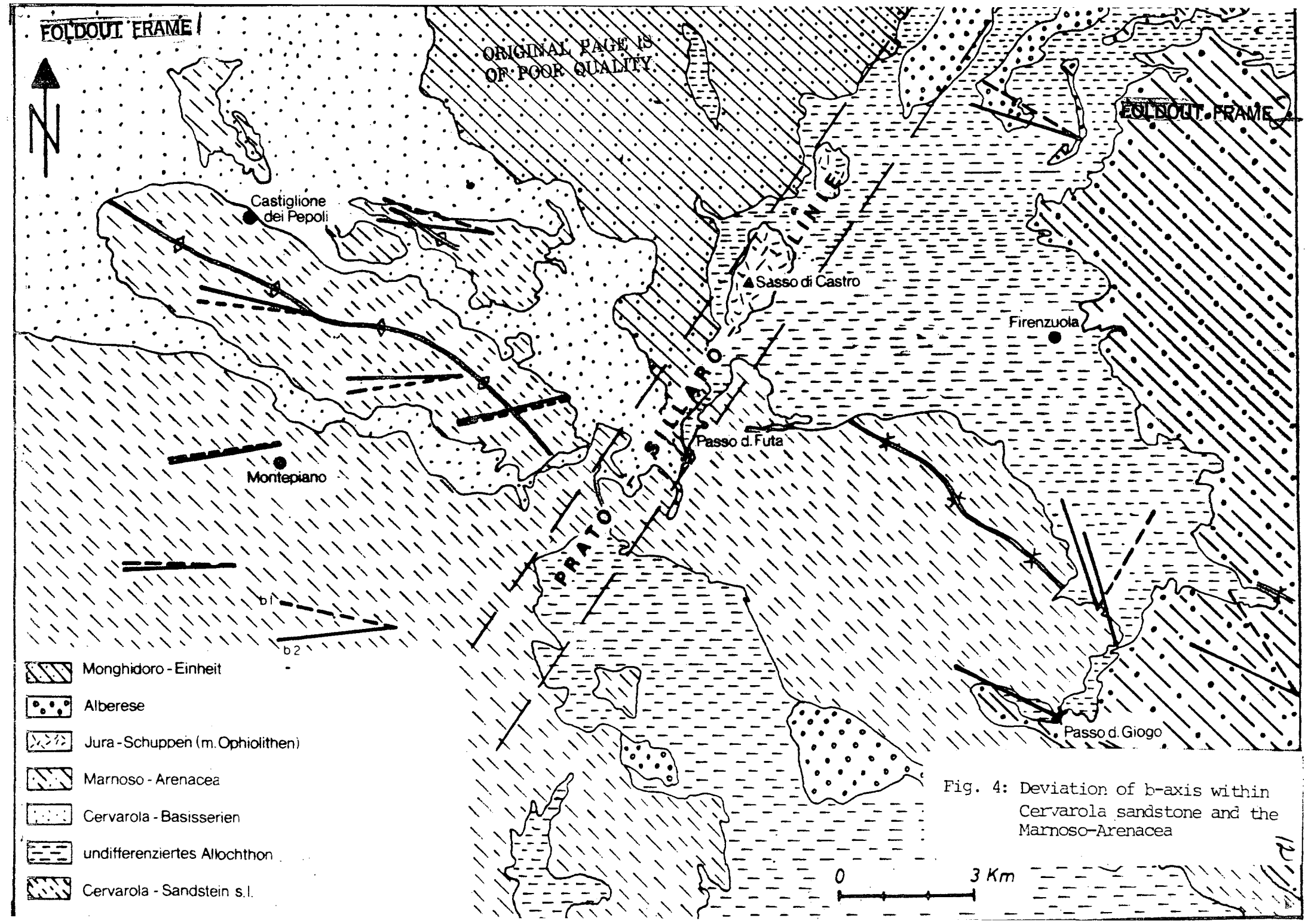

Fig. 4: Deviation of b-axis within Cervarola sandstone and the Marnoso-Arenacea

2. Evaluation of Satellite Imagery

On the basis of various data sources a lineation map was prepared in a scale of 1 : 500.000. The result is given in fig. 5. This map only exhibits lineations longer than 5 km. If detectable the sense of movement was marked and the major fold axes were traced.

For the Prato-Sillaro-Line and the southern adjacent profile zones a special map indicating satellite lineation and in situ mapped faults were prepared in a scale of 1:100.000 (fig. 6 a and b).

In addition to above interpretation, the lineament orientation has been systematically plotted over the entire region of interest (fig. 7).

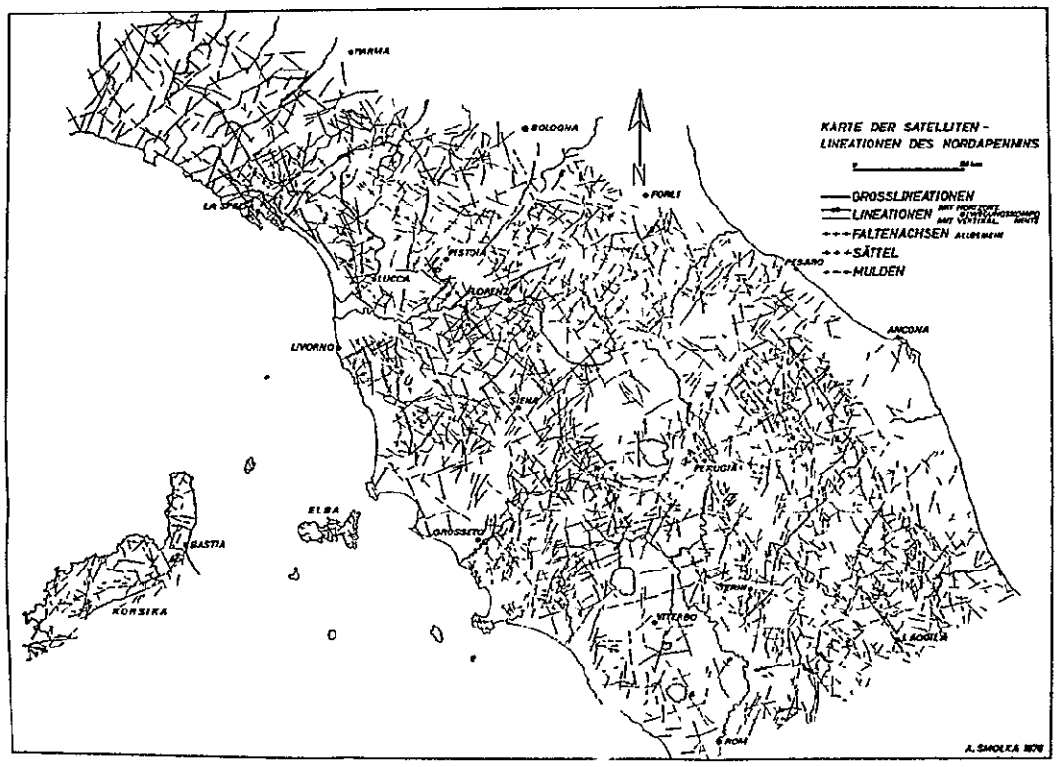

Fig. 5: Map of satellite lineations of the northern Apennine.

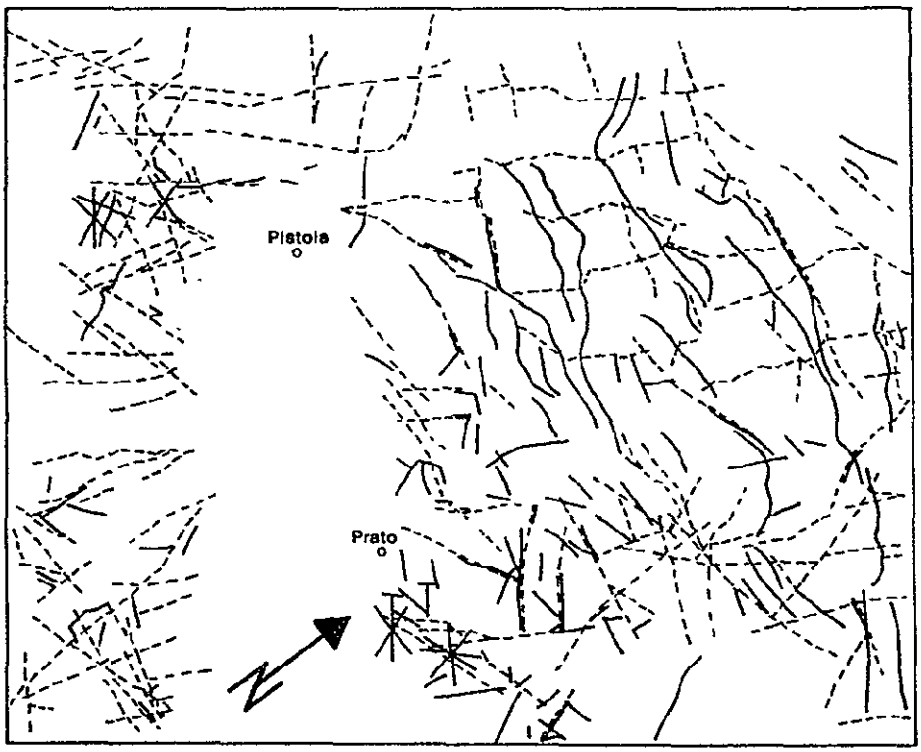

——— Faults mapped in the field (after Carta Geologica d'Italia, 1:100.000)

– – – Satellite linations

Fig. 6 a: Comparison of mapped faults with satellite lineations. Northern profile.

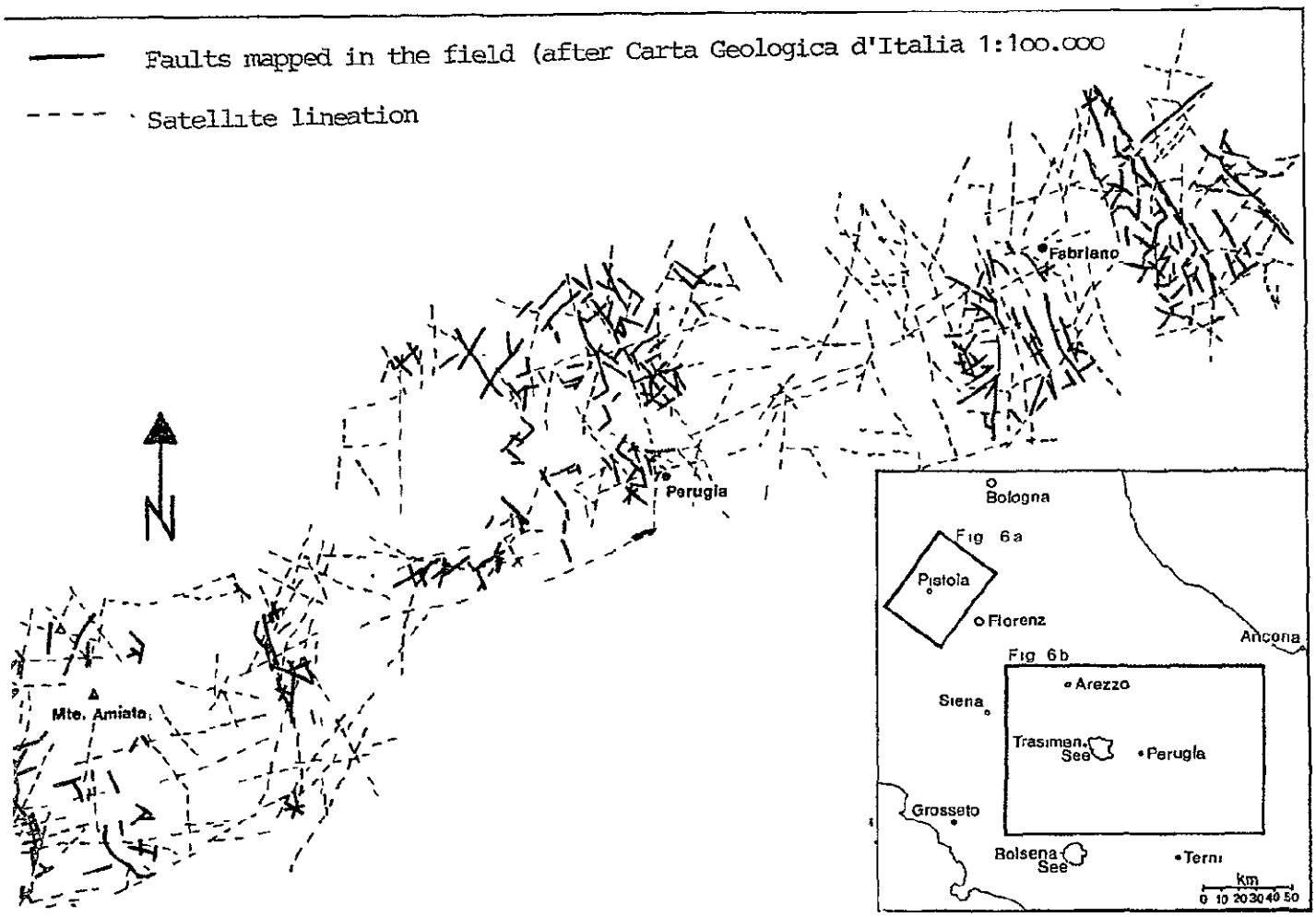

Fig. 6 b: Comparison of faults with satellite lineations. Southern profile.

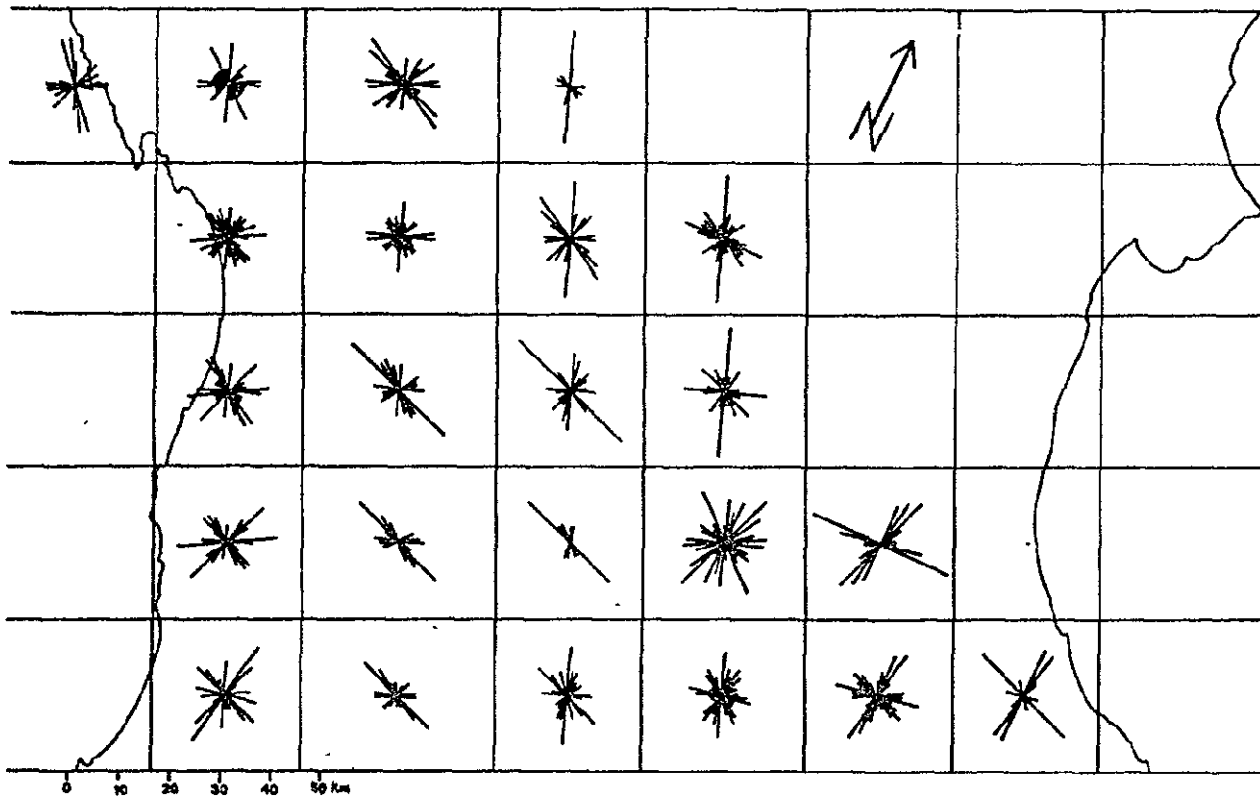

NORTHERN REGION

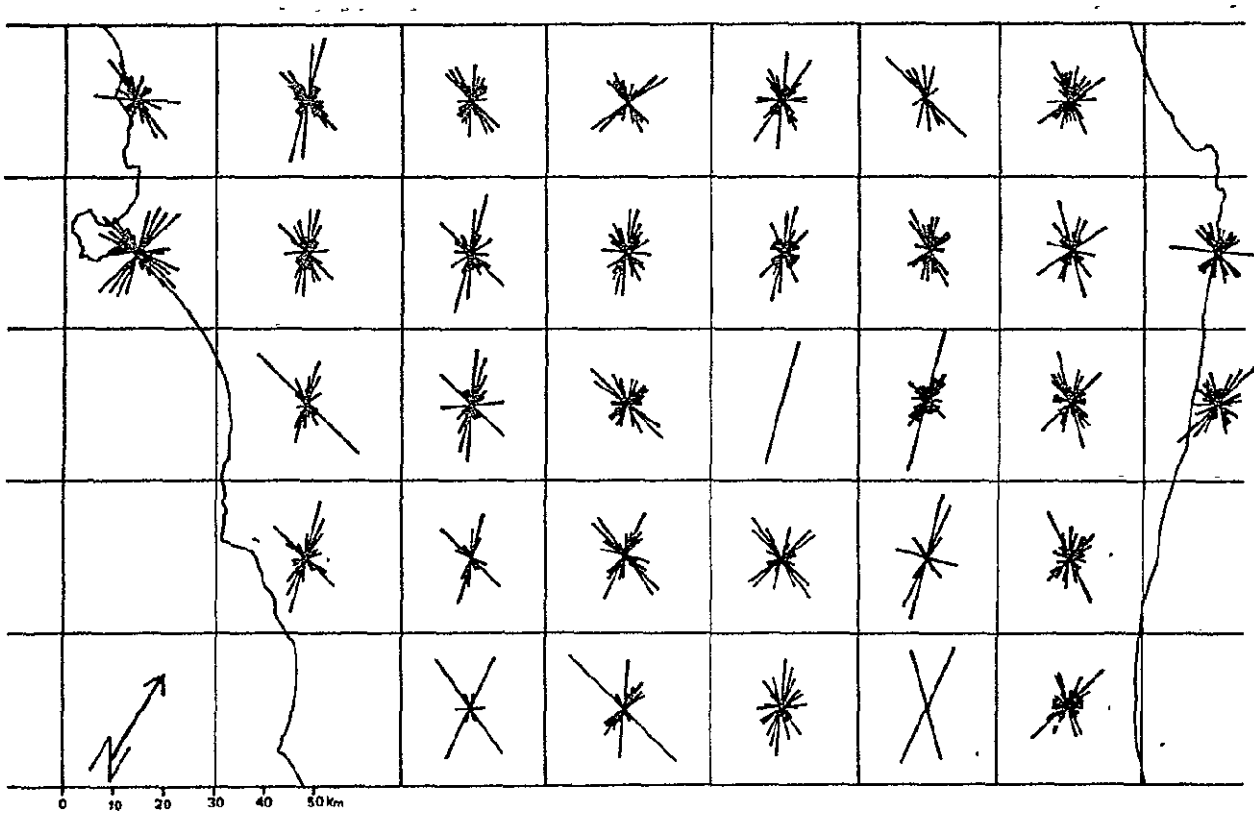

SOUTHERN REGION

Fig. 7: Statistical representation of lineament orientation.

From this work the following results could be obtained hitherto:

1. There are only few lineaments crossing several tectonic units, e.g. the Prato-Sillaro-Line, which touches Macigno, Morello-Alberese, Cervarola-Sandstone, Cantiere-Monghidoro-Unit, Bismantova-Sandstone and the Pliocene. Another lineament begins N of La Spezia and extends to the ENE along the Magra valley, over the Passo di Lagastrello to the Enza valley. This fault crosses the Tuscan formations, the Ligurian Ophiolith-Unit, the Orocco-Caio-Unit. Nearly all the other lineaments, even very long ones as the normal fault accompanying the Cetona-Orsaro-Structure are running within the same tectonic unit or separating diverse tectonic domains (e.g. Ancona-Anzio-Line). These lineations must be interpreted basement structures penetrating the young sedimentary cover.

2. There is neither morphological nor geological evidence for a large fault zone in the Arno valley and its prolongation to the E. On the contrary, the assumption of such a fault zone is in a strong contradiction to the strange turning of the Arno River around the Prato-magno.

3. The following main lineament trends can be derived from fig. 5 and 7.

   - a perpendicular set of lineaments ($65^{o}/155^{o}$) occupying the whole area mapped. This set corresponds to the antiapenninic and apenninic directions S of the Arno River
   - another perpendicular set of lineaments with a preferred 35^{o} - 45^{o} trend and a subordinated 125^{o} - 135^{o} trend. This set is well developed N of the

Arno River and corresponds to the antiapenninic and apenninic directions in this region. The 35° - 45° trend is still prominent in the southern Tuscany and the Nera valley (Umbria), whereas the 130° direction disappears almost totally S of the Arno River.

- some curved lineaments striking 350° - 25° (Prato-Sillaro-Line, Ancona-Anzio-Line; the long lineation beginning in the Mti. di Campiglia and running to the eastern border of the mesozoic nucleus of the Lima valley; the two large lineaments in the young volcanites). These lineations are not strongly referred to the orogenic structures. Therefore they should have existed already in the pre-apenninic crystalline basement. In the Umbrian arc the lineament pattern is generally more complicated because of the bending of the fold axis from NW/SE direction to NS direction.

4. Regarding the satellite image the main element of the Prato-Sillaro-Line is made up by a well recognizable lineament, which follows the Idice valley and limits the Cantiere-Monghidoro-Unit to E. The lineament prolonges southwards cutting the Morello-Alberese in direction of Calenzano.

   The detailed analysis of lineament directions for the Prato-Sillaro-Line and the adjacent areas shows some interesting aspects (fig. 8).

   - in the Mte. Albano the antiapenninic direction is still predominating in comparison to the Prato-Sillaro-Line direction (20°)
   - in the region S of the Cervarola-overthrust the Prato-Sillaro-Line direction becomes much more

prominent than the antiapenninic one

- N of the Cervarola-overthrust the Prato-Sillaro-Line direction changes to 5 - 10° striking.

In all the three zones subordinated maxima are developed at 75°, 95° and 160°. The first two directions have to be considered as shears to the 40°- and 65° directions respectively. It is very characteristic that only these shears are developed, which allow sinistral movements. The 160° trend is common in the entire Northern Apennines.

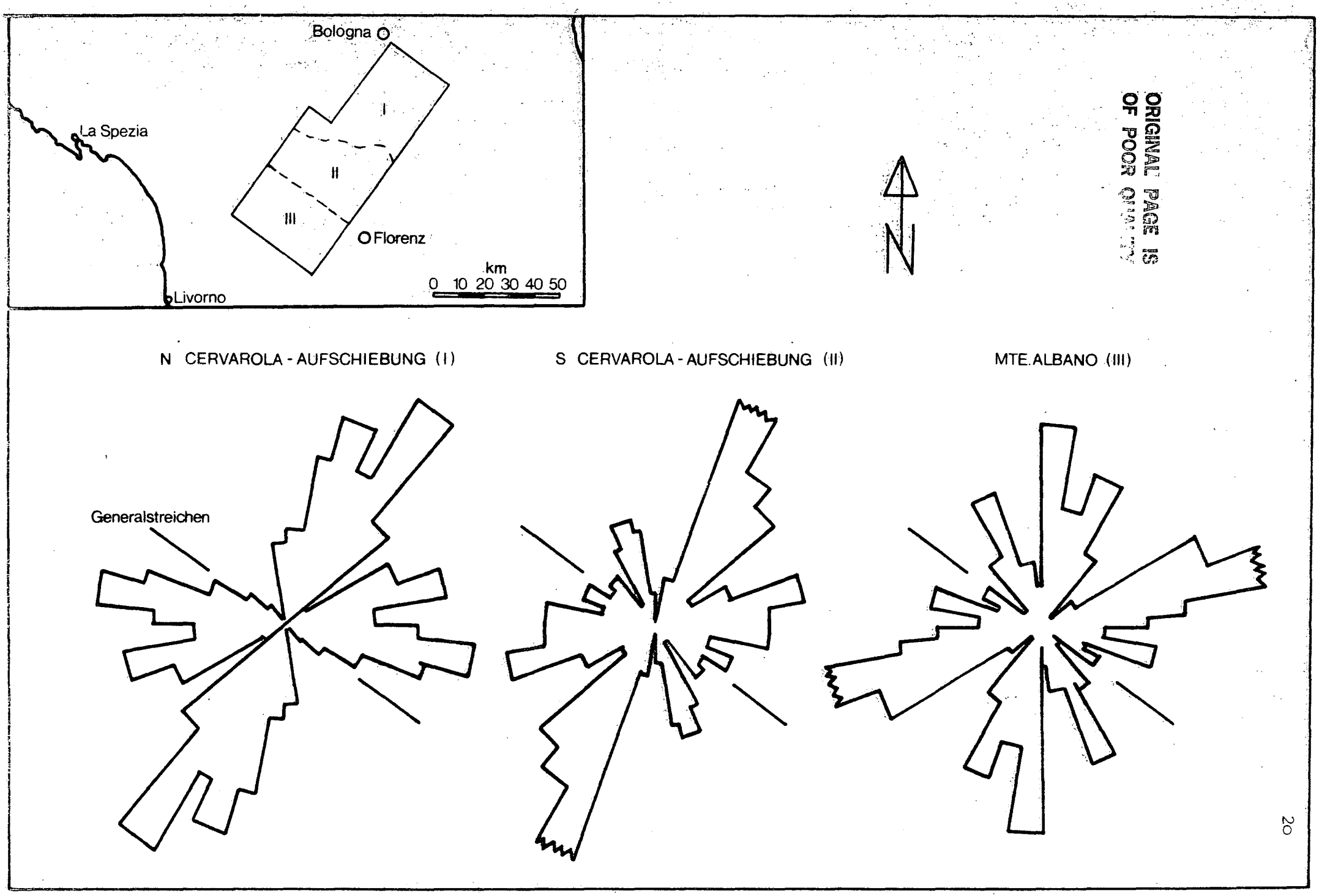

Fig. 8

3. Conclusions

The clockwise rotation of the Tuscan-Umbrian region stated in a previous publication (BODECHTEL & NITHACK 1975) can be regarded as well established by tectonic field measurements and satellite image interpretation. However, it has been proved by new results that the northern boundary of the rotated block is not given by the "Arno fault zone".
The part of the Arno fault in the proposed rotation model is taken over by the Prato-Sillaro-Line. From this is resulting a change in the shape of the rotated block, which represents a parallelogram instead of a triangle. Consequently, using the terms of the physics of solids the movement causing the rotation of the b_1-axes has to be described as torsion rather than as rotation. The horizontal movement component on the Ancona-Anzio-Line is considered rather small. Concerning the continuation of the Prato-Sillaro-Line to the SW the sinistral faults and the axis-deviations in the southern Mte. Albano region suggest a prolongation of the fault zone to the Tyrrhenian coast near Leghorn with slightly curved trend. The existence of two lineation systems visible on the satellite images (4o/13o^{o} and 65/155^{o} resp.) agrees well with the conception of clockwise rotation of the block S of the Prato-Sillaro-Line. Considering the extension of these two systems to N of the Prato-Sillaro-Line, BODECHTEL & NITHACK (1975) inferred a similar rotation of this northern block. However, such movement should be confirmed by additional field work.

It has to be emphasized, that the conception proposed here does not oppose to the idea of the anticlockwise rotation of Italy (ALVAREZ 1974, 1976; SOFFEL 1974, 1975). This rotation finished in the Eocene according to SOFFEL.

The above described clockwise torsion, however, took place between the two main orogenic phases in the Northern Apennines, that is between Aquitanian and Tortonian after BALDACCI et al. (1966).

B. Comparison of Photo Lineations Derived from Satellite Images and Aerial Photographs - A photogeological evaluation of Calabria and Sicily.

The entire southern part of Italy with an area of approximately 4900 km^2 (fig. 9) was mapped on the basis of MSS bands 5 and 7. The lineaments interpreted were displayed at a scale of 1:500.000 and statistically evaluated. By this a total of 12.500 elements with an overall length of 6500 km could be digitally registered. Some major lineations could be optimally derived from prints in a scale of 1:1.000.000 (fig. 10). Besides the interpretation of Landsat images aerial photographs (27 stereo-pairs, scale 1:10.000 and 1:20.000 were evaluated under same objectives.

Results.

The interpretation of the satellite images has clearly shown that above major lineations are accompanied by parallel striking minor elements. They occur either in the direct vicinity or as parallel elements at greater distances. The interelationship between major and minor lineations is strongly indicating the existance of large fracture zones described by CASSINIS et al.

The statistical representation of all counted lineations clearly reveals 3 directional maxima to N, NE, and SE (fig. 10). The evaluation on the basis of areal photographs shows a strong similarity between the directional distribution of lineation detectable on the island of Vulcano (fig. 10 and 11) with those from the Italian peninsula and Sicily. A further correlation can be observed between the major lineament directions and the areal distribution of the eolian islands.
The islands Salina Paraneo and Stromboli are arranged along the NE-SW striking lineament maximum whereas Salina, Lipari and Vulcano indicate above NW-SE direction. This phenomenon

Fig. 9: Landsat photo mosaic of Calabria and Sicily.

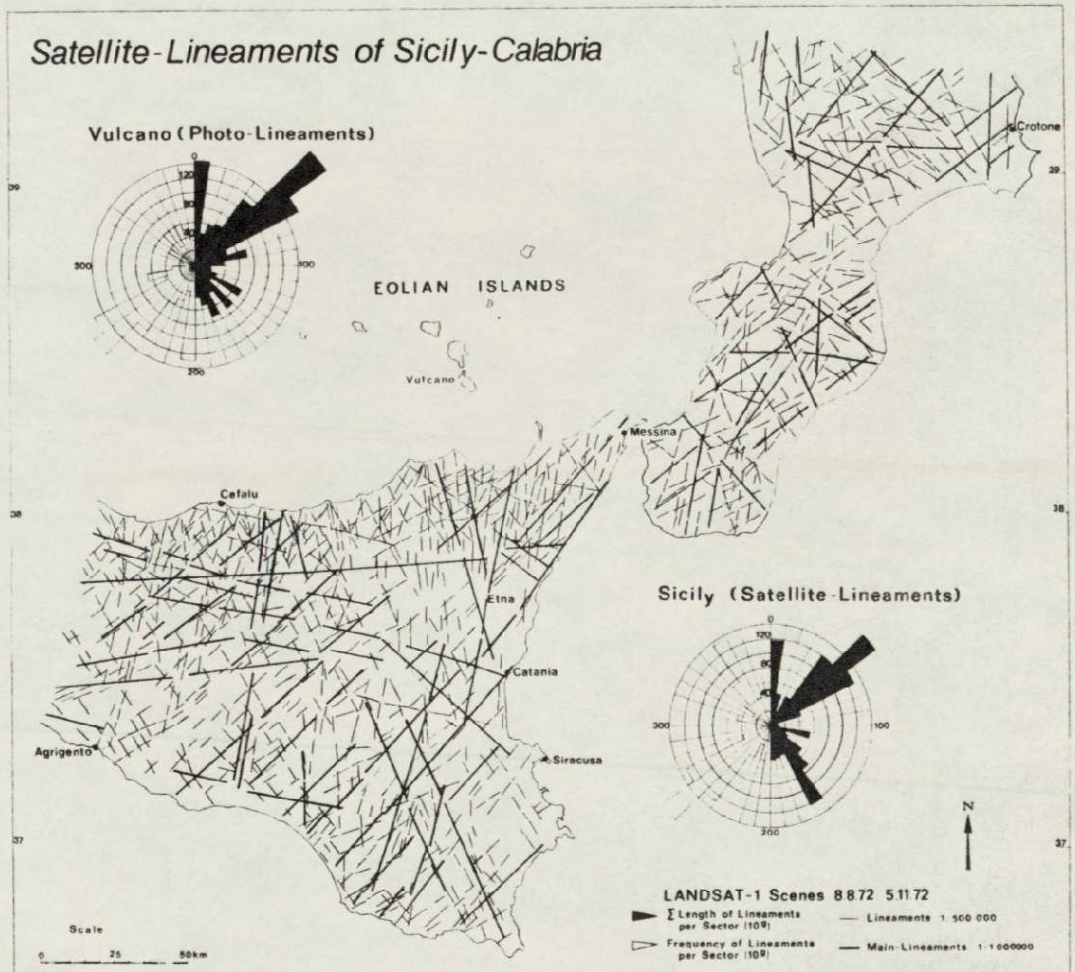

Fig. 1o: Photolineaments map derived from Landsat images of various scales.

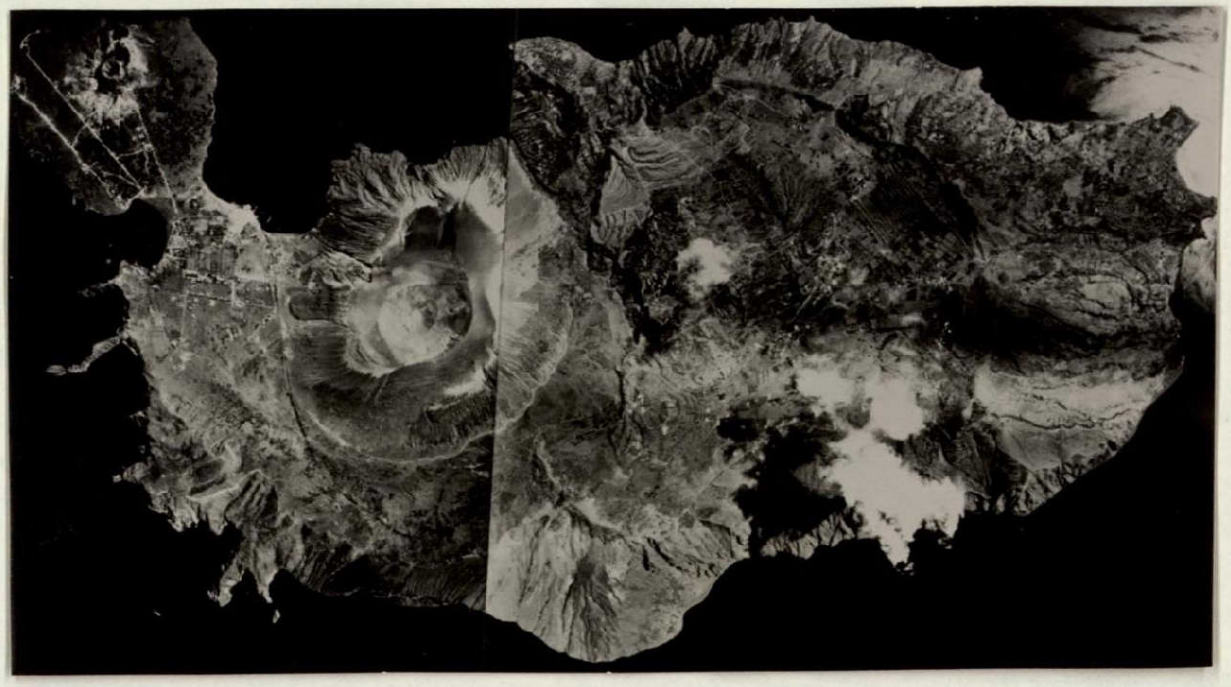

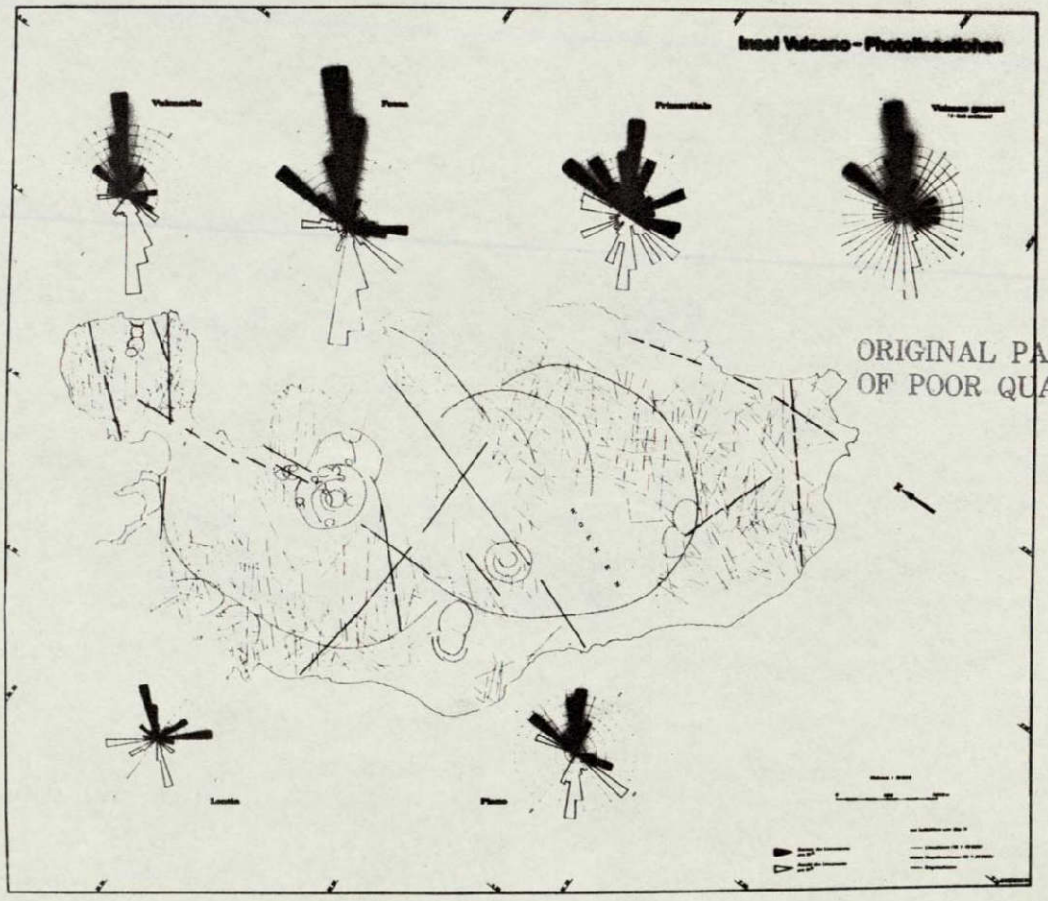

ORIGINAL PAGE IS
OF POOR QUALITY

Fig. 11: Photomosaic of Vulcano and photolineament evaluation.

characterizes the relationship of the volcanism with major fracture systems of the Tyrrhenian block.
The study demonstrated that the lineations derived from satellite images indicate a simplified structural pattern which is of special significance in defining the young fault tectonics of the southern Tyrrhenian block. The major directions of photo- and satellite lineaments coincide with seismotectonic results in the central mediterranean area and confirm also earlier results.

C. The Significance of Lineament Techniques for Practical Application in the North German Coal District.

1. Introduction

The coal reservoires in the southern and central part of the "Rheinisch-Westfälische" Coal Mining Region are far reaching exhausted. In order to keep up with the coal output, mining activities have to be extended to the northern part of the Ruhr Varlley. In this area the coal bearing layers are covered by mighty overlaying formations. Today prospection in this area is being carried out by drillings and seismological measurements above ground. Seismometer profiles deliver primarely information on the position of the coal bearing layers. In addition to this, large tectonical fracture systems can be detected, unter certain circumstances along the profiles.

Due to the basis of drillings only pointwise information on the petrography, the stratigraphy and the position of coal bearing layers is obtainable.
Clues on the fracture tectonical situation however can only be obtained if faults are sunk through.

Because of the lacking synoptic information obtainable by above prospection techniques the application of further methods such as photo-lineament evaluations is regarded to be of specific interest. Therefore, the following investigation has been directed towards an evaluation of the feasibility of "satellite lineaments " in order to describe the tectonical situation of the northern not yet explored mining region.

The area of interest (fig. 12) has been subdivided into 6 sub areas (fig. 13) which were individually investigated on the basis of Landsat frames representing various seasons and including Landsat-1 bulk products and Landsat-2 enhanced displays.

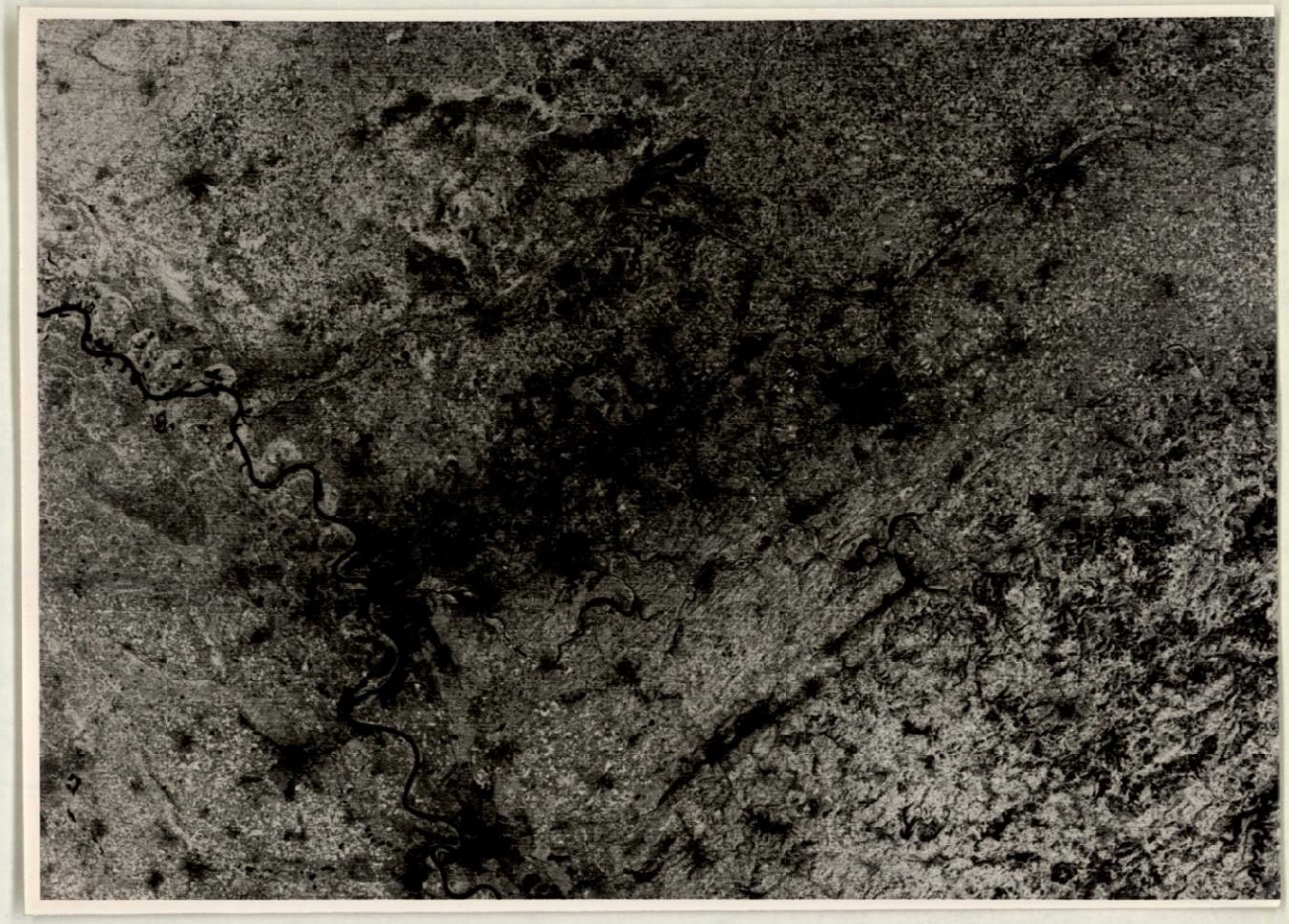

Scale 1 : 67o ooo

Fig. 12: Computer enhanced display of Landsat MSS exhibiting the north German coal mining area (Ruhr Valley).

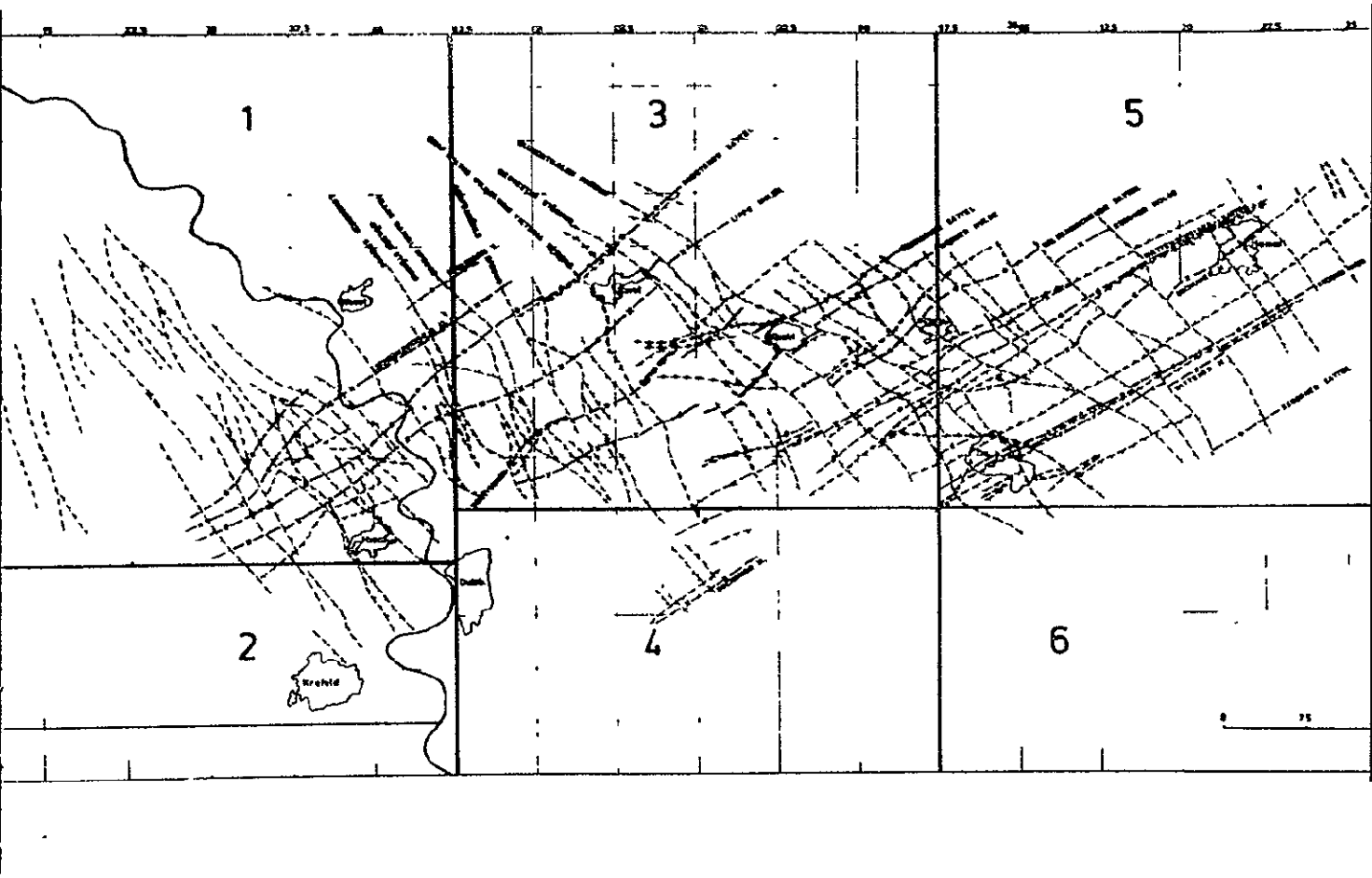

Fig. 13: Map of the major tectonical situation of the Ruhr-Valley with sub areas investigated individually.

In order to investigate the significance of the mapped photolineations with respect to the tectonical inventory obtained by intensive in situ measurements below ground (photogrammetric joint analysis), all photolineations which could be correlated to the known tectonical systems were indicated by special signatures (fig. 14 a,b).

An explanation of the signatures is given by fig. 15. The graphs indicate that the lineations could be interpreted with respect to two tectonical fracture systems - the B 1 -shear system (——) and the B 2 system (—·—) which is belonging to the asturian folding phase. Further indices represent lineations parallel to the system's B-axis ····» and B-parallel striking upthrusts or dip slip faults. Perpenticular to B striking lineations in direction of cross cutting dip slip faults and fractures are indicated by ····> . The remaining elements ····› represent transcurrent fault systems or diagonal shear ruptures typical for the tectonical systems of the Ruhr Valley.

The rose diagram of fig. 16 is a synoptic representation of all mapped photolineations (are 1 - 6) in combination with the striking directions of the main elements of the tectonical systems B_1 and B_2.
The fare reaching correspondence of photolineations with the major tectonical fracture systems of the Ruhr Valley indicates the high potential of linear features for the description of subsurfacial tectonics.

In the following a detailed lineament tectonical description of the various subareas demonstrated by fig. 13 is given.

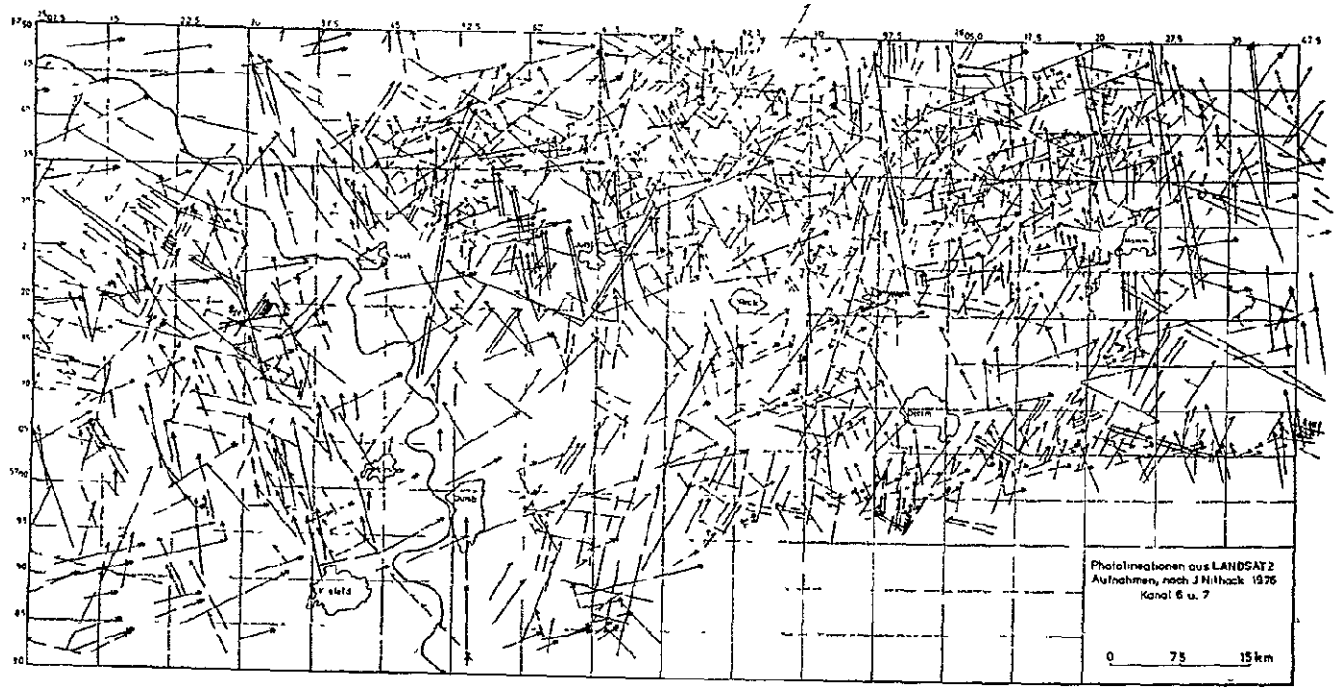

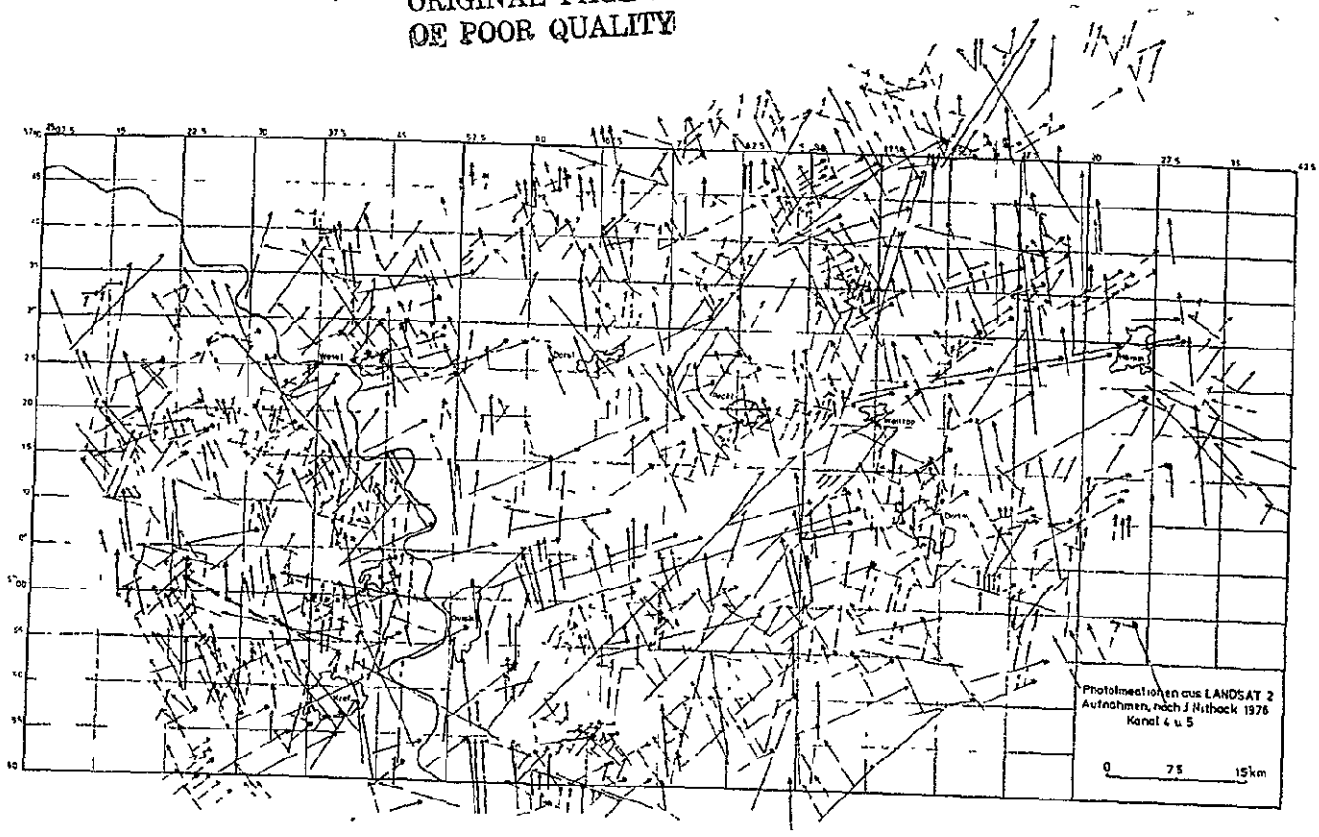

Fig. 14 a/b: Photo lineament maps of the Ruhr Valley derived from MSS bands 6/7 and 4/5 resp.

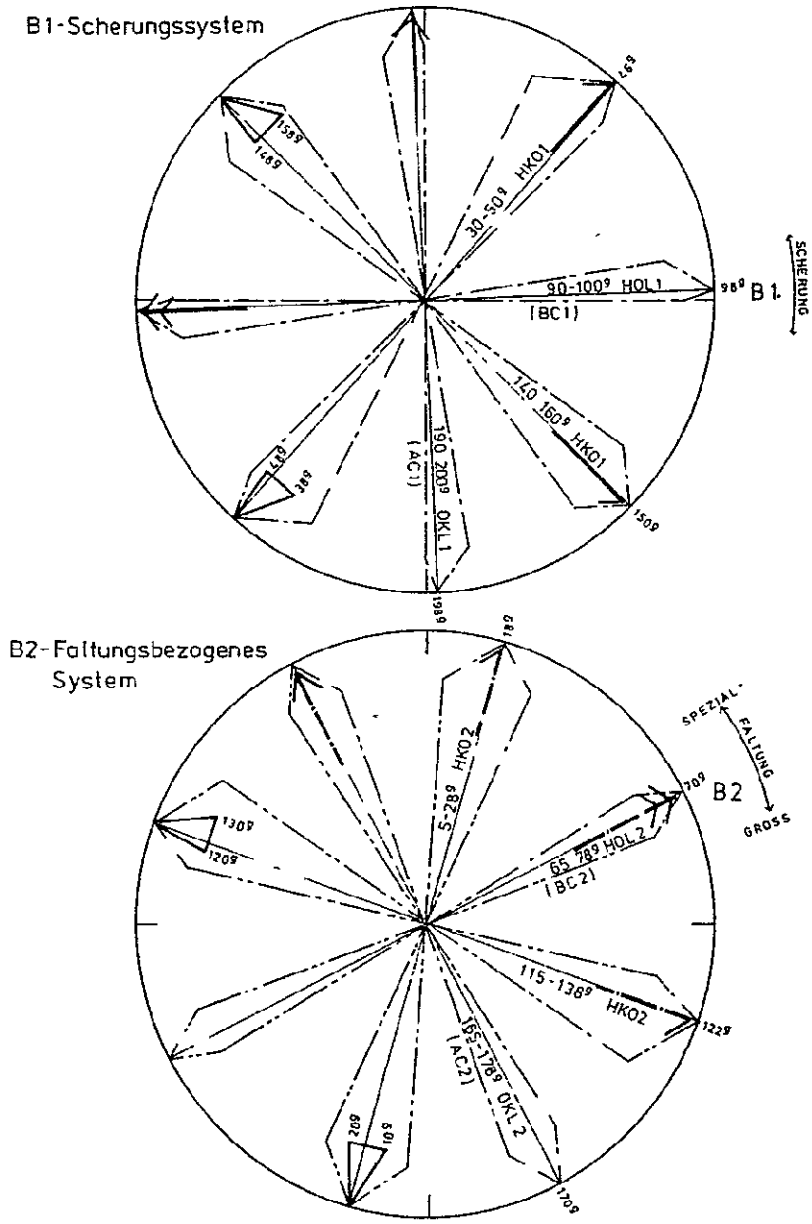

Fig. 15: Tectonical inventory of the Ruhr Valley. B1-shear system and B2 folding system with symbols indicating corresponding lineaments.

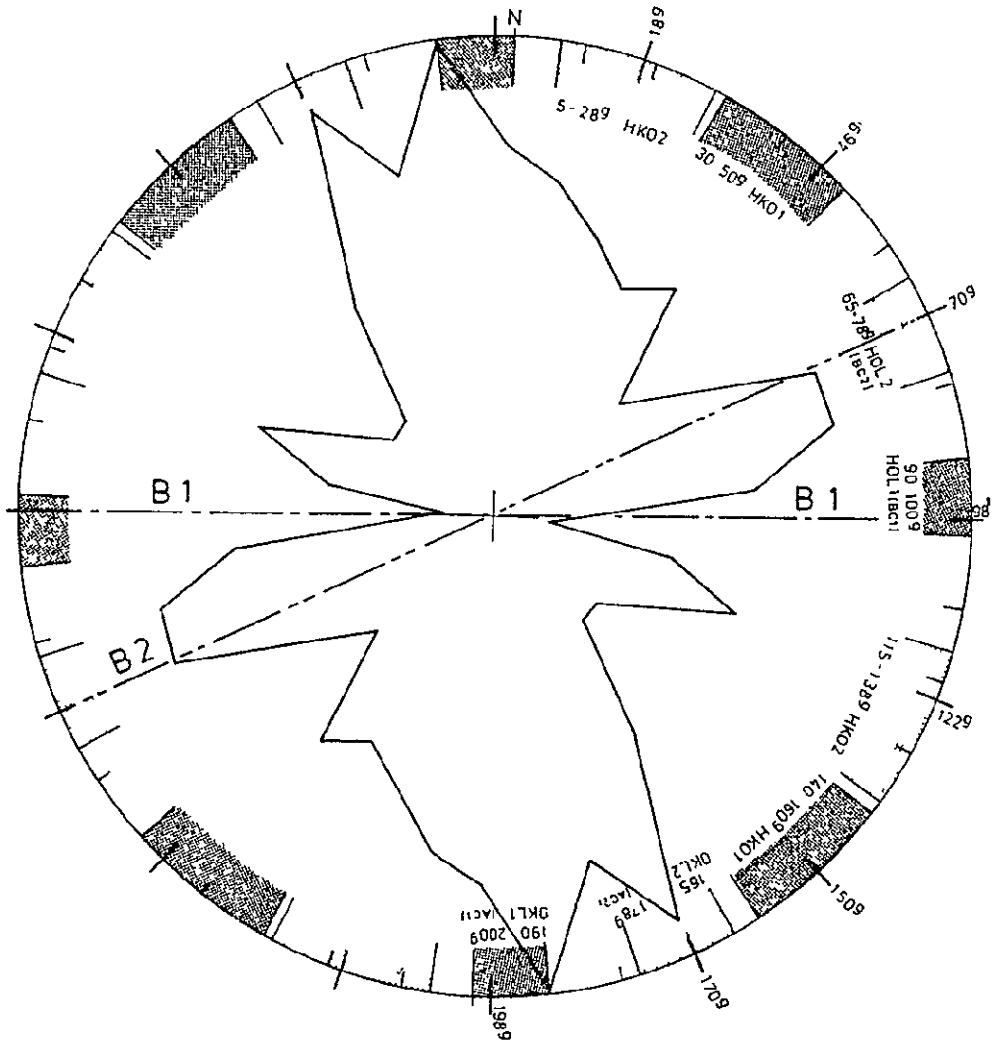

Fig. 16: Photo lineations of regions 1 - 6 in comparison with major tectonical systems B_1 B_2 (signatures around the circle).

2. Photolineations of the norther part of the Niederrhein (Area 1)

As it can be derived from the maps of figure 14 a,b and the rose diagram of fig. 17 area 1 is mainly characterized by lineations striking with 190g (oKL1). Additional diagonal striking shear structures HKo1 can be derived with two crossings. These lineations indicate fracture systems of the carbon layers, which have been active beyond the Mesozoicum.
In this area B_1-parallel striking elements are underrepresented.
The rose diagrams (fig. 18 a,b) obtained by analysing computer enhanced Landsat-2 images deliver additional information especially on elements indicating the fracture system of the asturian folding phase (B_2).
A comparison of the rose diagrams exhibited by fig. 18 a,b demonstrates a special phenomenon. MSS bands 6 and 7 deliver primarily good possibilities to extract lineations belonging to the B_1 system with NS striking elements accompanied by HKO-1 shear crossings (Fig. 18 a). MSS bands 4 and 5 mainly reveal those lineaments which characterize the B-2 system with a strong maximum of OK12 elements perpentricular to the direction of the B_2-axis (fig. 18 b) The same phenomenon could also be observed in other subregions where the coal bearing layers are covered with mighty overlaying formations.

MSS bands 6 and 7 exhibit more information on the drainage system which seems to be primarilly controlled by structures belonging to the earlier tectonical system (B 1).

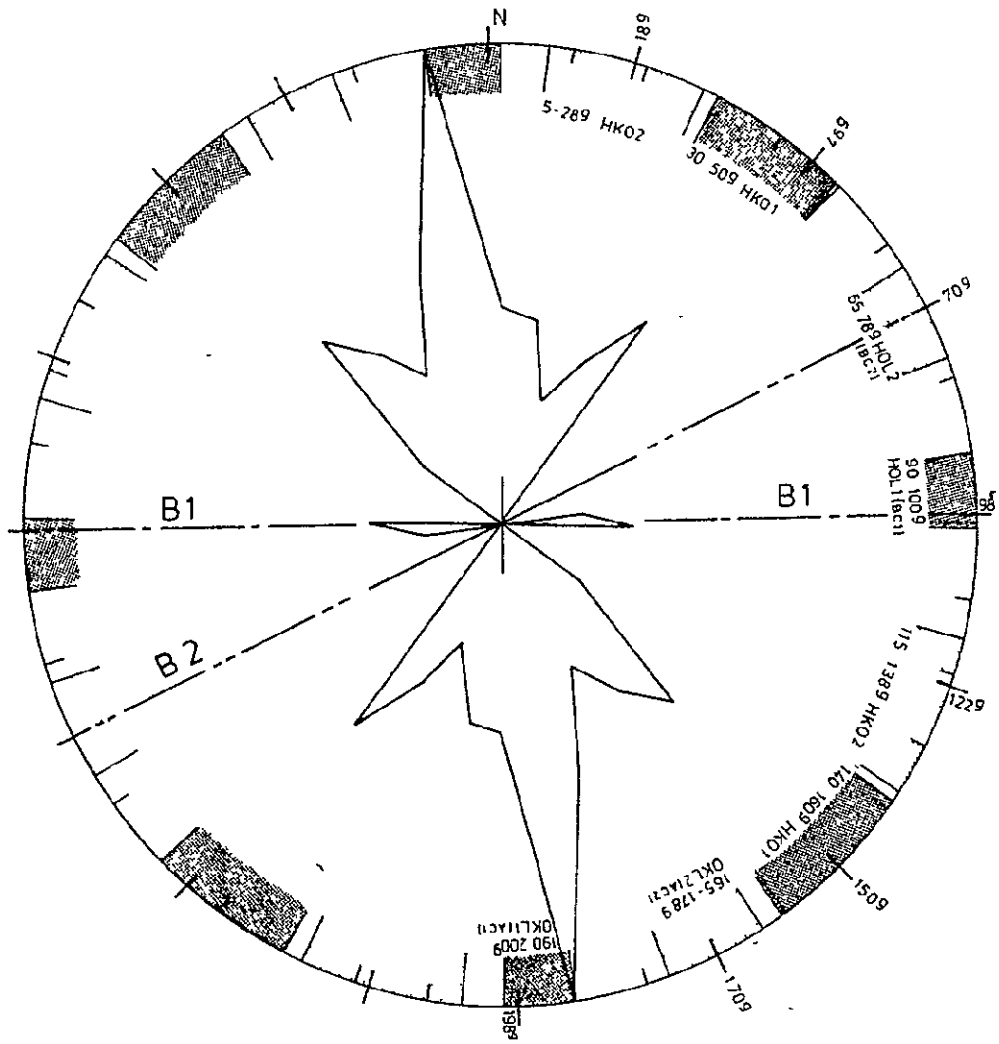

Fig. 17: Lineament distribution Area 1.
The major lineament orientation is NS
indication OKl 1.

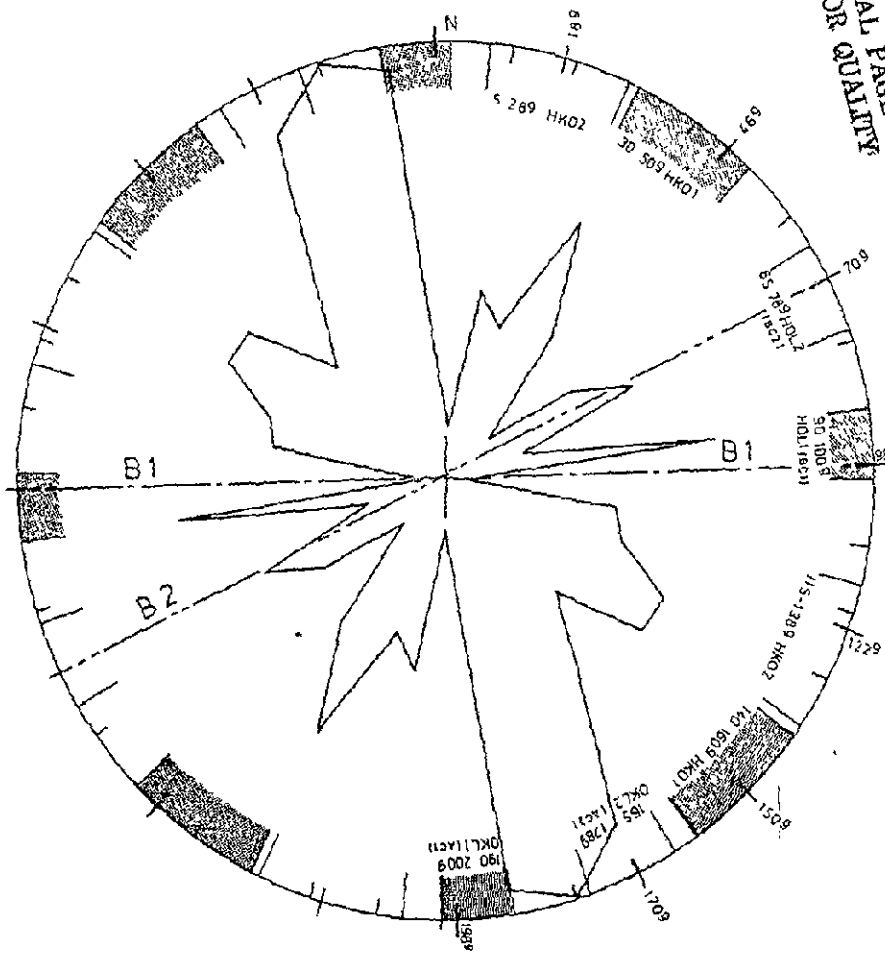

Fig. 18 a: Lineations derived from MSS bands 6 and 7.

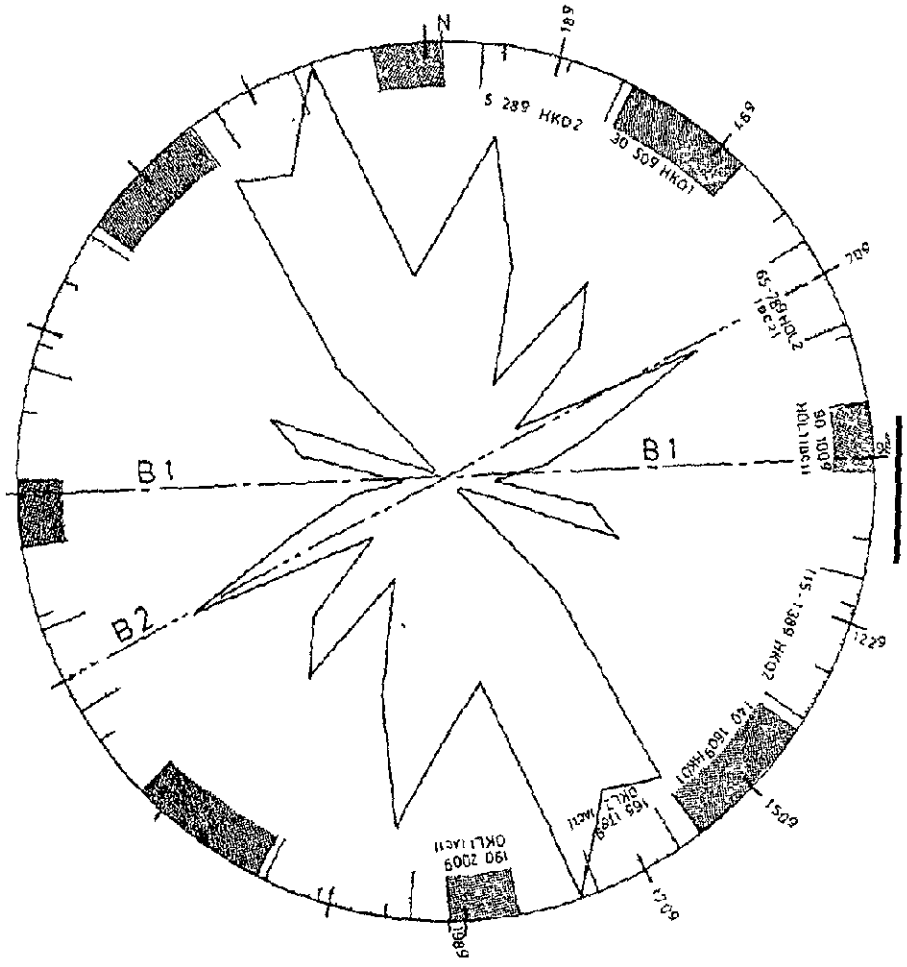

Fig. 18 b: Lineations derived from MSS bands 4 and 5.

3. Photolineations of the northern Ruhr Valley (Area 3)

This area covers the region of mining activities and its zone in front of the face.
The rose diagrams derived from Landsat-1 (fig. 19 a) (bulk product) indicates nearly the same situation as for area 1 with dominant NS striking (OKl-1) linear features. The interpretation on the basis of the enhanced Landsat-2 image again demonstrates a much higher degree of directional distributions indicating the presence of the B_2 system (fig. 19 b). Of special interest is the large number of lineations which follow the general direction of the B_2-axis (= fold axis) in connection with those lineaments striking perpenticular (OKl2).
Photogrammetric measurements below ground have shown that above situation is typical for this area.

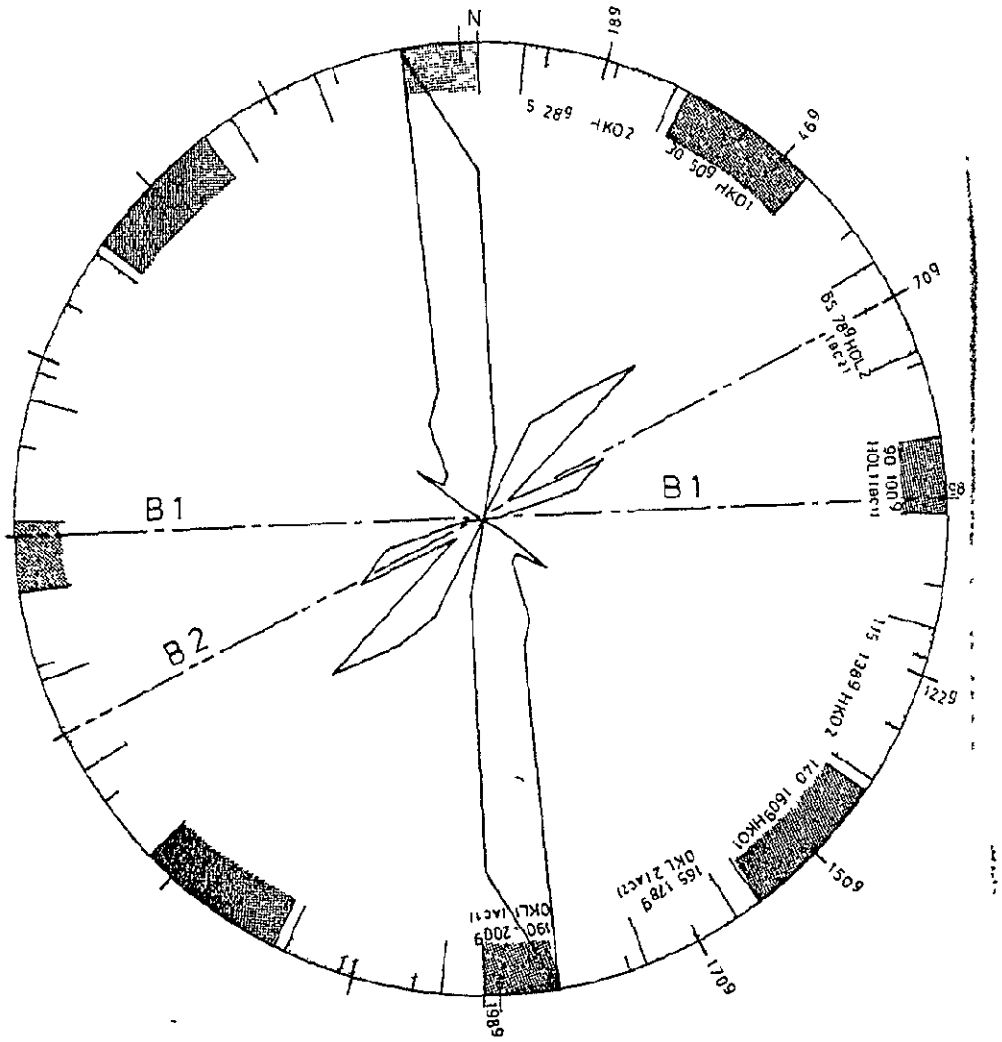

Fig. 19 a: Photolineation (Area 3) derived from Landsat-1 bulk products

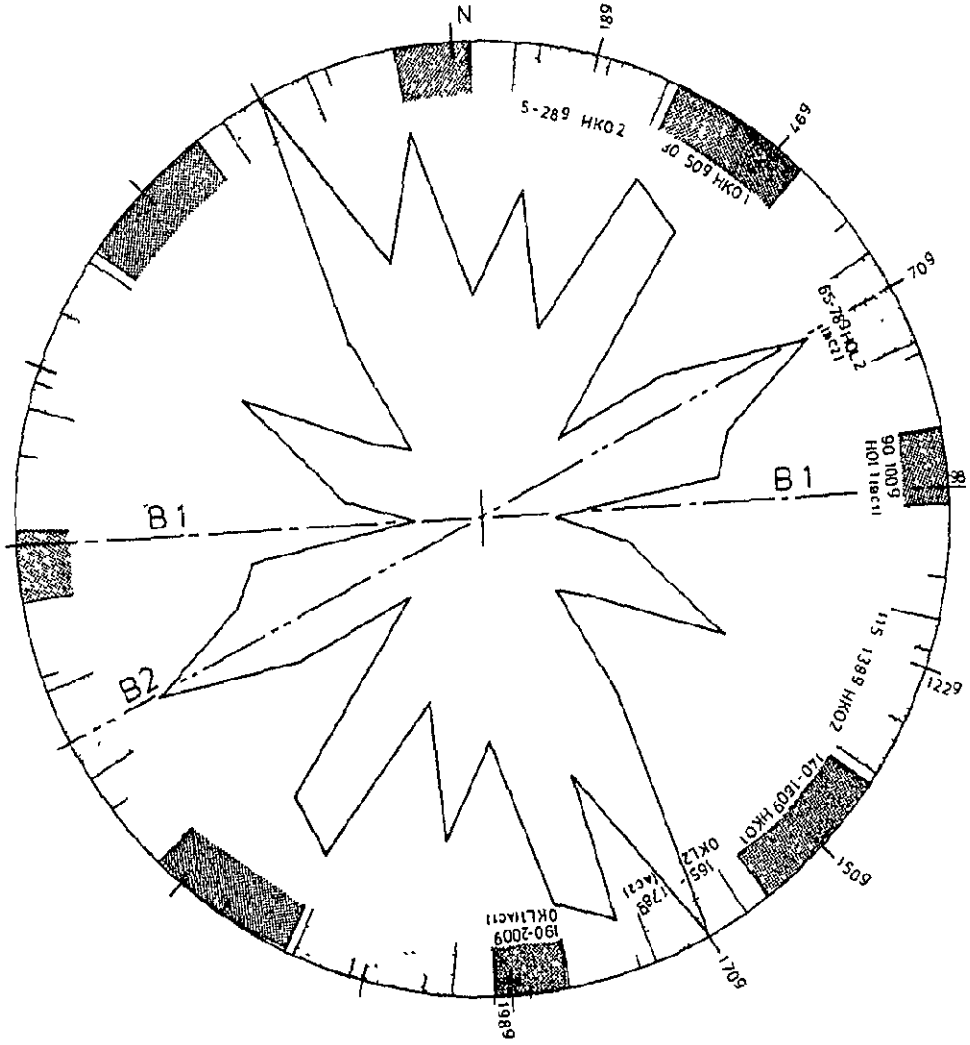

Fig. 19 b: Photolineations derived from Landsat-2. Computer enhanced images

4. Photolineations of the eastern Ruhr-Valley (Area 5)

The rose diagram of this area (fig. 2o) reveals besides the N/S striking elements HoL-parallel lineations which strike with 9o^g. In addition NE-, SW striking lineations represent diagonal shear structures (HKo1).

The weak maxima between 12o and 13o^g can be related to shear systems (HKo2) and 17o^g cross fractures which belong to the tectonic fabric of the folding phase which is not very expressed in this area.

5. Photolineations of the southern Ruhr-Valley (Area 4)

Area 4 ist characterized by an intensive folding of the coal layers. In correspondence to this tectonical situation, photolineations which occur parallel to the B2 system (folding system), are more expressed as those lineaments which indicate the B 1 system. This fact can be clearly demonstrated by the diagrams of fig 21.
Thus, these diagrams do not only represent north-south striking elements but also diagonal shear fractures indicating Ho2 and oKL2 tectonical elements.

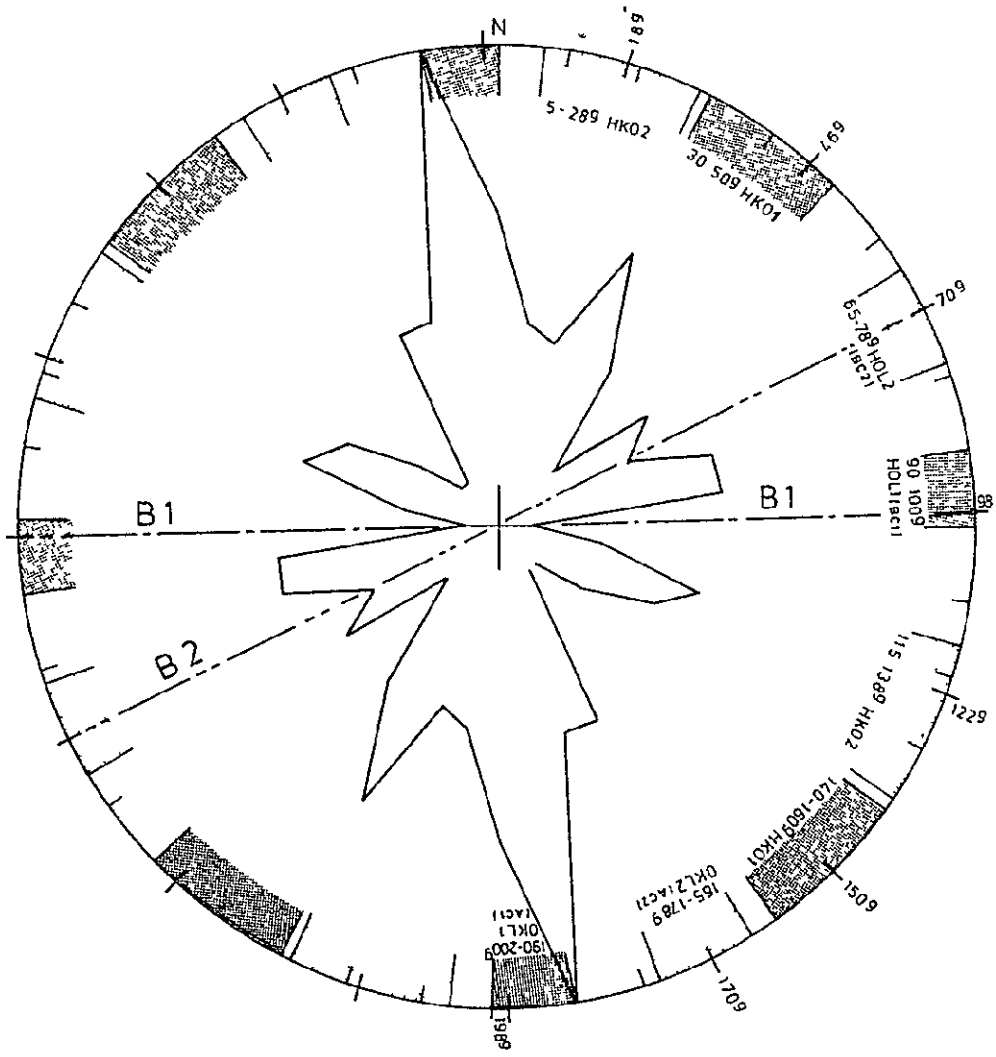

Fig. 2o: Photolineation (area 5)

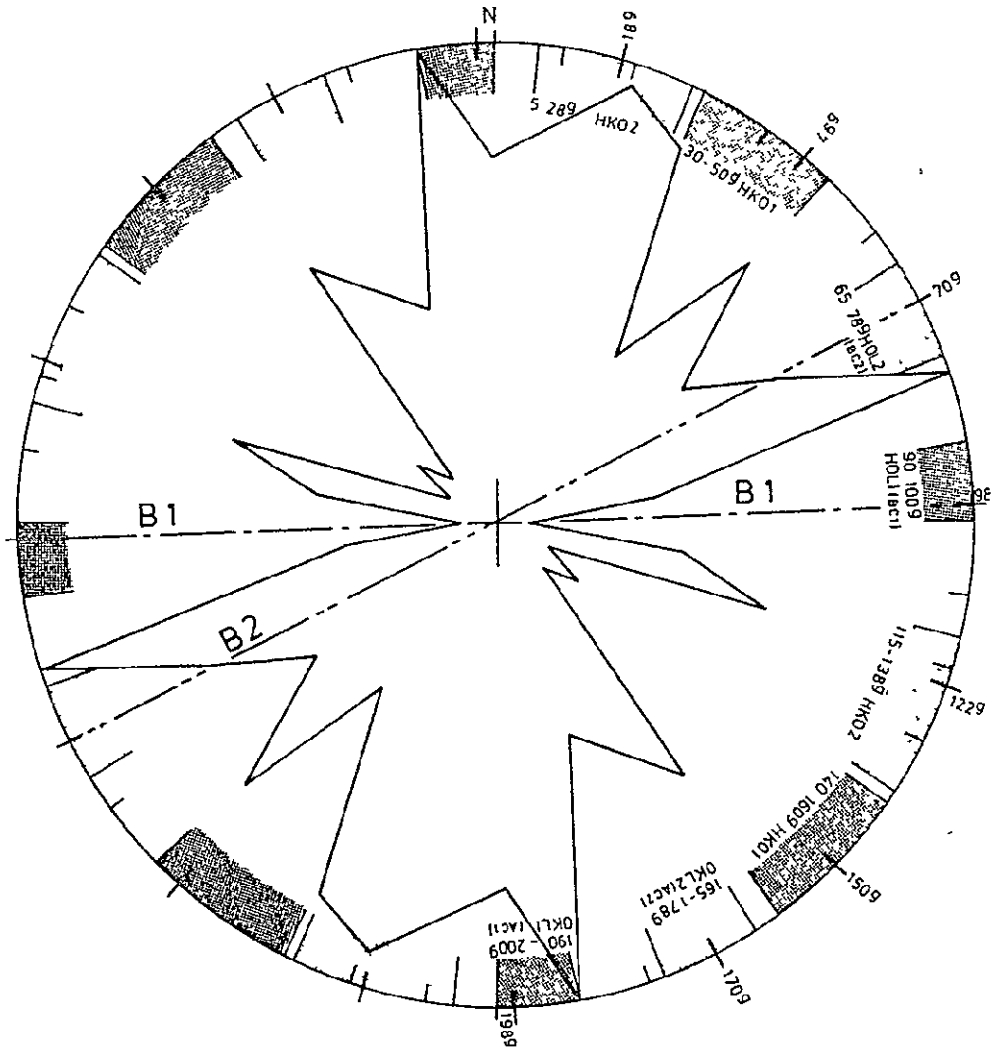

Fig. 21: Photolineation (area 4)

6. Density maps

Besides the statistical representation of photolineation on the basis of rose diagrams, special maps, indicating the density of lineation and the directions of "density axis" were produced.
The map of fig. 22 represents the density distribution of lineations on the basis of 5 x 5 km. The distribution of the maxima can be related to the major tectonic divisions in EW direction as it has been described by KIENOW (1955). In addition to that, the axis of zones with maximum density indicate NS occuring lineament zones which are characterized by intensive expressed fracture systems. The axis relating to density minima can be correlated with diagonal shearing zones (fig. 23).

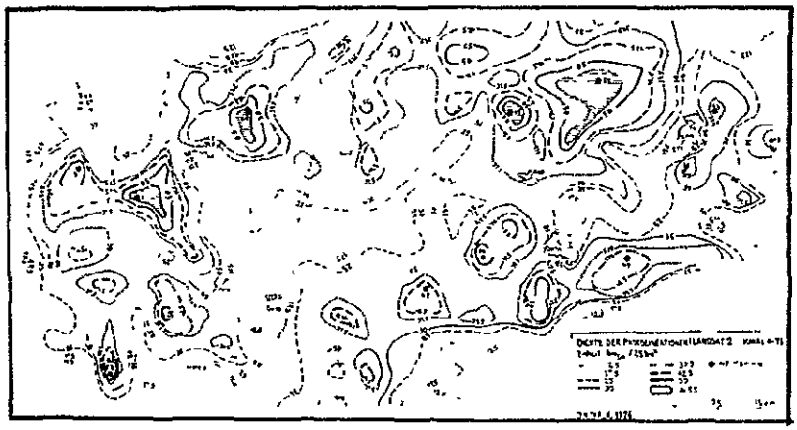

Fig. 22: Density map of photolineations (see also Fig. 12, 13 and 14)

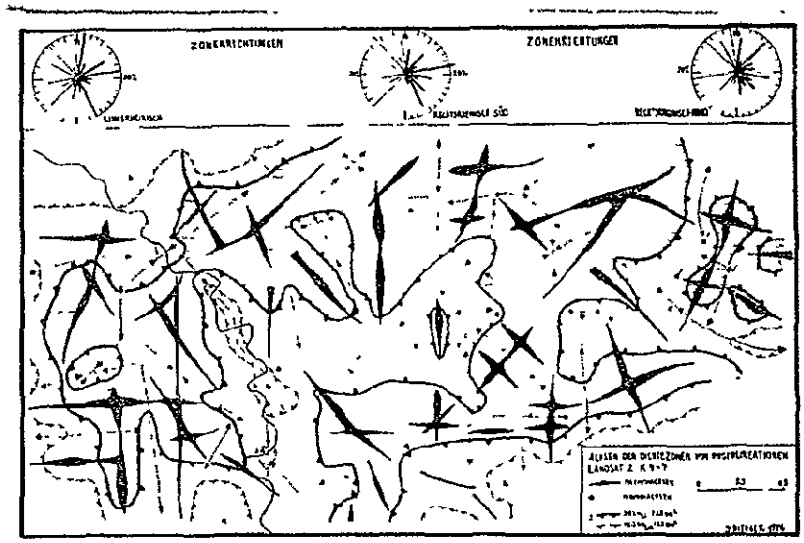

Fig. 23: Axis of zones with maximum( ) and minimum( ) lineament densities

7. Conclusion

Above demonstrated examples are derived from ongoing intensive investigations which are being carried out in the mining district of the Ruhr-Valley. A detailed comparison of photolineations with existing fracture systems has been possible because of the excellent tectonical inventory which is a result of a long term measurement program based on in situ measurements below ground. The additional application of Landsat imagery has definitely shown that there exists a close relationship between photolineations and the tectonical deformation plan of the Ruhr Valley. This corresponds not only to the distribution of directions but also to the detectability of structural elements of the deeper underground which have influenced the folding phase of the carbon.

The interpretability of photolineations with respect to the existing tectonical fracture systems leads to significant practical applications.
Today, coal breaking below ground is being carried out on the basis of far reaching automated machines. Experience has shown, that displacements of the coal bearing layers typical for regions with intensive tectonical influence may require to rebuild all technical coal breaking installations which is extremely costly.
A comparison with experienced difficulties in mining activities due to typical fracture configurations also identifiable by photolineations enable us to state, that in the northern not yet explored part of the Ruhr Valley, which bears a high potential for mining difficulties can be identified. These areas are characterized by cross cutting and to a certain degree diagonal striking elements.

REFERENCE

Photolineationen aus Landsat-2 Aufnahmen und ihre Beziehungen zur Tektonik im Ruhrkarbon.
Forsch.Ber. Ld. Nordrhein-Westfalen, Fachgr. Bergbau und Energie. 2556. Bd. 2. S. 137-143. 1977.

D. Application of Remote Sensing Data to Support Lignite Exploration in Northern Bavaria.

1. Introduction

The following section describes a research project which has been carried out under the objective to investigate remote sensing data in general for practical applications in the field of lignite exploration in Germany.
It has to be seen under the aspect of combining modern data and image data processing techniques with conventional interpretation methods. An approach which emphasizes the manifold possibilities to handle remote sensing information.

Within the frame of the project besides multispectral scanner data obtained by an airborne M^2S-system also Landsat data have been taken in consideration.

In the valley system of the "Urnaab" extensive lignite deposits have been built up during the Tertiary. Since the beginning of this century the known deposits in a depth of about 1o m are being exploited by the Bavarian Browncoal Industry.
With respect to problems in exploring new mining fields various conventional exploration techniques such as geo-electrcity, drillings and other geophysical methods have not been too successful.

The described study deals for the first time with the possibilities given by remote sensing techniques to support exploration activities in the area of the bavarian Brown-coal Industry. The basic idea that multispectral remote sensing techniques may be a valuable tool has been derived from the fact that brown coal is constantly releasing H_2S, NH_3, Co_2, Co.These products of the coalification process, are being absorbed by the surface vegetation directly, or via the water cycle. By this it is expected that the reflection characteristics of various vegetation types might be influenced in a detectable manner. Therefore the objective

of the study was directed towards an empirical investigation of a larger area (fig. 24) within the brown coal bearing valley systems due to spectral anomalies.

In order to meet above objectives the following data were acquired.

Fig. 24: Investigated area near Schwandorf

(- - - -) = known lignite deposits

——— = vegetation profiles.

2. Data Acquisition

During August 1976 the area of interest (fig.24) near Schwandorf in northern Bavaria was covered by an aircraft multispectral scanner flight from an altitude of ~ 4000 m above ground. From the same area Landsat data were processed from CCT's and compared with the results of the scanner flight. Unfortunately the Landsat data did not represent the same time frame, (year, season) of the aircraft mission.

On the basis of above aircraft, Landsat and additional collected ground truth data the following data evaluation approaches were selected:

1) Statistical investigation of aircraft scanner data with respect to vegetation signatures.
2) Application of image processing techniques applied on M^2S and Landsat CCT's for enhancement and detection of possible spectral anomalies.

3. Statistical Investigation of Spectral Signatures

In order to statistically evaluate spectral characteristics of selected vegetation types and to correlate these measurements with the geological information an intensive and detailed vegetation map along selected profiles was carried out. As it can be derived from fig. 24 the selection of profiles was related to areas with known lignite horizons below ground to areas without lignite bearing layers and to those areas which have not yet been explored. With respect to ground truth activities, information about the plant species (crop types), vegetation associations and soil moisture was provided. A typical vegetation map along a profile is given in fig. 25 . It shows that the major vegetation types have been wheat, winter wheat, barley, maize and grass land.

For the correlation of spectral signatures with ground truth information the image processing system of the Central Lab was used and special software programs to establish a data bank were implemented.

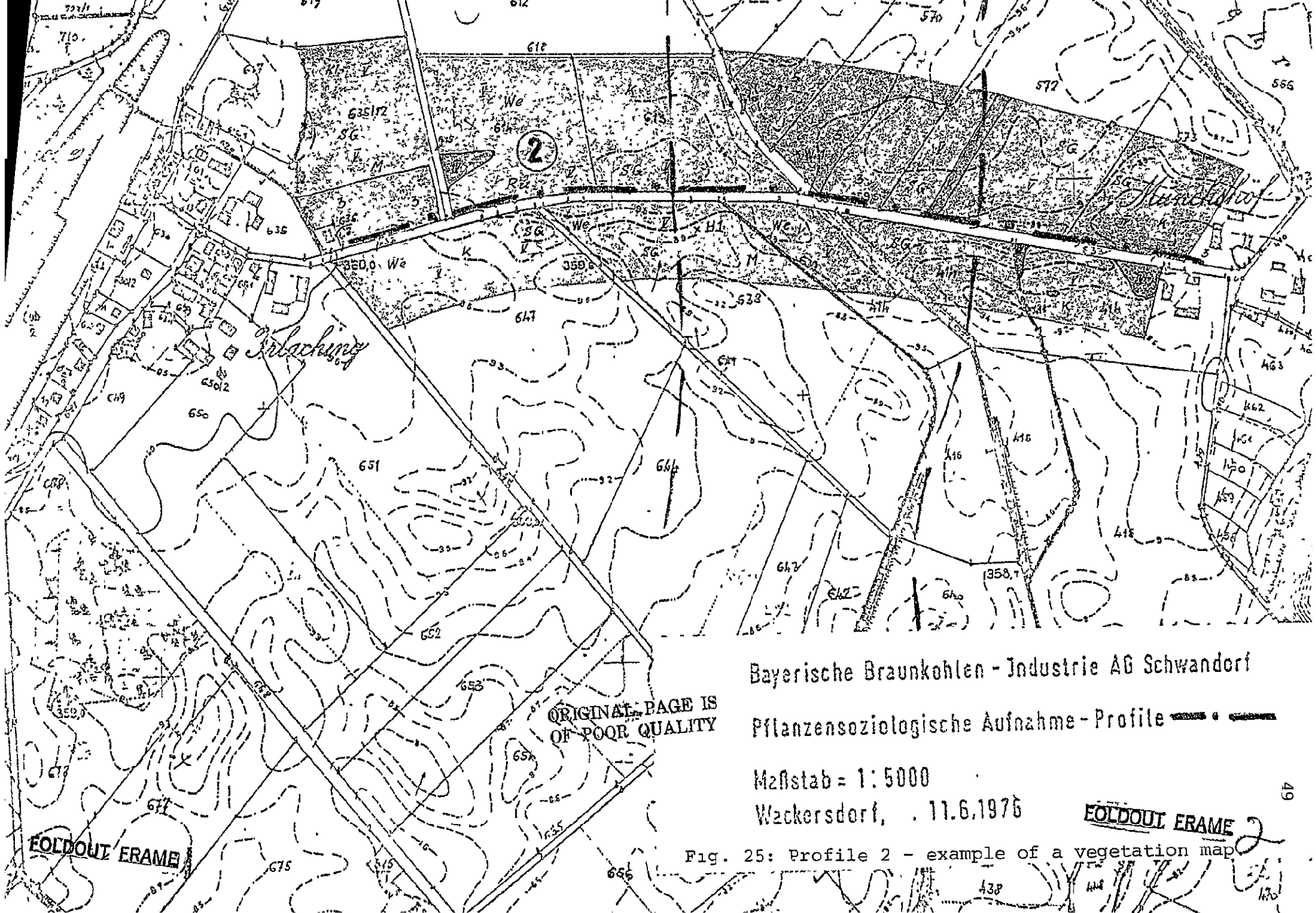

Fig. 25: Profile 2 - example of a vegetation map

The Data Bank

As it can be derived from fig. 26 larger areas containing profiles with ground truth information can be displayed on a color TV screen. The displayed image consists either of three selected spectral bands within the visible and infrared region or of preprocessed bands such as PC-transformations

Fig. 26: Enlargement of M^2S exhibiting an area covering profile No. 1 and 2.

in order to obtain maximum grey-tone or color separation for the visual identification of mapped fields.
In a next step (see fig. 27) the spectral signatures of unumbiguously identifyable fields can be selected interactively via the TV screen and stored into the data bank by adding information on crop type, soil moisture, profile number, position within scan stripe and information about the occurrence of lignite in the underground.
The corresponding information is coded with symbols (f.e. wheat = w, soil moisture levels $F_{1 \ldots 3}$ etc.).
For each measurement point the spectral information contains the meanvalue, standard deviation and minimum/maximum intensities.

Fig. 28 demonstrates the use of the data bank for the statistical investigation. By special filter programs (F 1) the stored signatures can be retrieved due to ground truth information described above. The execution is carried out by keying in the corresponding symbols
Fig. 29 demonstrates a listing showing the ID-symbols in the first line.
By this a fast evaluation of signatures is possible. By using another set of filter programs (F 2) a further selection of prefiltered data due to individual spectral bands can be achieved in combination with the calculation of several ratio transforms etc.

Results.

With respect to the manifold crop and vegetation types covered by the mapped profiles only summer barley, wheat- and corn-fields were selected for the comparative signature study. The restriction of above vegetation types was necessary because the other crop types were statistically underrepresented within the profiles.
Out of a total of $\sim$ 400 signature measurements the following results could be derived:

DATA BANK - DATA STORAGE

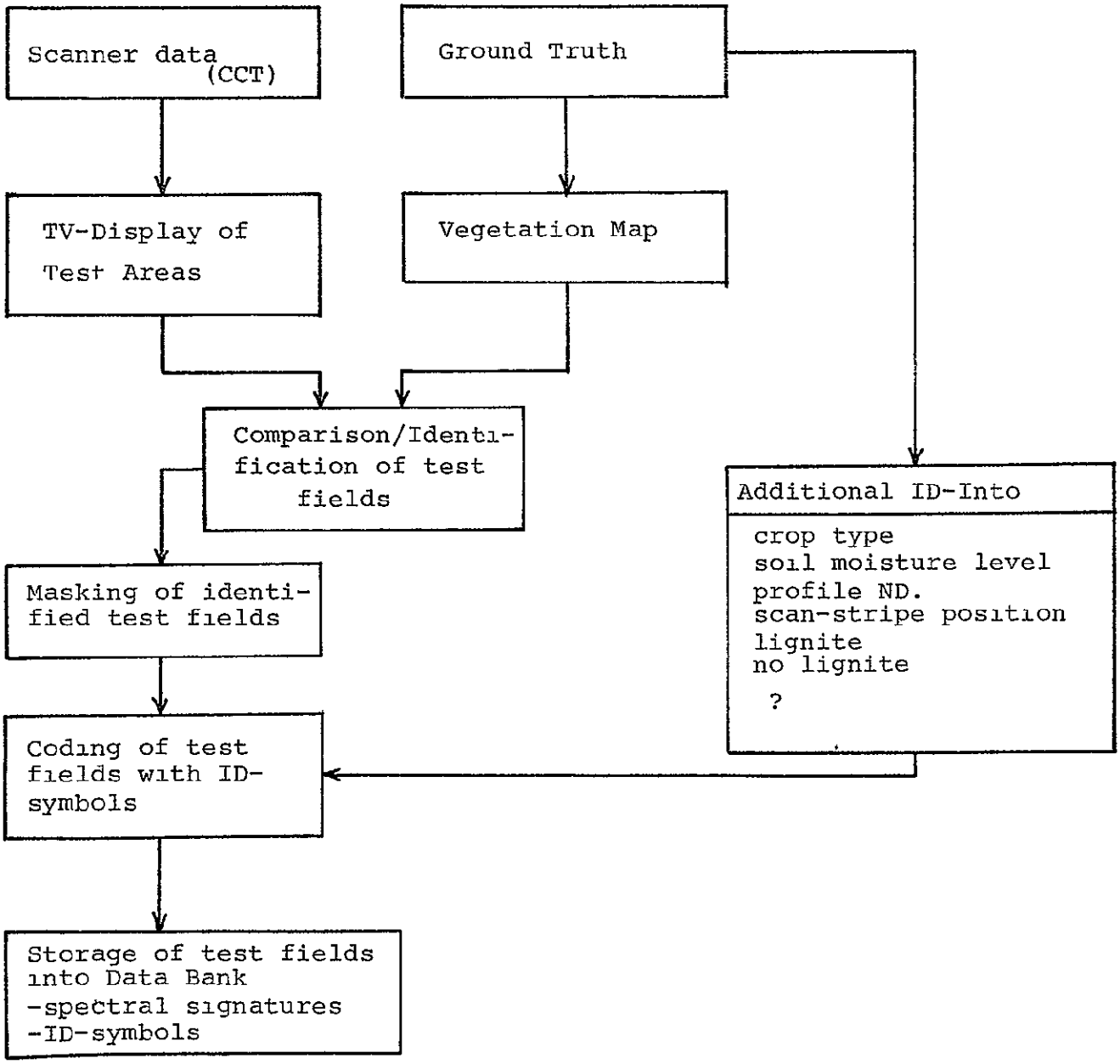

Fig. 27

DATA-BANK - DATA RETRIEVAL

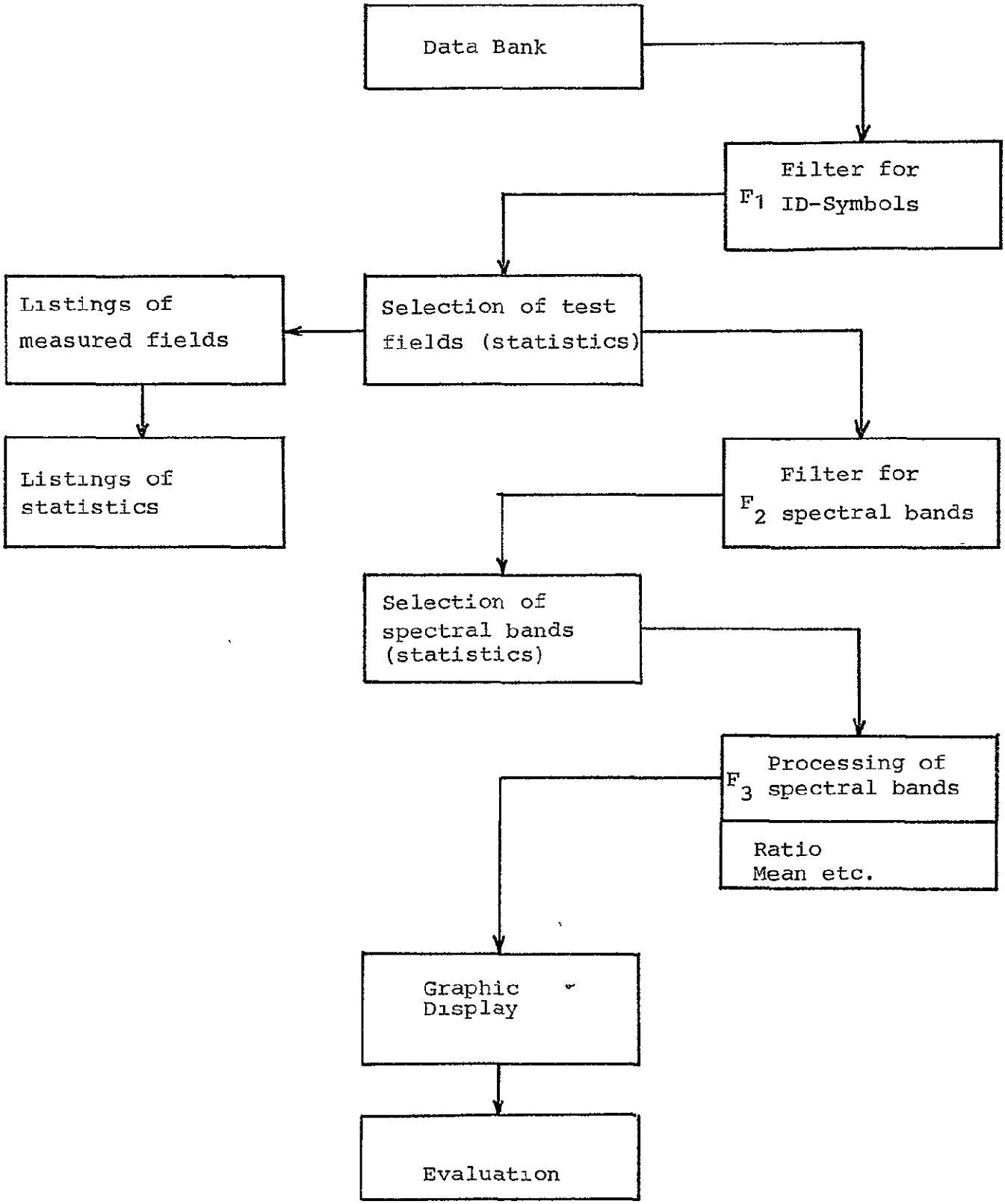

Fig. 28

FIELD IDENTIFICATION = SGF2S300P2
NUMBER OF PIXELS = 11
ANBAU = SOMMERGERSTE
FEUCHTIGKEIT = IV
STREIFEN = 3TER
KOHLE? = KEINE KOHLE
PROFIL = 2. PROFIL

CH	0	1	2	3	4	5	6	7	8	9	10
MIN	161	84	53	49	29	37	27	53	124	101	0
MAX	170	91	56	51	32	40	30	54	126	109	0
MEAN	164	86	54	49	30	37	27	53	125	104	0
STDD	3	2	1	0	1	1	1	0	1	3	0

FIELD IDENTIFICATION = K0F2S300P2
NUMBER OF PIXELS = 170
ANBAU = KOHL
FEUCHTIGKEIT = IV
STREIFEN = 3TER
KOHLE? = KEINE KOHLE
PROFIL = 2. PROFIL

CH	0	1	2	3	4	5	6	7	8	9	10
MIN	158	82	48	42	25	1	24	49	117	0	0
MAX	170	89	53	46	30	36	28	50	129	128	0
MEAN	164	85	49	43	27	33	25	49	122	113	0
STDD	3	2	1	1	1	3	1	0	3	31	0

Fig. 29: Print out of selected vegetation types.

The spectral measurements taken from fields with summer barley have clearly shown that those spectral signatures which were derived from areas above lignite layers are characterized by slightly decreased intensity values if compared with those measurements over areas where drillings did not indicate lignite.
Of special interest has been the fact that changes in reflection intensities are not restricted only to the infrared band .

Comparisons of wheat measurements demonstrated a reverse behaviour of spectral signatures. By this the intensity values above lignite layers are higher than the others.

Corresponding measurements taken from maizefields and grassland also indicate increased intensities derived above lignite horizons.

Similar investigations have been carried out over various other crop types. These measurements, however, didn't show the same correlations as they could be observed with above vegetation types.

In order to select the optimum spectral regions for the discrimination of above described phenomena, two-dimensional representations of selected bands were visually interpreted. Fig. 3o demonstrates an intensity plot of band 4 versus band 7. The circle indicate the standard deviations.

The good separation between those measurements derived from lignite bearing and lignite free areas can be clearly seen.

In order to compare spectral vegetation measurements from profiles over yet unexplored areas an "intensity signature" was established with respect to the positions of summer-barley-, wheat- and maize values within above (fig. 3o) two-dimensional space given by bands 4 and 7 (fig. 31). The corresponding measurements were separated due to information about lignite in the underground.

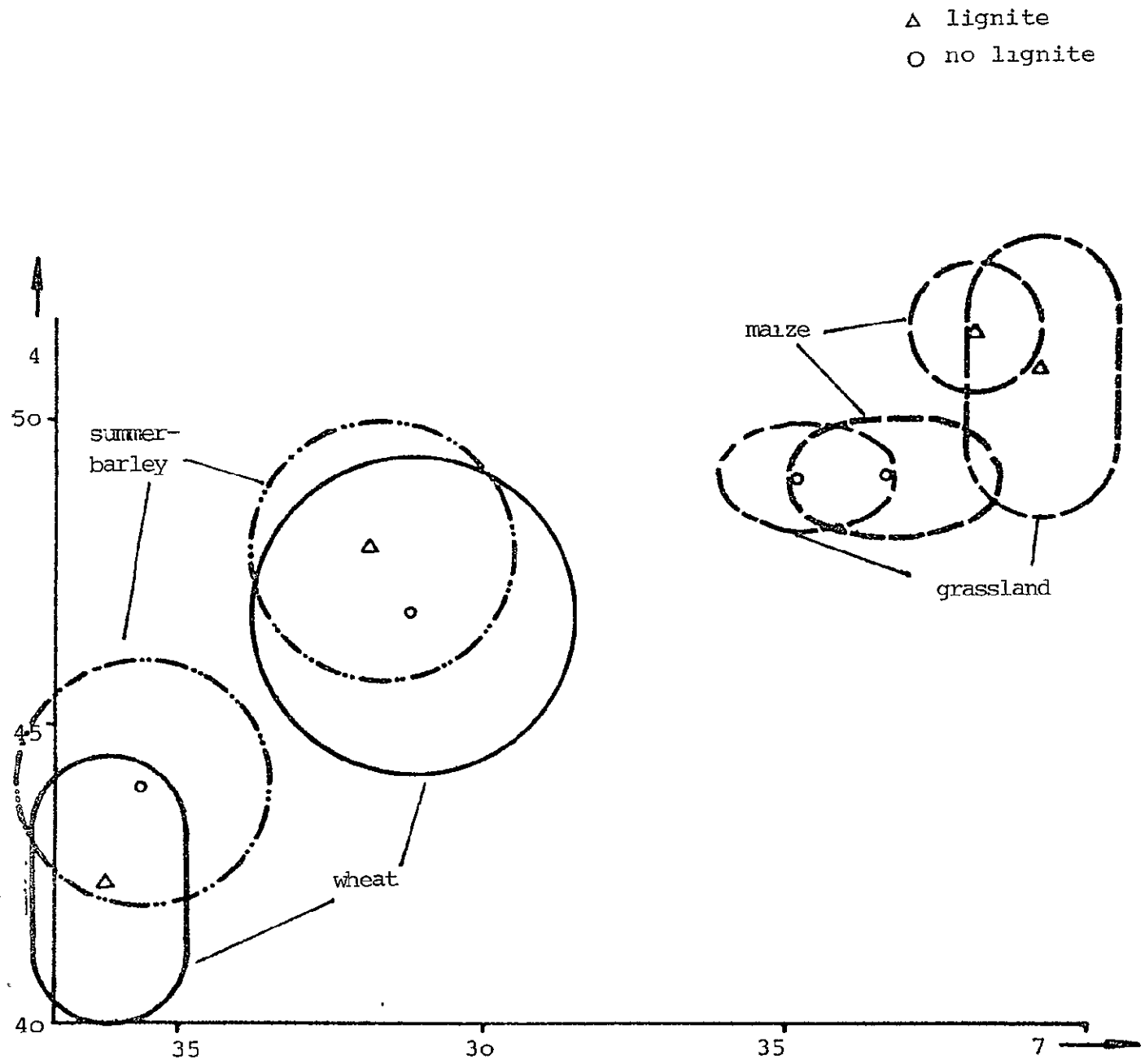

Fig. 3o: Two-dimensional display of intensity measurements band 4 and 7.

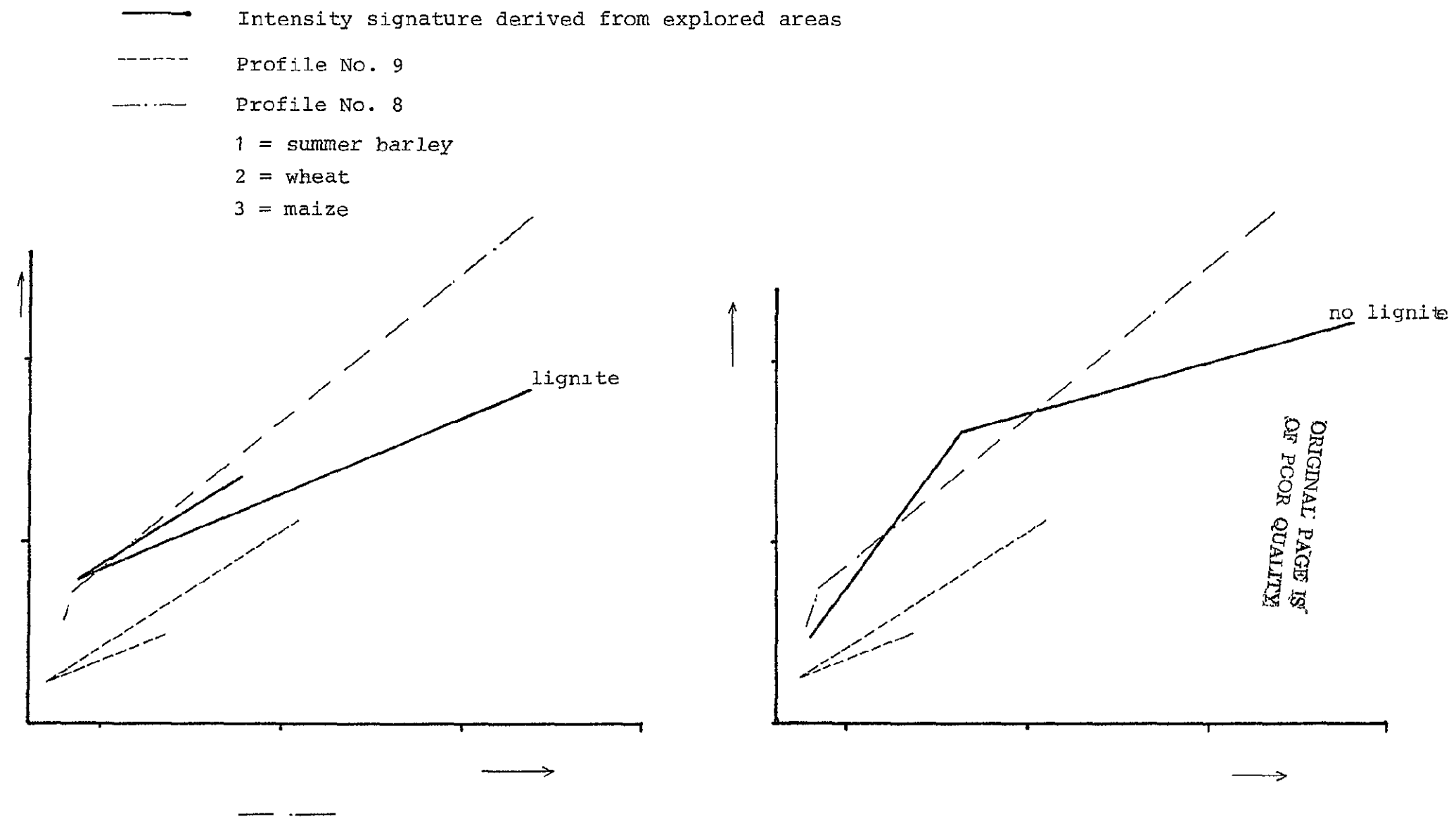

Fig. 31: Note the similarity of Profile No. 9 with measurements above lignite.

In a next step the measurements derived from profiles over unexplored areas were transformed into the same "signature" space". The comparative representation of fig. 3o shows that the summer-barley-, wheat- and maize-measurements taken over profile No. 9 indicate a trend similar to those measurements above lignite horizons.
The corresponding data representing profile No. 8, however, expresses a trend which indicates the absence of lignite.

The results obtained by above empirical approach only describe spectral phenomena. The matter of fact that the near IR measurements did not show any correlations with lignite occurrence leads to the conclusion that a possible impact of trace gases on vegetation is very unlikely.

4. Enhancement of spectral anomalies by image processing

In order to obtain more indications with respect to the obtained results, various image enhancement techniques were tested on the basis of M^2S and Landsat data.
Besides ratio transformations of selected bands, analog carried out linear combinations and PC transformations of all bands were produced. Best results could be obtained by support of the PC transformations, in terms of interpreting the first PC transform or evaluating enhanced low order transformations. The results of two selected areas are demonstrated below. Area I (fig. 26) is located north of Schwandorf (fig. 24) and covers Profile No. 1 and 2.

For a further interpretation a PC transformation was carried out on the basis of all bands available. The corresponding covariance matrix was obtained from samples representing various vegetation types.
In order to enhance the low order transformations, a 3 x 3 convolusion and subsequent histogram stretch was carried out. Out of the available transforms No. 6 and 8 were selected. No. 8 (fig. 32) exhibits a grey tone distribution which ca be related to somewhat increased soil moisture along the river NAAB. The circular light area detectable on the PC transformation No. 6 is very distinct - nevertheless it could not be related to an a priori recorded earth scientific phenomenon (fig. 33).

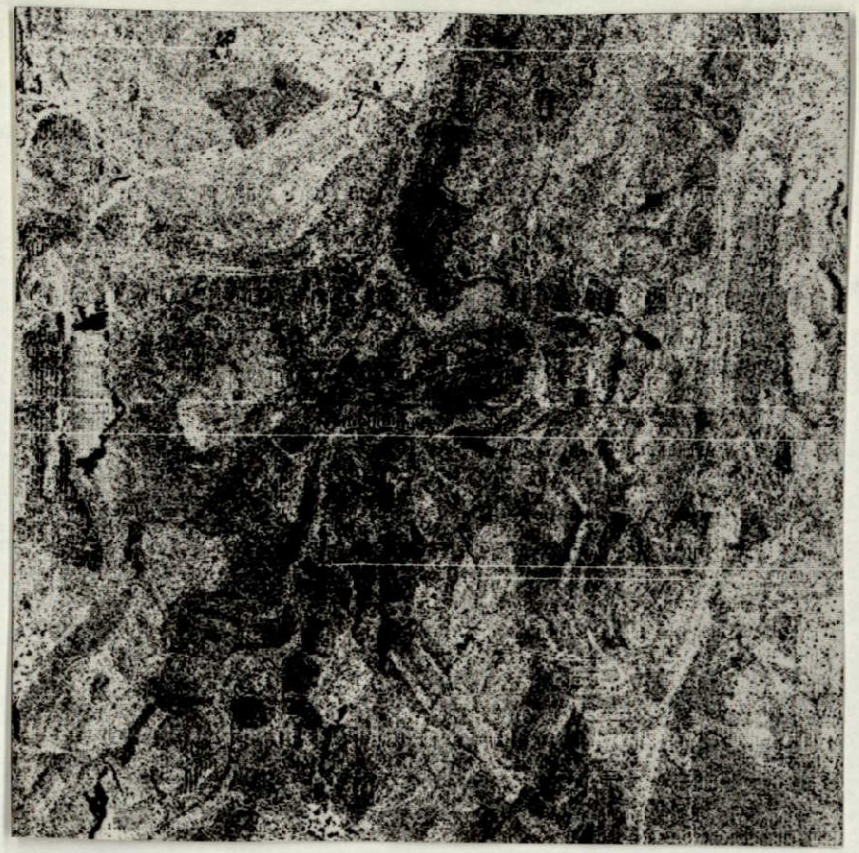

Fig. 32: 8th principal component

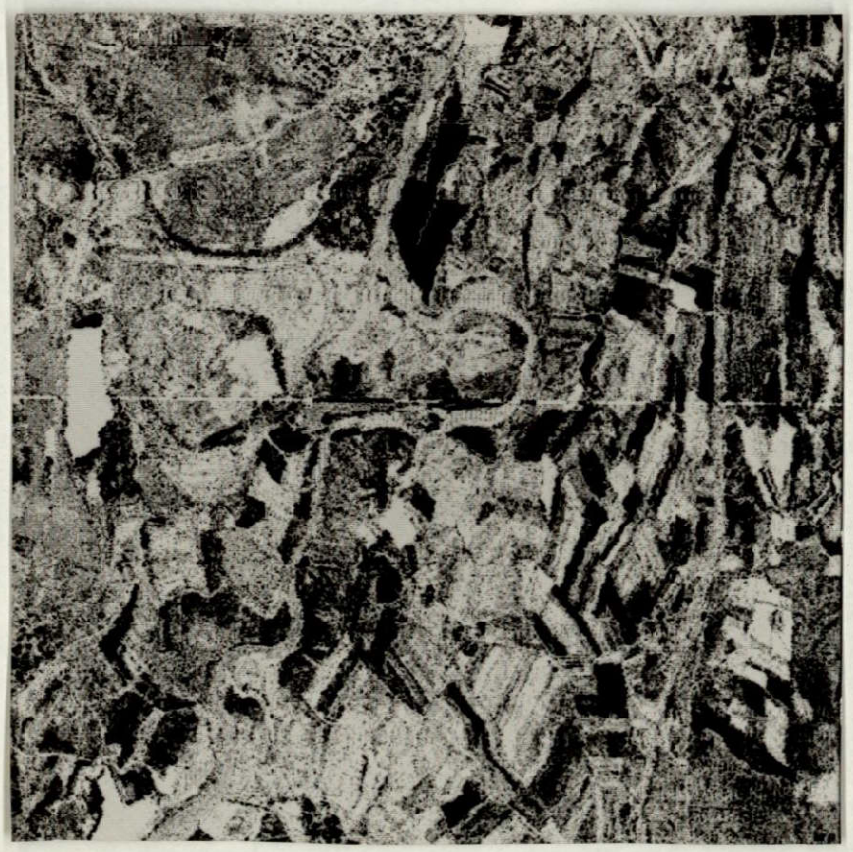

Fig. 33: 6th principal component

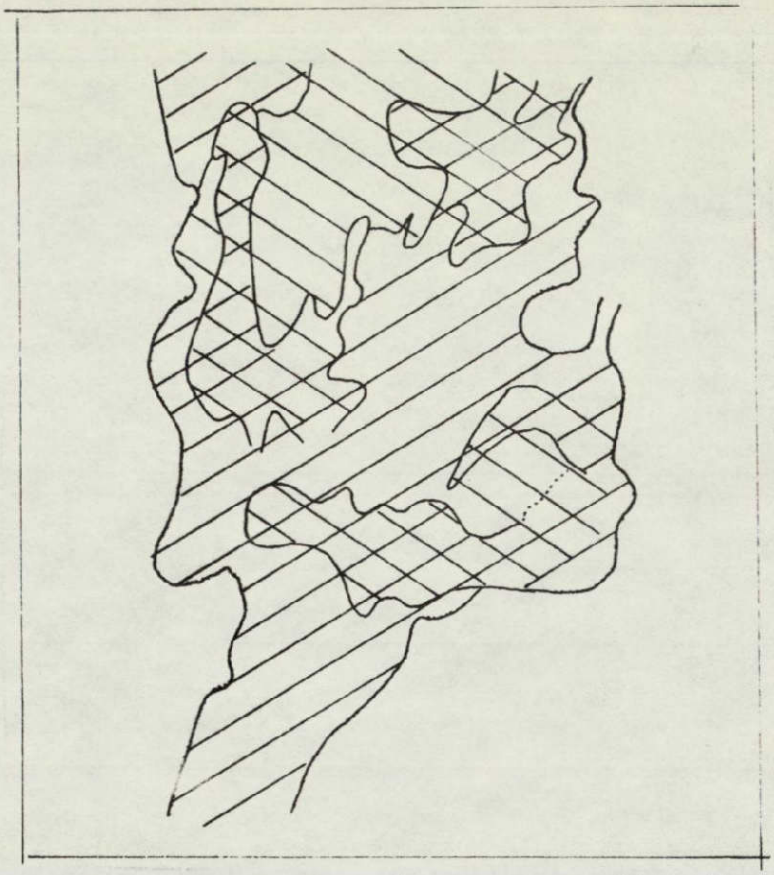

Fig. 34: Schematic overlay of grey tone distribution derived from PC-axis No. 6 and 8.

Fig. 35: Overlay of extracted areas.

Fig. 34 represents a schematic overlay of both features. Areas which indicate the overlapping of the two grey tone phenomena represent a surprising correlation with explored and mapped lignite horizons (compare fig. 35 and fig. 24).

The second area which has been digitally processed includes profile No. 8 and 9 (fig. 24).
This time it is the 1st PC-transform which reveals an unambignously detectable grey-tone anomaly (fig. 36).
This anomaly can be related to the occurrence of lignite due to the fact that it covers exactly the already discussed profile No. 9.
In addition to that, the anomaly can be interpreted as a prolongation of a mapped lignite horizon in the north (fig. 24).

Fig. 36: 1st PC transform exhibiting a distinct grey tone anomaly.

Further processing of Landsat data (fig. 37) did not bring comparable results. This however does not lead to any conclusions because of the seasonal difference between the aircraft scanner flight and the Landsat overpass. In addition it has to be mentioned that the scanner flight was carried out after an unusual dry period in 1976.

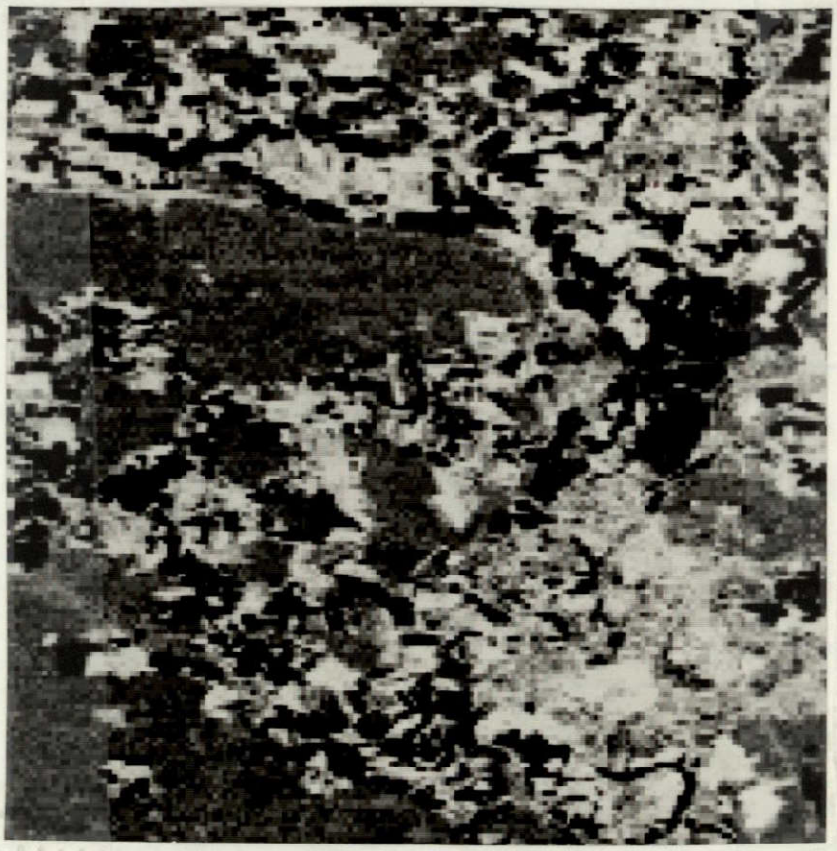

Fig. 37: Landsat, 1st principal component

E. Application of Landsat to Support Thematic Mapping in Geology

1. Introduction

During the last two years the experience was made, that the utilization of Landsat data for activities in the field of geology and thus exploration purposes is one of the applications which have proved to be of great practical potential.

In the beginning Landsat images acquired over arid and semi-arid areas have been primarily inspected and interpreted with an eye on linear features and textural information detectable on small scale synoptic data. The mapping of lineaments on the basis of aerial and satellite images can be regarded as an important approach to photogeological investigations, as it is demonstrated in the previous chapters. Lineaments and textural pattern often reveal tectonical phenomena on a small scale and thus contribute to a better understanding of the geological frame.

The application of conventional photogeological interpretation techniques with the analysis of grey- and color-tone variations for the determination and discrimination of litho-logical phenomena has not been very successful.

Based on physiological limitation, the human interpreter is not able to distinguish subtle grey and color-tone variations or even to recognize tonal phenomena in a quantitative way. Also grey tone variations in images as an expression of the spectral surface characteristics are not very indicative if the available spectral bands are interpreted individually. Even the interpretation of color representations composed by the MSS bands 4, 5 and 7 does not lead to satisfactory results. With respect to Landsat images this is mainly due to the similar reflection characteristics of various rock types within the wavelength regions covered by this MSS scanner system.

2. Requirements Towards Data Processing for Geology.

In order to fully utilize the spectral information available in Landsat images, data processing techniques have to be applied. For landuse purposes thematic maps have been produced by fully automated image processing. For geological purposes, however, the application of digital processing can not be fully automated. Experience in using spaceborne images for geological applications has shown that the capabilities of the interpreter in deriving significant information is indispensible. Therefore, from a geological point of view certain requirements concerning the data base, and the kind of preprocessing methods applied have to be established:

a) Processing of multispectral and multitemporal information in order to enhance the spectral separability inherent in the reflection properties of the surface;

b) Preservation of textural information exhibited in the original data;

c) Utilization of the synoptic properties provided by spaceborne images. Ths requires technological capabilities permitting the evaluation of full Landsat frames;

d) Production of processing results in form of orthophotos like images af a scale of 1:500.000 and 1:250.000. This requires high precision display capabilities.

Due to the manifold requirements we have constantly increased our image processing software and have tested and still are testing various methodological approaches to provide the user with data products exhibiting an optimum information basis.

In the following chapter some examples of data processing are given. With respect to above mentioned requirements the examples do not take into consideration the analysis of multitemporal data, because software development for geometric

corrections could not yet be finished. For demonstration purposes examples, taken from scenes covering a part of Saudi Arabia and Iran were selected. The corresponding frames (EROS -bulk products) are exhibited by fig. 38 and fig. 39.

The selected data were processed and displayed by applying the various methods available through the ISI system 47o and the extensive software package (see part II).
With respect to the user requirements and an optimized use of our processing unit, the various processing methods are applied in terms of problem oriented processing (POP) and post processing (PTP).

Problem oriented processing involves all the procedures which may enhance the interpretability of data by digitally combining multispectral information in one or the other way. By this it is understood to perform f.e. logical operations taking into account intensity values of pixels derived from the multispectral data set, and any multispectral feature transformations such as ratio processing principal components or other linear and non linear transformations.
POP requires the presence of the earth scientist during the processing phase in order to obtain optimum enhancements for his task. The procedure of optimizing this process is explained in part II.

Post processing includes more or less routine operations to take full advantage of POP-processed images and to provide the user with an acceptable data base for subsequent interpretation purposes. Under this aspect post processing means

- supression of noise
- further enhancement of tonal variations
- enhancement of linear features
- generation of color composits
- geometric correction.

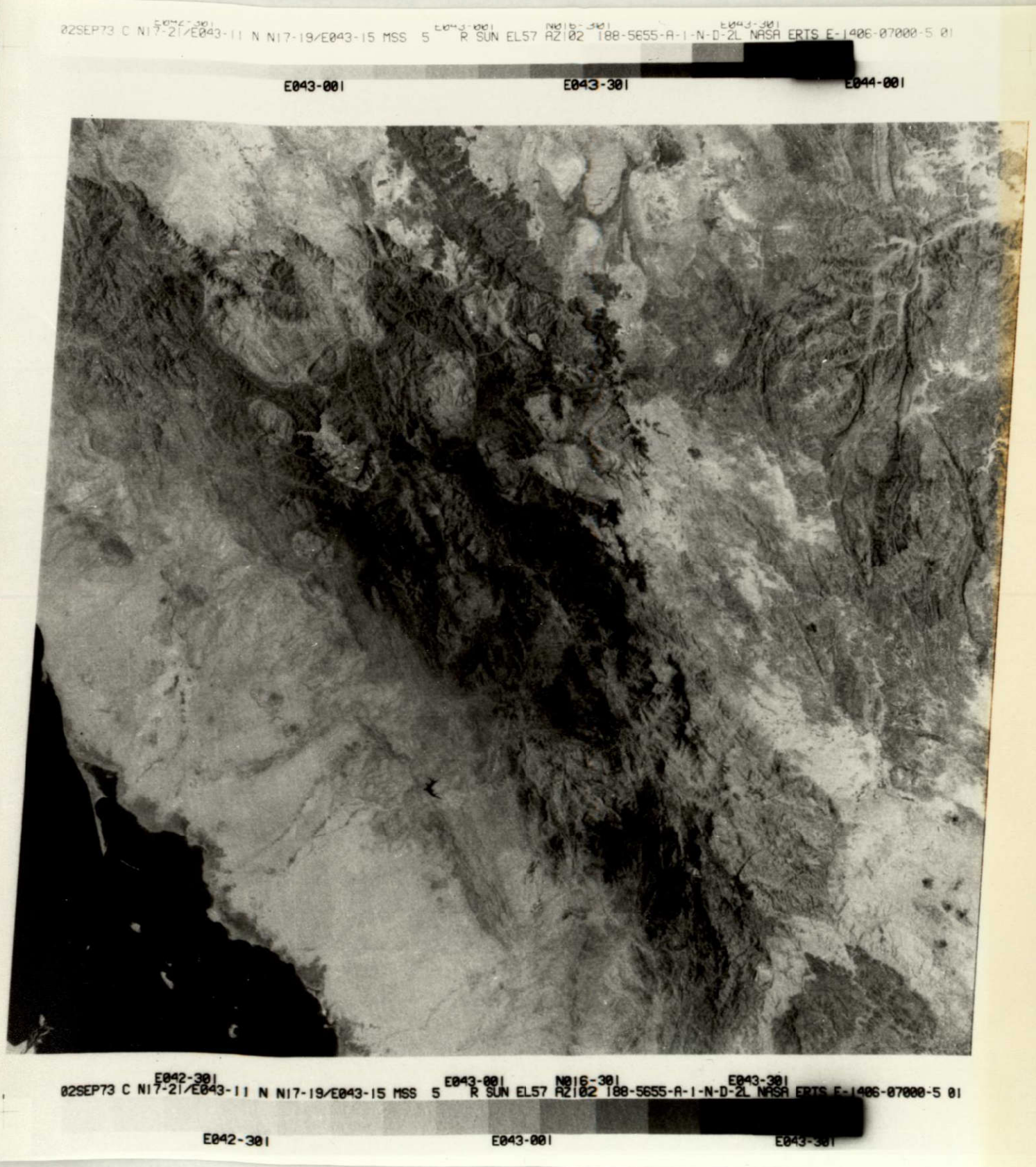

Fig. 38: Landsat MSS 5 Saudi Arabia EROS buld products

Fig. 39: Landsat MSS 5 Iran EROS bulk products

On the basis of above Landsat scenes our capabilities and work in applying POP and PTP-techniques are demonstrated.

3. Ratio Processing (POP)

Ratio processing is understood to result from dividing intensity values of corresponding picture elements in adjacent spectral bands. New ratio values are presented in the form of a new image. There are two properties of band ratioing which makes this simple technique extremely useful especially for geological applications:

a) Suppression of unwanted atmospheric and illumination effects:
   If we assume that the physical characteristics of electromagnetic radiation are very similar in adjacent narrow spectral bands, the impact of atmosphere and illumination variations should also be very similar. Thus by band-ratioing it is possible to decrease the above effects e.g. to eliminate shadows as a disturbing feature which depend on the illumination angle and the surface relief.

b) Enhancement of spectral properties of lithological units:
   It has been reported, that ratio intensities of adjacent wavelength regions are very sensitive to variations in the mineralocial composition of rock types. By this it is an excellent tool to discriminate between various rock types or even to enhance lithological boundaries not visible on the basis of the original spectral bands.

The examples of fig. 4o which represent an entire Landsat frame may illustrate above mentioned properties. Fig. 4o, a,b,c exhibits MSS bands 4, 5 and 6. The ratios defined on a subset of the Landsat frame are displayed by fig. 4o d,e. Fig. 4o d which corresponds to the ratio 4/5 clearly demonstrates the suppression of intense shadow effects exhibited by the strong relief. Furthermore the appearance of various

geological phenomena become visible. Above ratio image in combination with the original spectral bands provides for some areas information not recorded on geological maps available.
A further ratio image (fig. 4o e) between MSS bands 5/6 shows rather vegetated areas in dark and black than an increased differenciation of geological features.

A typical case for post processing (PTP) is f.e. the geometrical rectification of POP-results or their representation in form of color composites. Fig. 41 demonstrates a geometrical corrected sub-area and fig. 42 a,b the comparison between a normal false color and a ratio color display. The examples of fig. 42 a,b are photographed from a TV screen and are characterized by a decreased quality.

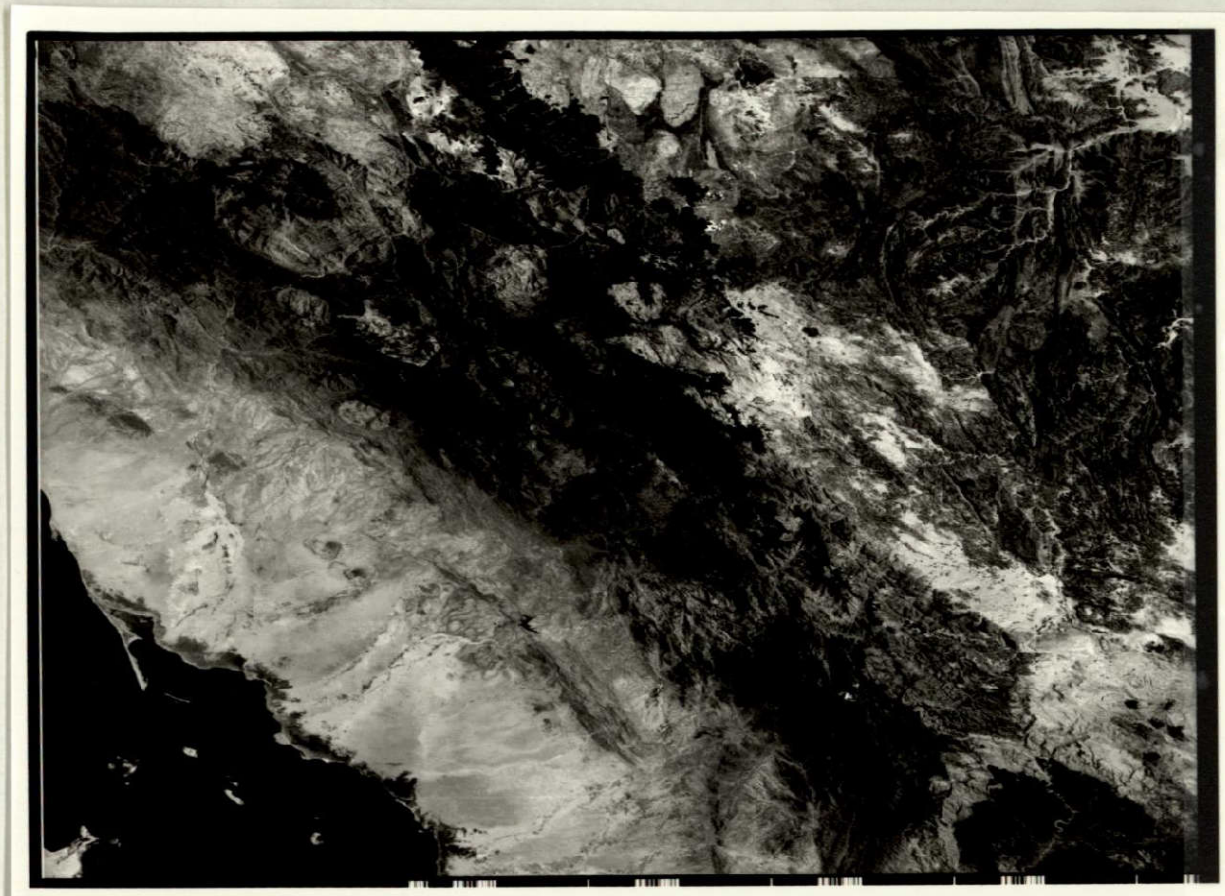

Fig. 4o a: Landsat MSS band 4

Fig. 4o b: Landsat MSS band 5

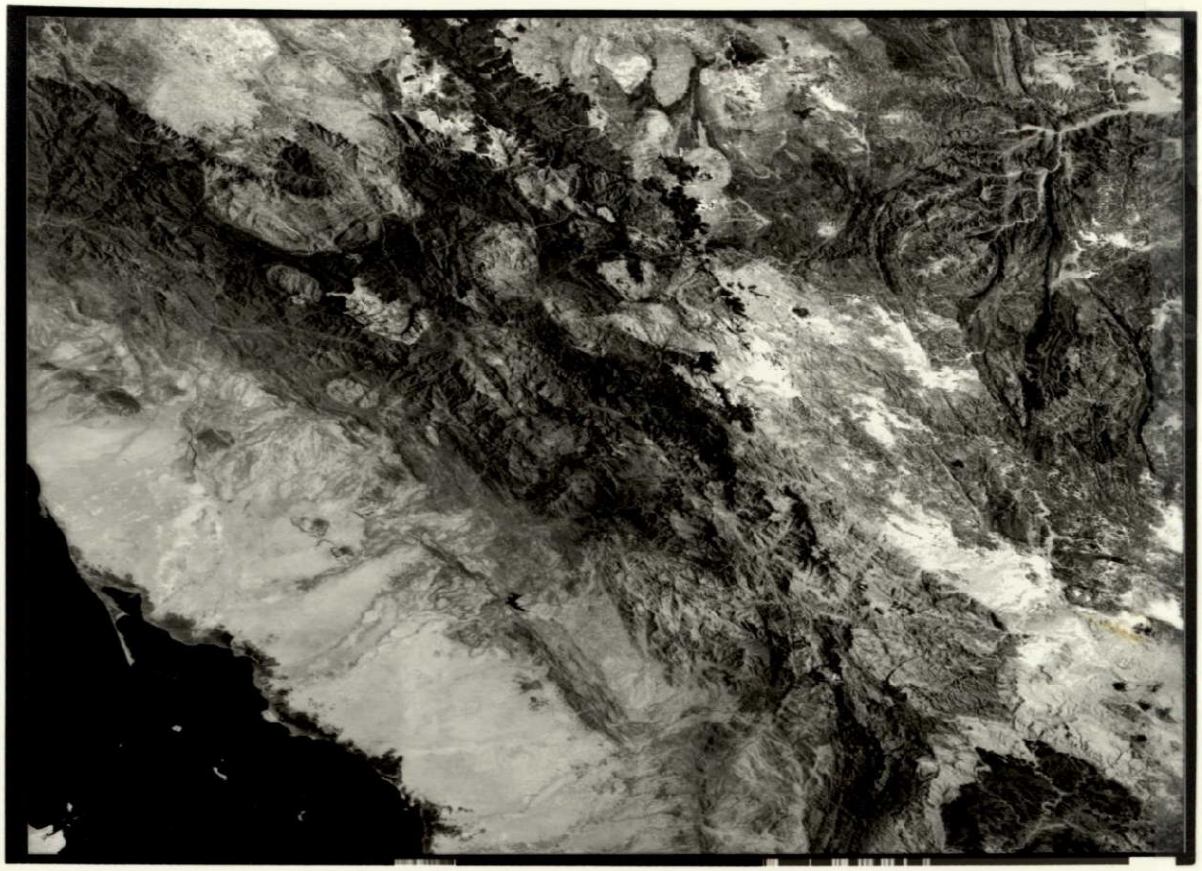

Fig. 4o c: Landsat MSS band 6

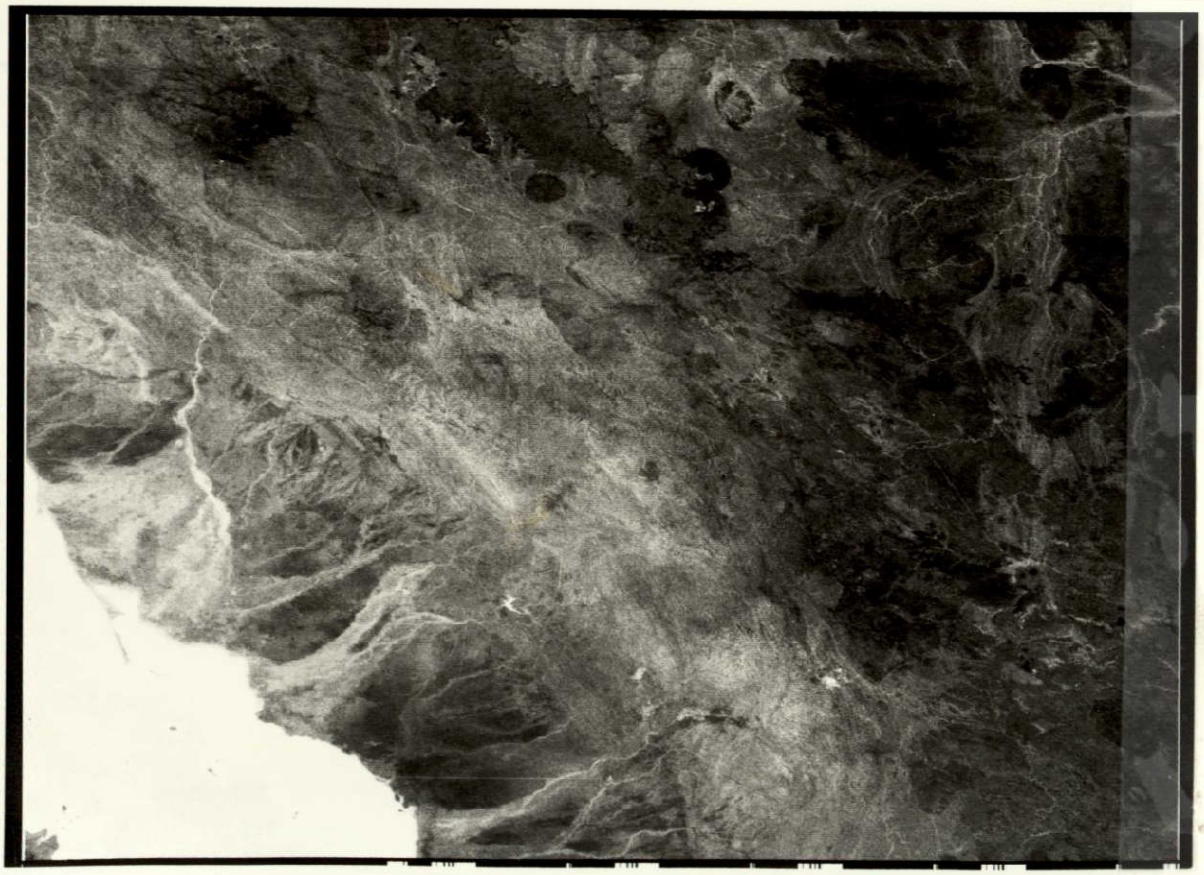

Fig. 4o d: Ratio MSS 4/ MSS 5

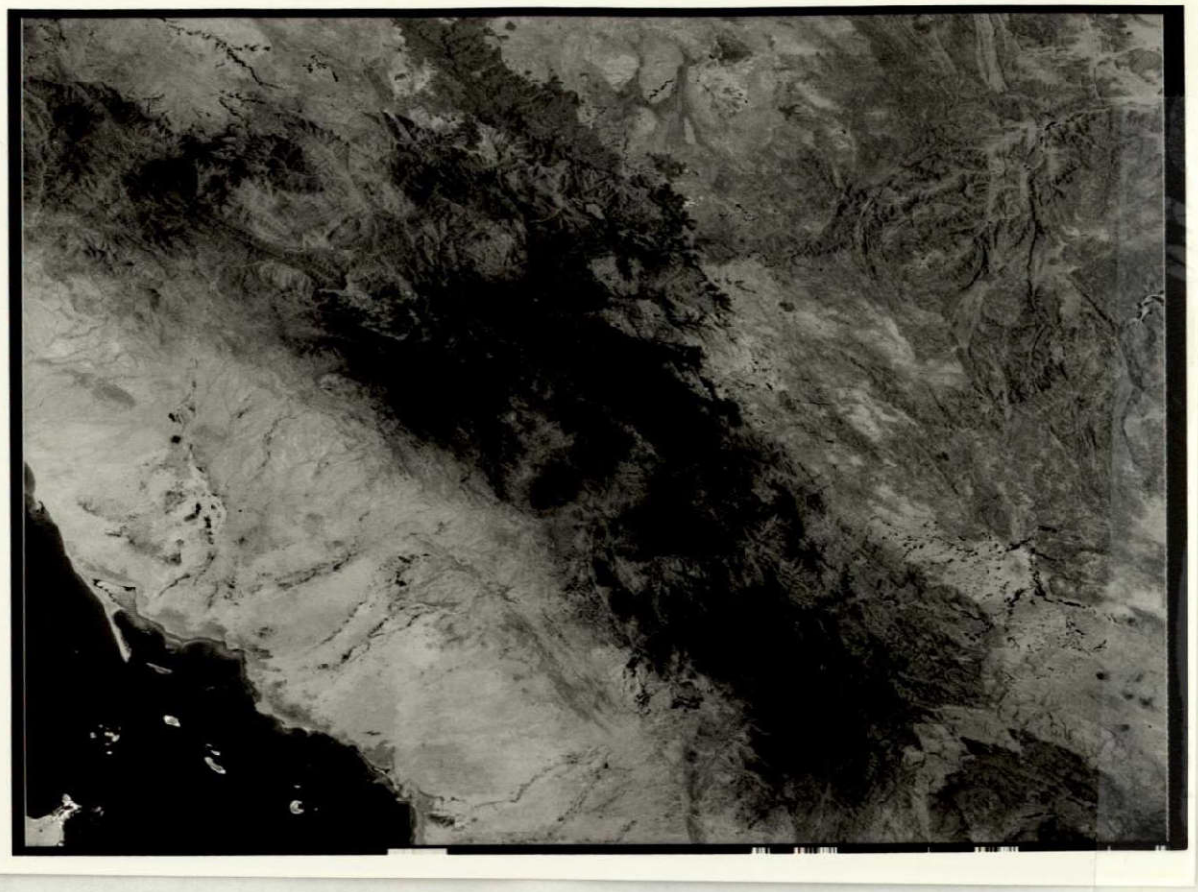

Fig. 4o e: Ratio MSS 5/MSS 6

Fig. 41: MSS 4 geometrically rectified.

Fig. 42 a: False color representation

Fig. 42 b: Ratio color representation.

4. Principal-Component-Transformation (POP)

The principal-component (PC) -transformation is a well known technique and of special significance for data reduction purposes. The PC-transformation represents basically a linear combination of the original bands by calculating the weighting factors for the transformed images via the covariance matrix. So f.e. out of 4 spectral bands 4 new, transformed and now not correlated images of decreasing information content can be calculated. Experience with multispectral data has shown, that by the first component normally more than 5o percent of the information present in the original bands can be expressed. The remaining percentage is distributed over the lower order transformations also in a decreasing way. By this the 3rd and 4th components only contribute with a few percent of information.

The transformed images of the test area clearly demonstrate how most of the grey-tone variance (information) is contained in the first component (fig. 43 a).

Of special interest for the photogeological interpretation are the transformations of lower information content after problem oriented processing.
The 2nd, 3rd and 4th axis of fig. 43 a,b,c,d have been post processed by carrying out a 3 x 3 convolution in combination of a histogram egalisation. Above low order transformations are characterized by some tonal contrast not detectable on the original data.
Of special interest is the enhancement of a rock border within the granite. Fig. 44 a,b exhibits two color renditions based on enhanced lower order transformation.

Fig. 43: Principal components of a 512 x 512 subarea taken from Landsat scene (fig. 39).

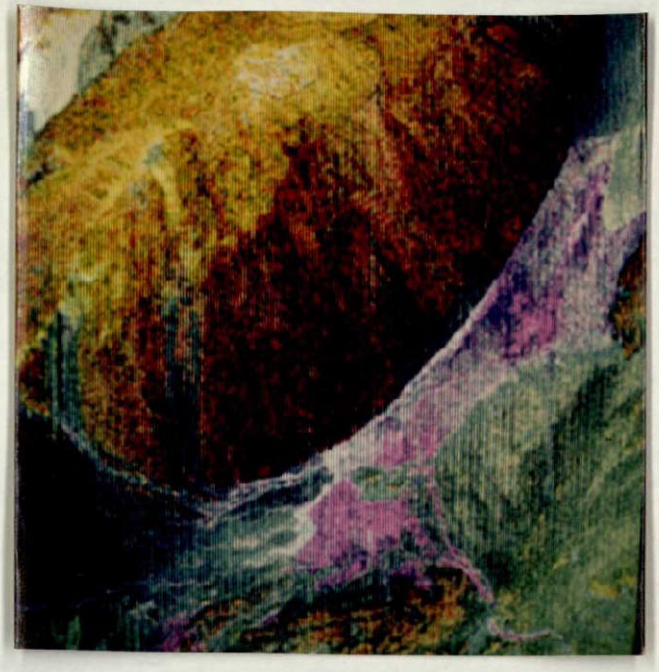

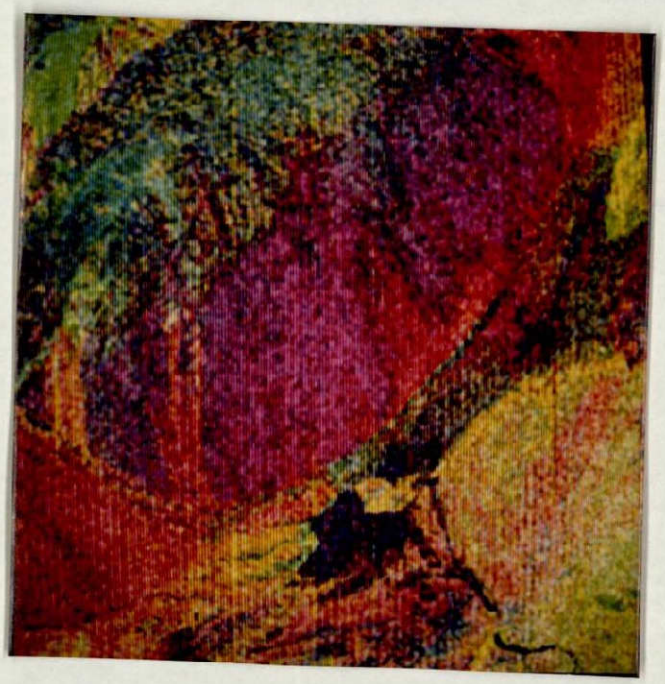

Fig. 44: Color renditions composed of enhanced low order transformations.

5. Image Filtering (PTP)

Very often it can be observed that especially the problem oriented processed data (ratios, PC-transforms are characterized by also enhanced noise pattern.
With respect to Scanner data striping noise is very critical.

This noise manifests itself in the form of stripes in the scanning direction, and can be under some circumstances very disturbing for an interpretation or an automatic processing of the image. Since this is a totally technology-dependent problem, it can be foreseen that an improvement in the sensor technology in the next Landsat-series satellites will tend to elliminate this problem. However, the Landsat-1 satellite has been sending image data to earth for three years and the Landsat-2 will possibly do well a long time also.

That represents an extraordinarily amount of data which will have to be processed for years to come, for its own sake and also in conjunction with images from future systems.

Therefore, a method for the ellimination of this problem in already existing imagery is of very great importance. Some restrictions should be imposed on such a method: First, it must be fast. Second, it must be a standard algorithm applicable to all data without the need to be adjusted to each new picture and third, and perhaps most important, it must not destroy information contained in the picture.

In the following chapter very recently started work in above field of post processing is discussed.

Problem Description and Already Existent Methods

The nature of the problem source can be easily understood considering the structure of the MSS. In each spectral channel six lines are scanned through six different detectors. Obviously, if each one of the detectors had exactly the same characteristics the problem wouldn't exist, but they have different gain and offset.
This produces the undesired effect that even an homogeneous object will not produce an homogeneous picture.
In most of the pictures, this noise cannot be appreciated at first glance. As example, four spectral channels of a sub-scene of a Landsat frame are shown in fig. 45. In fact, only in picture regions where the signal to noise (S/N) ratio is very low, can it be observed easily.

In some cases, however, the effect of processing is a reduction of the S/N ratio, as in the case of channel ratios and differences, and for the principal components transformation. This last processing is shown in fig.46 . As can be seen, the third and fourth principal components have a lower S/N ratio and therefore the striping noise is easily visible.

Various methods have been proposed for correcting this effect. The most obvious would be to measure the gain an offset of each different detector (as is actually done in most scanners through a calibration lamp) and afterwards to modify the data according to the obtained coefficients.

This is perhaps the most reasonable method, and it has the single disadvantage that the coefficients can vary from time to time.

Another method uses local statistics in the picture to elliminate the variation produced in each line due to the detectors. We will concentrate here on a method based on the coherency of the noise, that is, on its frequency characteristics.

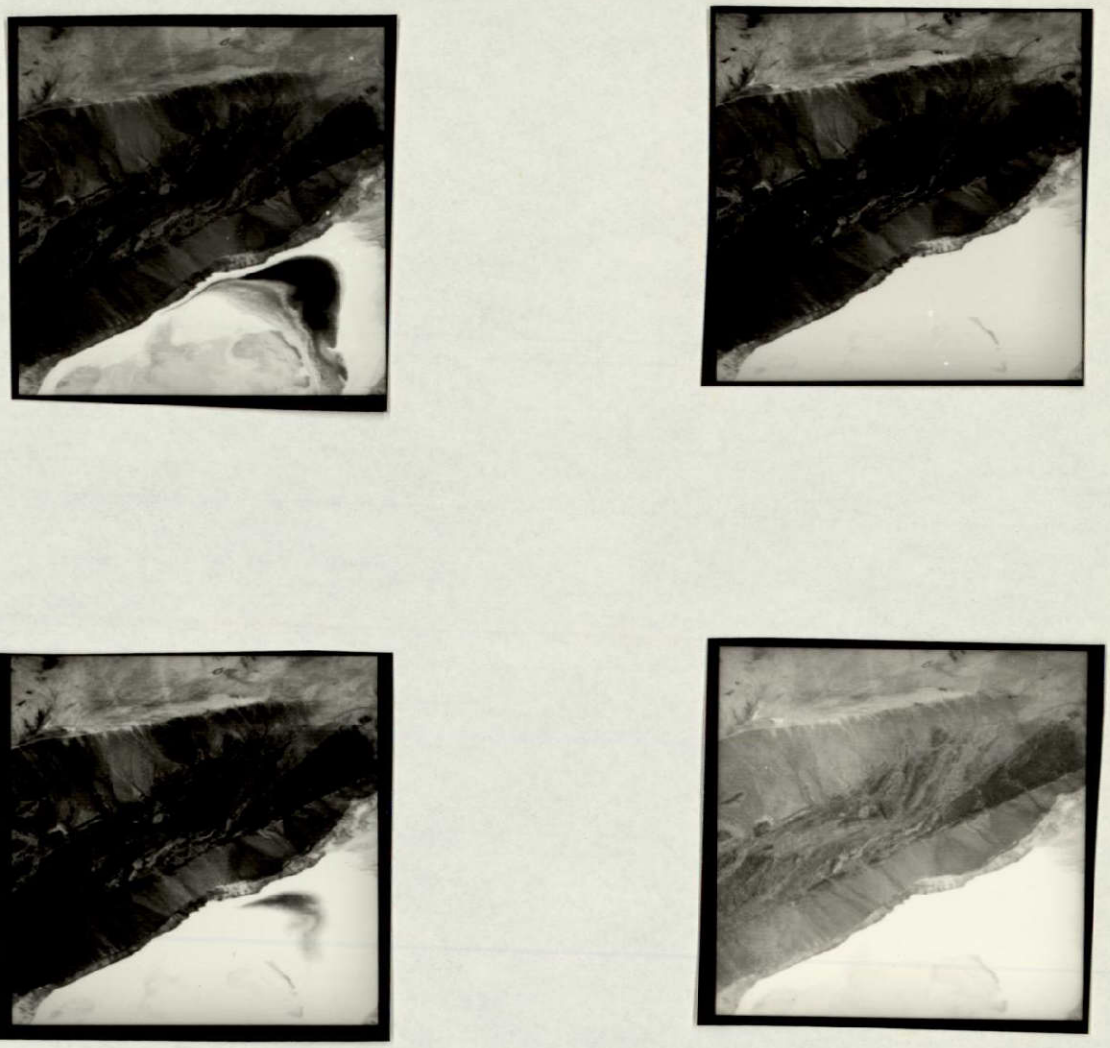

Fig. 45: Display of the 4 Landsat MSS bands striping effect detectable only in areas with low S/N ratio.

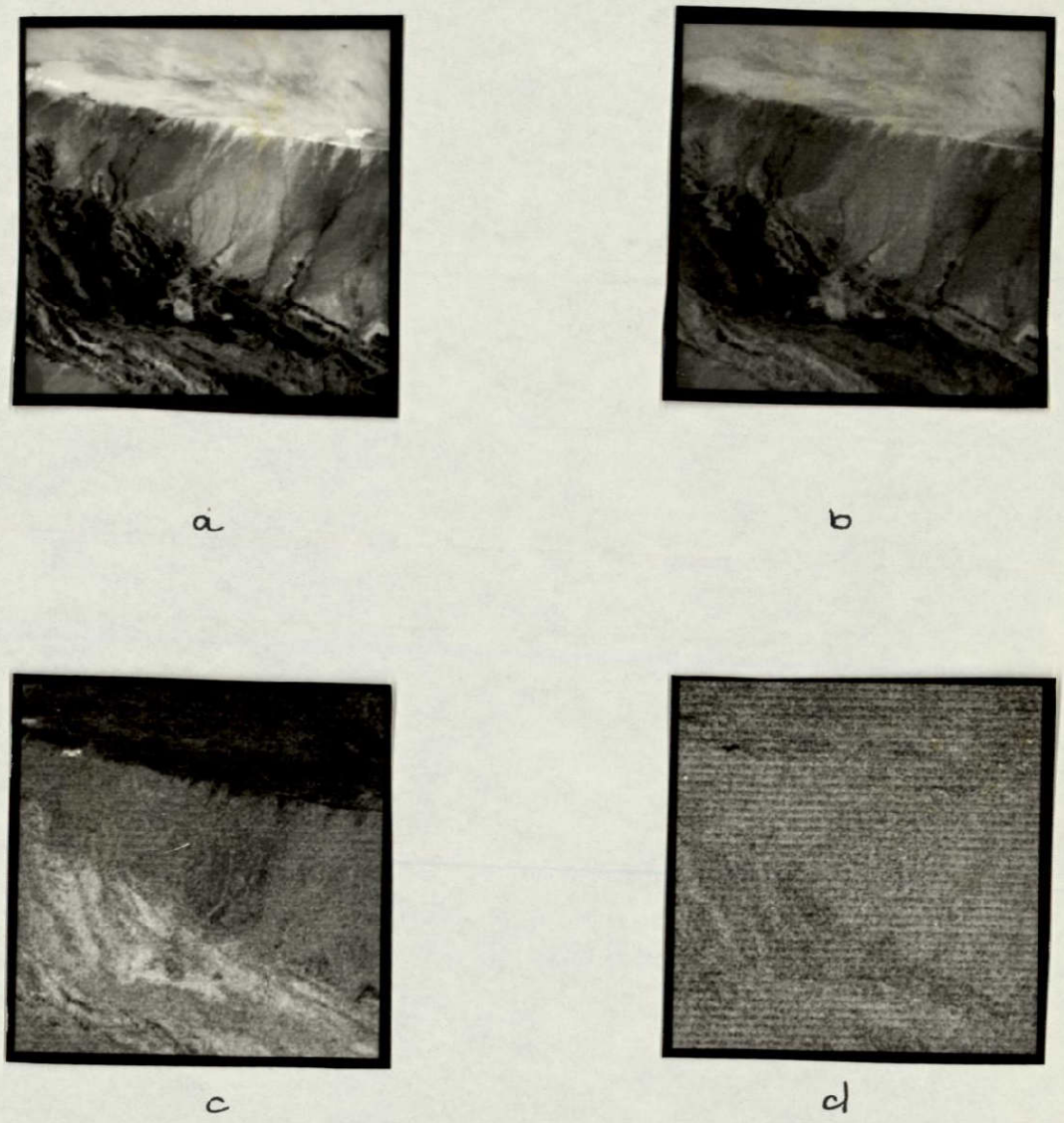

Fig. 46: Principal component transformation of Landsat MSS bands, fig. 45 (256 x 256 pixels).

Spectrum Analysis

Since it is known that the noise is one-dimensional, an also one-dimensional Fourier transform will be enough in order to evaluat its frequency characteristics. For this transformations we choose the image of fig.46 d, and applied the fast Fourier transform along the columns. The result is shown in fig. 47 .

The noise can be seen to consist of two components of two very well defined frequencies, namely

$$f_1 = \frac{21}{128} \frac{1}{\Delta x} \qquad (a)$$

$$f_2 = \frac{42}{128} \frac{1}{\Delta x} = 2 f_1$$

$\frac{1}{\Delta x}$ = sample frequency, in this case could be assumed to be $\frac{1}{79}$ m

Obviously, after the Nyquist theorem, we can only have frequencies such that $f \leq \frac{1}{2\Delta x}$ and with this rule the frequencies mentioned above can be easily deduced from fig. 47.

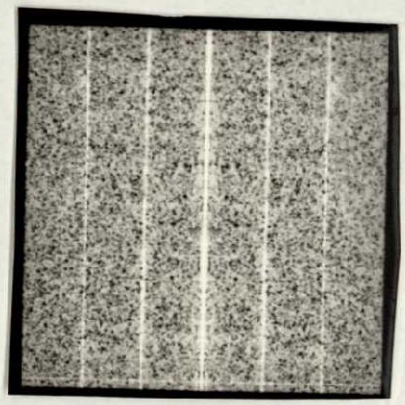

Fig. 47: One-dimensional fourier transformation of fig. 46 d.

Filtering in the Frequency Domain

From the known relation for two signals and their respective Fourier transforms:

$$S * f = S \cdot F \qquad (b)$$

Where * devotes convolution and S and F are the Fourier transforms of s and f, it can be easily seen that the multiplication of the signal transform S with an adequate filter and doing afterwards the inverse Fourier transform would eliminate the noise correponding to the filter transform F. In our case it would mean to apply a filter which eliminates the frequencies f_1 and f_2 (a filter transform with zeroes at this frequencies) and which presses all other frequencies (ones). That would be an idealized multiband bandpass filter.

This method was applied to the last two images in fig.46 and the results can be observed in fig.48 .

It should be pointed out that this is a relatively very time consuming algorithm, because of the double application of the Fourier transform (direct and inverse) and because the picture must be transformed in column direction and is normally linewise stored in mass storage, a transposing operation being therefore necessary prior to the filtering operation.

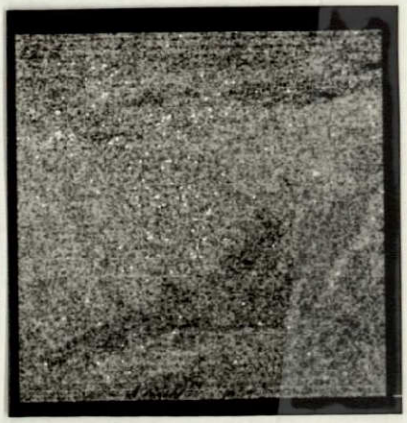

Fig. 48 a/b: 3rd and 4th principal component after filtering in the frequency domain.

Design of a One-Dimensional Finite Impulse Response Filter

A very well known class of filters, the finite impulse response (FIR) filters, is specially attractive for implementation, because very efficient algorithms already exist for the design. A general expression for such a filter can be written as follows

$$y(k) = \sum_{i=0}^{N-1} h(i)\, x(k-i) \qquad (c)$$

where N is the length of the filter, h (i), i = o ... N-1 its coefficients (A) and x (k) is the input sequence or signal (in our case a picture line or column) y (k) is the output or filtered sequence.

That is the expression for a discrete convolution, and obviously, if we succeed in designing a filter which approximates the ideal frequency response of the desired bandpass filter, with only few coefficients, a considerable increase with respect to the implementation with the Fourier transform could be attained.

A first problem must be in our case mentioned. We cannot approximate a band pass filter with a finite number of coefficients, so that

1) the relation (b) does not apply for the method applied in the foregoing section and therefore the results obtained in fig. 48 are not totally correct;

2) the FIR filter we will obtain only approximates the desired frequency response. Moreover, since we want to use as few coefficients as possible, this approximation cannot be very good;

3) if we increase the number of coefficients, a direct implementation through convolution will be impossible, so that we will be obliged to use the implementation in the frequency domain.

The expression for a bandstop filter is:

$$H(u) = \begin{cases} \emptyset, W_1 < u < W_2 \\ 1, u \leq W_1,\ u \geq W_2 \end{cases} \qquad 0 \leq u \leq \pi$$

The inverse Fourier transform of this expression would be:

$$h(n) = \frac{1}{\pi} \left(\frac{\sin W_1 n}{n} - \frac{\sin W_2 n}{n} \right)$$

which has coefficients extending to $+\infty$, and therefore such filters cannot be exactly approximated by the filters of (c).

In our case we limited ourselves to the design of such a filter following an algorithm proposed by Mc CLELLAN and reducing the number of coefficients to 15.

The resulting filter has linear phase and is antisymmetric. Because of this antisymmetry we can save almost half the multiplications because the expression (c) can be written.

$$y(k) = \sum_{i=0}^{\frac{N-1}{2}-1} h(i)\ X(k-i) - x(k-N+i+1) + h\left(\frac{N-1}{2}\right) \cdot X\left(k-\frac{N-1}{2}\right) \qquad (d)$$

The coefficients and design parameters of this filter is shown in fig. 5o

As already mentioned, the filter is only an approximation to the ideal case, first because it can only approximate the given frequency response, and second because we cannot specify frequency bands as narrow as desired. Obviously, the filter will cause a degradation because it will filter frequencies we don't actually wish to filter and moreover because of the ripple introduced by the approximation.

The result of filtering are shown in fig.51, for all four spectral channels, and even if we have filtered the striping noise, the degradation caused by the filter itself is evident.

****

FINITE IMPULSE RESPONSE (FIR)
LINEAR PHASE DIGITALFILTER DESIGN
REMEZ EXCHANGE ALGORITHM

BANDPASS FILTER

FILTER LENGTH = 15

IMPULSE RESPONSE

```
H(  1) =  -.68341404E-02 = H(  15)
H(  2) =  -.19531188E+00 = H(  14)
H(  3) =   .16992465E-01 = H(  13)
H(  4) =   .69750877E-01 = H(  12)
H(  5) =   .38706068E-03 = H(  11)
H(  6) =   .16015114E+00 = H(  10)
H(  7) =  -.10545385E-01 = H(   9)
H(  8) =   .58824886E+00 = H(   8)
```

	BAND 1	BAND 2	BAND 3	BAND 4
LOWER BAND EDGE	0.000000000	.150000000	.230000000	.315000000
UPPER BAND EDGE	.100000000	.180000000	.270000000	.345000000
DESIRED VALUE	1.000000000	0.000000000	1.000000000	0.000000000
WEIGHTING	1.000000000	10.000000000	1.000000000	10.000000000
DEVIATION	.342570848	.034257085	.342570848	.034257085
DEVIATION IN DB	-9.304991948	-29.304991948	-9.304991948	-29.304991948

	BAND 5	BAND
LOWER BAND EDGE	.390000000	
UPPER BAND EDGE	.500000000	
DESIRED VALUE	1.000000000	
WEIGHTING	1.000000000	
DEVIATION	.342570848	
DEVIATION IN DB	-9.304991948	

EXTREMAL FREQUENCIES

```
  0.0000000     .1500000     .1656250     .1800000     .2700000
   .3150000     .3306250     .3450000     .5000000
```

****

Fig.: 5o

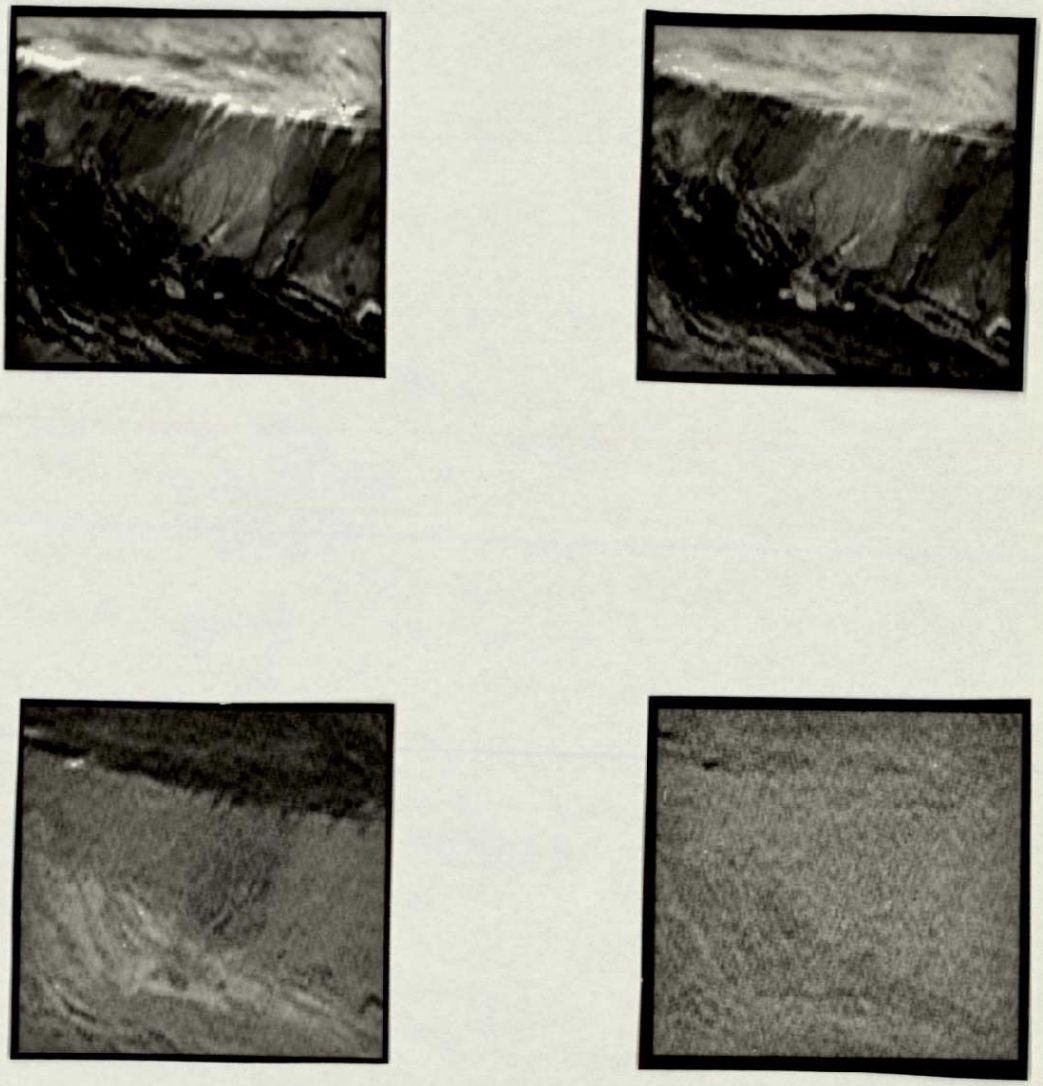

Fig. 51: FIR filter PC components.

Control Number

BLANKET RELEASE FORM

In accordance with Memorandum of Understanding No. ____ between STID and OSSA ____; OART ____; OTDA ____; OMSF ____; the attached document can be Announced ✓; Not Announced ____; and has a distribution limitation as follows:

- ☑ UNLIMITED
- ☐ U.S. GOVERNMENT AGENCIES AND CONTRACTORS ONLY
- ☐ U.S. GOVERNMENT AGENCIES ONLY
- ☐ NASA AND NASA CONTRACTORS ONLY
- ☐ NASA HEADQUARTERS OFFICES AND CENTERS ONLY
- ☐ NASA HEADQUARTERS ONLY

Remarks:

☑ NASA CR 158858 ☐ TMX _____ ACCESSION NO. _____

Analyst F 3/5/79

FF No. 864

Conclusions

Some aspects of the difficulties in the application of an FIR filter for our particular problem are evident.
First, the effect of different band widths on the resulting filter and therefore on the filtered image should be studied.
This must include also the number of coefficients, but it seems to be impossible to approximate a filter with so few coefficients as to allow the implementation as a convolution sum. Therefore, the design with a large number of coefficients and the filtering in the frequency domain should be carried out.
This would obviously not be an operative solution.

The second approach would be to design an infinite impulse response filter (IIR), which can be implemented in a recursive form and can provide sharper edges in the frequency response with fewer coefficients than the FIR.

PART II

TECHNICAL DESCRIPTION OF THE IMAGE PROCESSING SYSTEM ISI 47o AND ITS USE FOR EDUCATIONAL PURPOSES

Technical description of the analog-digital image processing system ISI 47o

1. Software

Introduction

In this section the structure and capabilities ofthe ımage processing system software (originally called SWING) will be descrıbed. If the reader ıs ınterested ın details of the programmıng system FORTH, which served as frame for the implementation of SWING, or if he needs some basıc concepts for understanding the mechanics of SWING, he wıll fınd enough material ın the lıterature referenced in this report (1), (2), (3), (4), (5).
The basıc elements of SWING are:
- the Image Control Block (ICB)
- the Image Stack (IS)
- the Image Processing Loop (IPL).

In the following the structure of thıs elements and the interactions between each other will be described.

The Image Control Block

This is practically a list of variables resident in a core area. Each one of this variables or table entries, identifıed with a specıfic name contains an attribute of the image associated wıth the table.
Several of this areas are reserved at time of SWING loadıng, so that when the user wishes to get access to a defınite physical image he only needs to associate it with any of the already existing tables.

A physıcal image can be a fıle on dısc or one of the existing devıces (TV monıtor, optronics, magtape format, etc.).
The relation between physical ımages and ICBs can be represented graphıcally as in fig.52.
Fıg. 53 represents an ICB and how its entries are referenced.

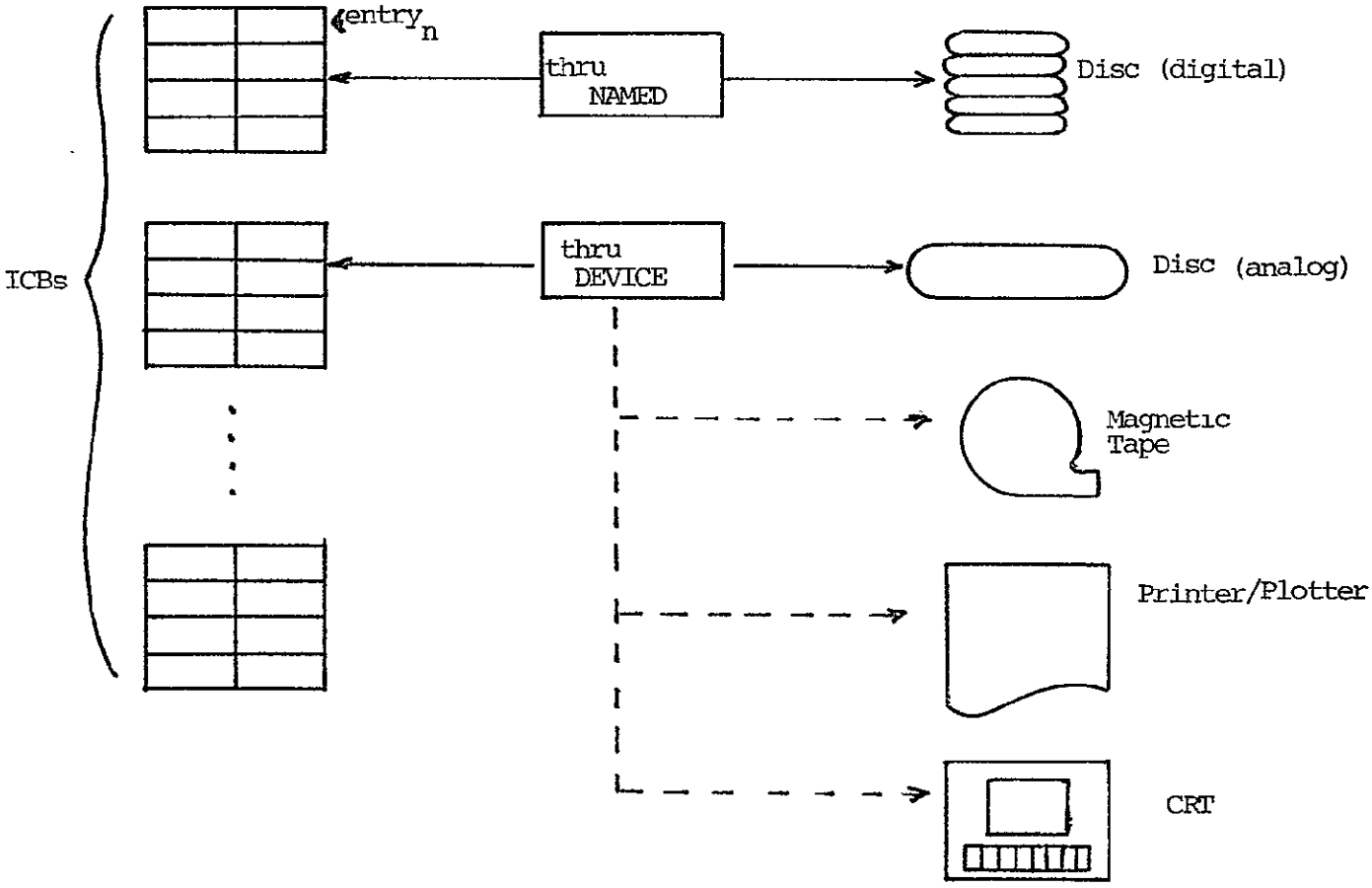

Fig.52: Allocation Image/ICB

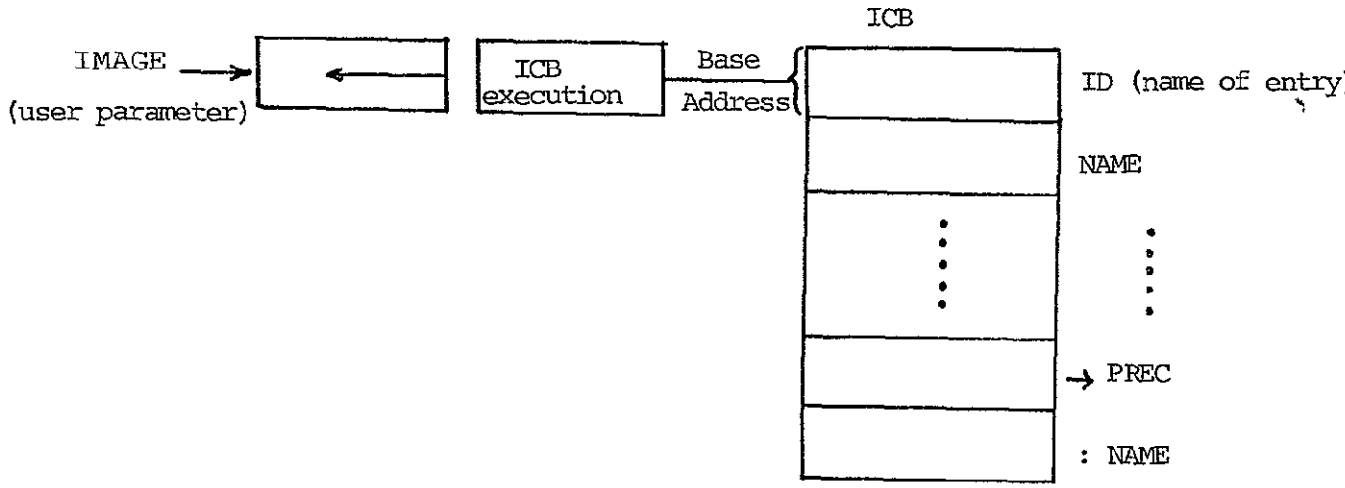

Fig.53 : ICB's entries reference

Some of the entries in the ICB can be changed before starting the processing so as to allow a choice of bands, subimage to be processed, etc. Furthermore, an image file on disc will be created by association of the file with an ICB and setting interactively the parameters which define the image.
Each ICB has a name, and this is the name of a FORTH word which at execution time will put the basis address of the ICB on an entry of the user's control block. To obtain the contents of a specified entry in the primary ICB only the bias of this entry with respect to the basis address need to be known, as shown in fig. 53. The ICB entry will be in the newest referenced IBC.

The Image Stack

It works like a normal first in-last out list, where the basis address of the ICB is stored each time that an ICB is referenced by its name as mentioned above.
In this way several ICBs can be stored and afterwards retrieved for processing. This characteristic allows the concatenation of processing commands.

The Image Processing Loop

A large class of image processing algorithms works on the argument picture in a sequential mode, normally processing the whole picture line by line.
At each picture element the same operation will be applied for the whole picture, depending on the result desired.
Independently the whole input/output management and the supervising of the sequential process don't need to be of concern for the person interested in the processing.
The aim of the IPL is to assume this control of a previously defined process, and the mechanics of the IPL are shown in fig. 53.

The key to the whole is the value of a status indicator, the variable ISTATE, which tells in which stage of the operation the system is.
The PROCESS area of fig.54 is given in more detail in fig. 55. This table is filled by the user with arguments (images and parameters) through the processing commands. It could be assumed to be a program at the highest possible level (the image processing language).
The user enters data and addresses pointing to executable code in the process in the following way

image $_1$ ... image $_n$ parameter$_1$ ... parameter$_m$ command

The command fills the PROCESS as shown, but the contents of it will not be executed.
The command TRANSFER includes the contents of the PROCESS within an IPL and starts it.
The process will be executed beginning with the first ICB, which puts its basis address on the stack, then the second and so forth. The parameter list will be jumped over and the sequence continues entering the operation driver.
The code executed by the operation driver depends also on the status variable ISTATE and its structure is shown in fig. 56. If this variable has the value 3, the code defined by the user will be executed.
The user can easily determine which operation driver he needs for a specified operation and which parameters his program will receive at execution time. Usually they are byte addresses of input and output data and number of pixels. He can retrieve the parameters entered before the TRANSFER from the PROCESS and operate with them and with the picture data.
Normally he only needs to observe some easy rules and can write in FORTH or symbolic assembler the code he wants to be executed.

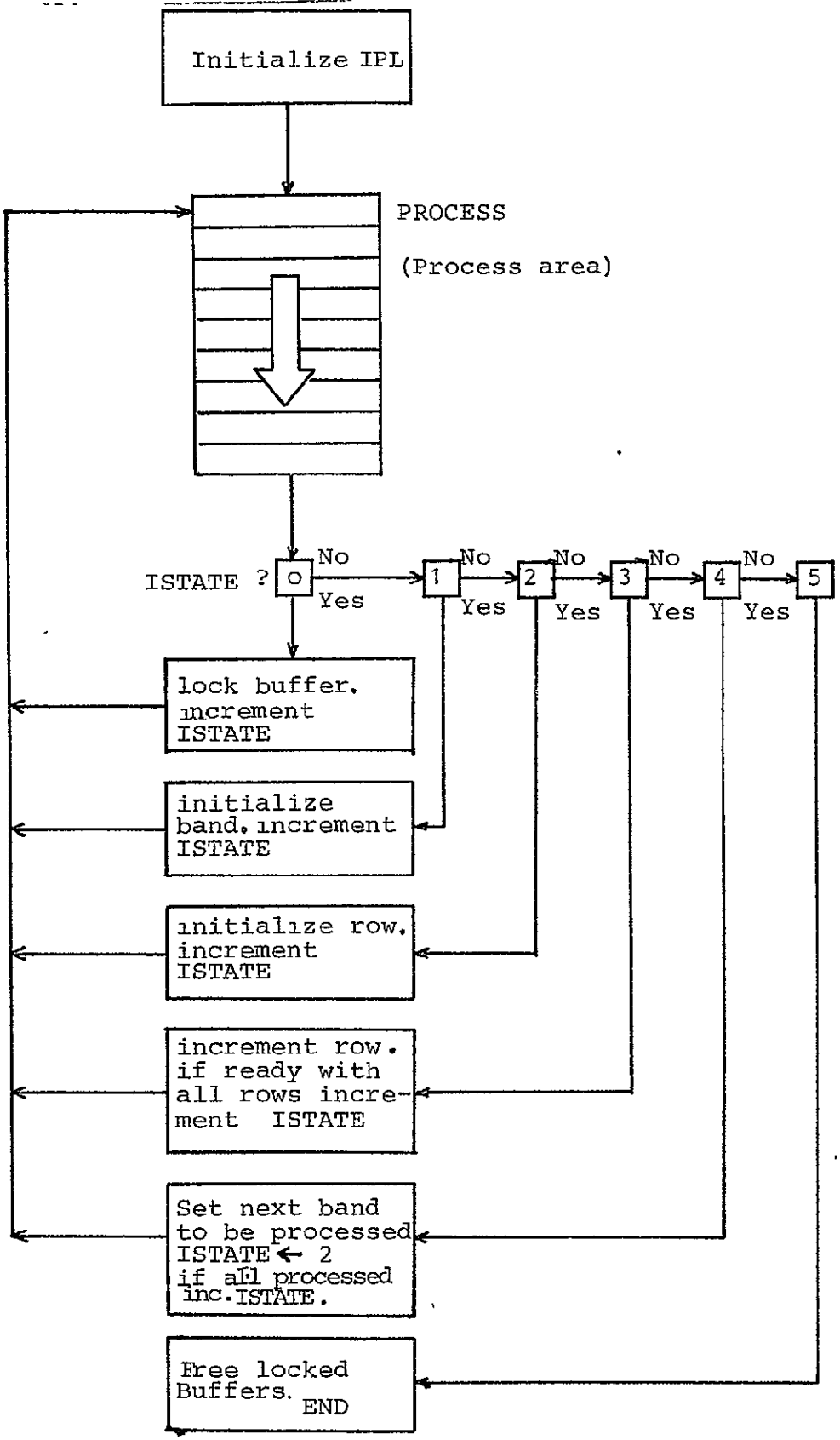

Fig.54: Control Flow of Image Processing Loop.

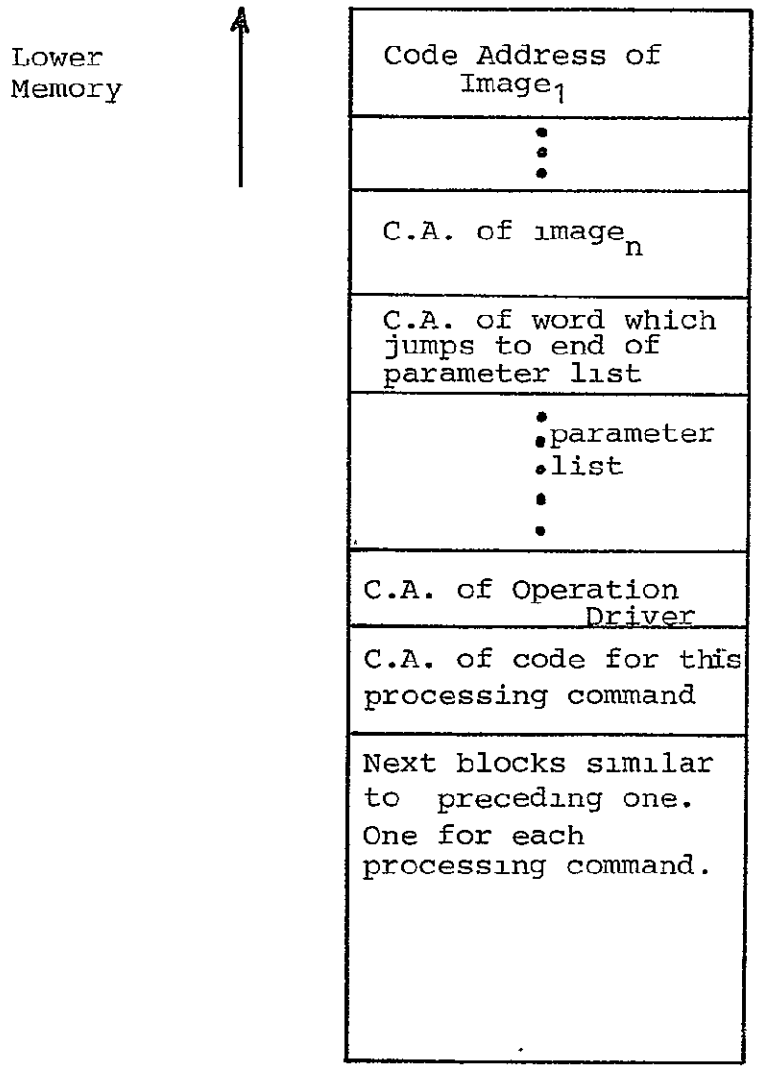

Fig. 55: Contents of Process Area.

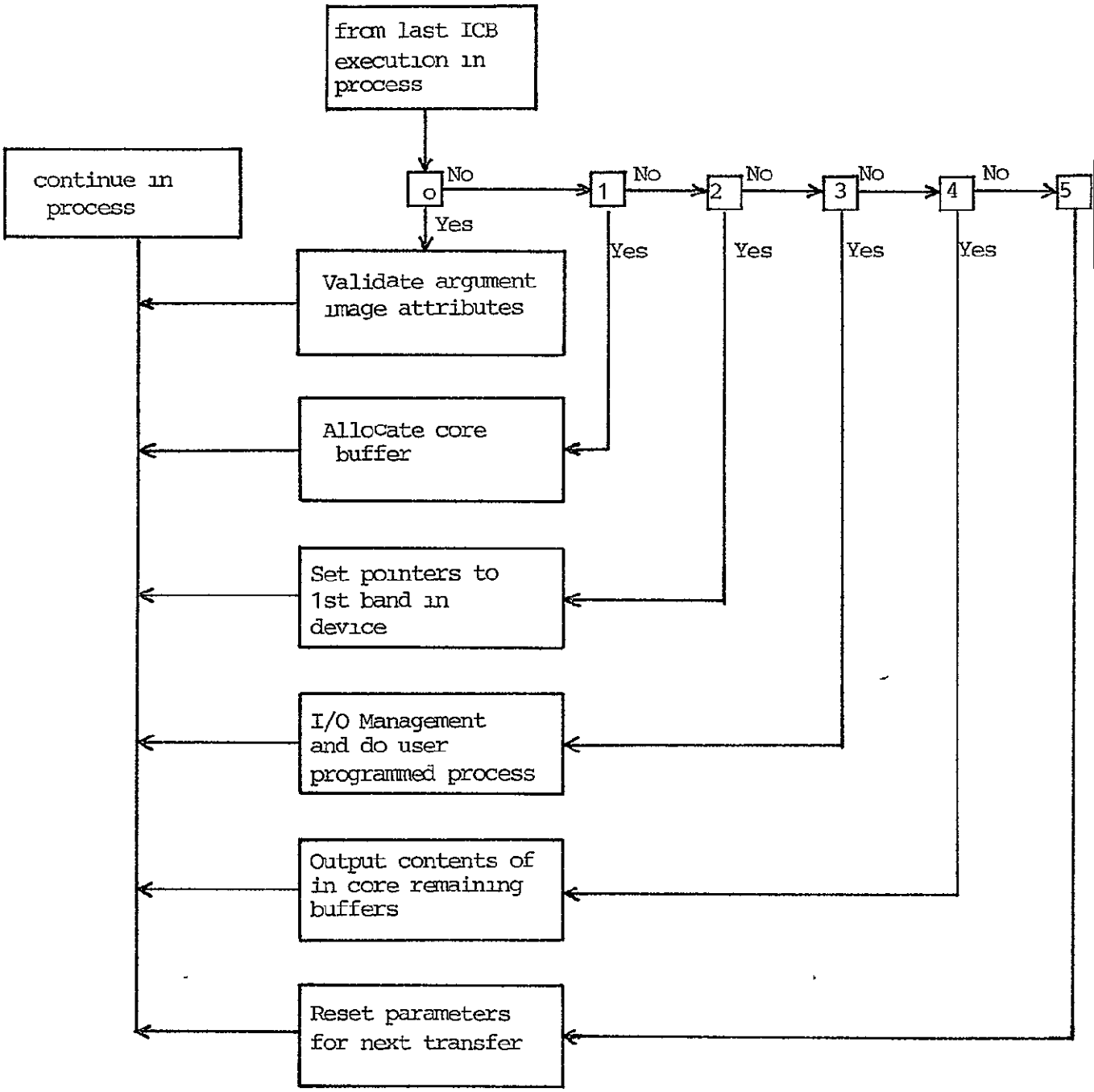

Fig.56: Basic Structure of Operation Driver.

1) FORTH - An application oriented language - Introductory Programmer's Guide
Forth, Inc. - Manhattan Beach, California

2) FORTH Technical Mannual
Forth, Inc.

3) FORTH-PDP-11 Supplement
Forth Inc.

4) Minicomputer Programming in FORTH. E.D. Rather, C.H. Moore, Forth Inc.

5) FORTH: A New Way to Program a Mini-Computer.
C.H. Moore, Astron. Astrophys. Suppl. 15, pp 497-511.

Image Processing Language Syntax and Available Commands

The syntax was already specified in the previous section.
The language consists of commands preceded (or followed) by arguments.
These arguments can be images (input, output) and parameters (constants).
After the arguments and the code corresponding to a command have been prepared for a posterior execution by TRANSFER, the output ICB remains on the image stack. This ICB can serveas input image for the following command, so that more of them can be chained together. The chaining images don't need to be existing ones, because since the process is executed line by line, only the first and the last in the line need to be physical images where the results will be stored. Of course, some processes cannot be chained because they require global information of the proceeding step, as is the case for the principal components transformation, where the covariance matrix of the whole image is needed before. Other cannot be included in the process because they don't work in a sequential way, as is the case for the image transpose.
Nevertheless, there are a large class of processes which can be carried out sequentially and therefore can be programmed as a chain of already existing processes, like the hyperbox classification.
Finally, the next pages show a list of the available commands with a short description of the operation associated with them.

Transient and buffer management utilities

	BUFFERGET	Modify buffer area in order to allow processing of images larger than 1 K byte x 1 K byte
	TEGSPACE	Restore original configuration of buffer area modified previously by BUFFERGET.
	$WORDS	
Loading word		Load transients loaded by loading word (after that not deletable by C)
	CWORDS	Delete commands loaded by $WORDS

Optronics Commands

inimage	raster size	!OPTRONICS	Enter a field corresponding to the size of inimage and raster size in the optronics film map file, with the position determined by the MAF.
		OPTRONICSHOW	Display on TV-monitor the optronics film map file.
		OPCLEAR	Clear the optronics film map file (for a new sheet of film)

Loading Words

GRIDS	Load support for the GRID processing command
PATTERNS	Load pattern generator
PRINTING	Load system diagnostic support
TAPING	Load magnetic tape support

Words associated with the PROCESS

C	clear the PROCESS and FORGET all transients
R	clear the PROCESS
MORE	allows adding more commands to the PROCESS after a TRANSFER
CDUMP	print a PROCESS dump
TRANSFER	execute the PROCESS

Image and system status utilities

	*HEADING	Print disk image heading content report
	*STATUS	Print ICB content report
	ICBS	Print report of all ICBS
n	ISTATUS	Print a STATUS report for top n images on the image stock
	STATUS	Print STATUS report.

Image File Management

*ALLOCATE	Allocate a disk image file
*CLOSE	Close a disk image file
*CREATE	Create a disk image file (ALLOCATE is faster, use CREATE only if a zeroed file is needed)
*OPEN	Open a disk file image

Other commands

	TMP	Generate a TEMPORARY ICB
	1 NULL	Generate a NULL ICB
image	ITRANSPOSE	transpose image (allowed size = 2^n x 2^n)

Image Statistics Utilities

	QHIST	Print 16 category histogram
at	NHIST	Print detail of histogram beginning with at
n	ZGFHIST	Print histogram with adjusted maximal percentage n
	STATISTICS	Print STATISTICS report
	?HISTOGRAM	Print STATISTICS report and histogram content report
	?COVMAT	Print actual covariance matrix
	?PRINCIPAL	Print actual eigenvalues and eigenvectors
	CORREL	Print actual matrix of correlation coefficients
	?MAPPED	Print mapped histogram

inimage	COVMAT	b	Calculates covariance matrix
inimage outimage	HCTRANS	bw	Principal components (inimage)→outimage
inimage outimage h.scale v.scale 1st col. 1st row	?TEXT	b	Writes a text on outimage beginning at 1st row 1st col. and extending horizontally. The character size is given by h.scale and v.scale
inimage (1) outimage (1)	1 > FFT	dw	one-dimensional Fourier Transform
inimage (1) outimage (1)	1 < FFT	dw	one-dimensional Fourier Transform (Backwards)
inimage (1) outimage	POWER	dw	power spectrum (inimage) → outimage
$inimage_1$ $inimage_2$ outimage	IFMUL	dw	$(inimage_1) * (inimage_2)$ → outimage
inimage(dwnd) outimage(word)	SF > W		(inimage)+n → outimage
outimage width position	STEPFILT	dw	create notch symmetric filter at (position) with (width)
outimage width position	EXPFILT	dw	create exponential filter (smooth notch) at (position) with (width)
inimage (byte) outimage(word)	FIRFILTER		Filter inimage with filter coefficients stored on tape
inimage(DWORD) outimage(byte)	PSCALE		logarithm (inimage)→ outimage with output values between ∅ - 255
inimage	WEXTREM	w	Determine maximum and minimum of inimage and store on inimage file
inimage	FEXTREM	dw	Determine max. and min. of inimage and store in inimage file.

(1) two band image (real and imaginary)

Piecewise Table Mapping Utilities

	PIECEWISE	Load piecewise mapping table words
	TBLGET	Gets are for piecewise table
	RELTBL	Releases table per piecewise table
start end value	FILLTBL	Fill piecewise table from start to end with value
startpos endpos startval endval	LINEAR	Sets piecewise table from startpos to endpos with values from startval to endval
start end	LSEG	Sets piecewise table from start to end with own values
start end	PASS	Sets piecewise table from start to end with own values, ø below, 255 above
	TBLSHOW	Print piecewise table
position value	VSET	Stores value at position of the piecewise table
	ZAPTBL	Zeroes piecewise table
	?MAPPING	Print mapping table

Processing Commands

inimage outimage gain bias	*+TBL	b	(inimage * gain) + bias --| outimage
inimage outimage mult div	*/TBL	b	(inimage * mult) / div --> outimage
inimage outimage mult	*TBL	b	inimage * mult --> outimage
inimage outimage div	/TBL	b	inimage / div --> outimage
outimage	+DIAG	b	Send an upward sloping diagonal ramp (up from left to right) to outimage
inlimage in2image outimage	+SCATTERGRAM		Add the scattergram of inlimage (byte) and in2image (byte) to outimage (word)
outimage	-DIAG	b	Send a downward sloping diagonal ramp (down from left to right) to outimage
inimage outimage low high	-NOTCH	b	Map values between low and high (inclusive) to 0, others to 255
inimage outimage	16STEPS	b	Map continuous inimage to 16 steps in outimage
inimage outimage	8STEPS	b	Map continuous inimage to 8 steps in outimage
inimage outimage adj gain atten bias	<BYTE		(((inimage (byte) + adj) * gain / atten) + bias --| outimage (wor
inimage outimage adj gain atten bias	<WORD		(((inimage (word) + adj) * gain / atten) + bias --| outimage (byte
inlimage in2image outimage	ADD	bw	inlimage + in2image --> outimage
inimage outimage	B>W		inimage (byte) --| outimage (word)
inimage outimage	BITCOUNT	b	bitcount (inimage) --> outimage
inimage outimage low high	BTWN	b	Map values between low and high (inclusive) to 255, others to 0 (Does nor generate a mapping table.)
inimage outimage	CLASSIFY values	b	Classify inimage --> outimage, 0 is not in, 255 is in, values specify a hyperbox

inimage outimage thresh n	CLEAN	b	Zeroes non-zero cells with fewer than n neighbors which are greater than or equal to thresh and sets to 255 all cells with n or more neighbors which are greater than or equal to thresh
inimage outimage adj gain atten bias	CNVT		(((inimage + adj) * gain) / atten) + bias --▷ outimage (byte --▷ word or word --▷ byte)
inimage outimage	CONTOUR	b	Contour inimage --▷ outimage
inimage outimage	CONV	b	Convolve inimage --▷ outimage (3 x 3 blocks)
inimage outimage	COPY	bw	inimage --▷ outimage
inlimage in2image outimage	DIV	bw	inlimage / in2images --▷ outimage
inlimage in2image outimage	EQ	b	inlimage = in2image ⇨ 255 --▷ outimage else 0 --▷ outimage
inimage outimage thresh n	EQINT	b	Map inimage --▷ outimage in n equal-width levels based on the histogram of inimage ignoring values with less than thresh occurrences
inimage outimage n	EQPROB	b	Map inimage --▷ outimage in n levels each having equal probability as determined by the histogram of inimage
inimage outimage	EXPMAP	b	Adjusted exponential function
inimage outimage	GRID	b	Superimpose a grid on inimage. Requires GRIDS.
inlimage in2image outimage	GT	b	inlimage > in2image ⇨ 255 --▷ outimage else 0 --▷ outimage
inimage outimage	HISTOGRAM	b	Gather histogram of inimage and place with outimage if possible
outimage	HRAMP	b	Send a horizontal (constant left to right) ramp to outimage
inlimage in2image outimage	LAND	bw	inlimage AND in2image --▷ outimage
inlimage outimage	LNMAP	b	Adjusted logarithm function
inlimage in2image outimage	LOR	bw	inlimage OR in2image --▷ outimage
inlimage in2image outimage	LT	b	inlimage < in2image ⇨ 255 --▷ outimage else 0 --▷ outimage

inlimage in2image outimage	LXOR	bw	inlimage Exclusiv OR in2image --> outimage
inimage outimage mod	MODTBL	b	inimage modulu mod --> outimage
inlimage in2image outimage	MUL	bw	inlimage * in2image --> outimage
inimage outimage thresh max	NMAX	b	Normalize to maximum max using thresh as the threshold based on histogram
inimage outimage thresh min	NMIN	b	Normalize to minimum min using thresh as the threshold based on histogram
inimage outimage thresh min max	NORM	b	Normalize to minimum min and maximum max using thresh as a threshold. Based on histogram
inimage outimage low high	NOTCH	b	low ≤ inimage ≤ high => 255 --> outimage else 0 --> outimage
	PRESERVE		Preserve mapping table with disk file of input image
inlimage in2image outimage numgain numbias dengain denbias	RATIO	b	Compute ratio: $\frac{(\text{inlimage} * \text{numgain}) + \text{numbias}}{(\text{in2image} * \text{dengain}) + \text{denbias}}$ --> outimage
inimage outlimage out2image	REPLICATE	b	Replicate inimage to both outlimage and out2image
inimage outimage inlow inhigh outlow outhigh	RERANGE	b	Rerange inlow to inhigh to the range of outlow to outhigh
inimage outimage	REVERSE	b	Reverse the values, (255 minus inimage) --> outimage
n	SCALAR	b	Create an image with a value of n; used in place of an ICB reference
inimage outimage vnum vden hnum hden	SCALE	b	Scale up or down by vnum/vden in the vertical direction and by hnum/hden in the horizontal direction
inlimage in2image outimage	SCATTERGRAM		Create the scattergram of inlimage and in2image in outimage

inimage outimage	SDSTRETCH	b	Map using standard deviation stretch
inimage outimage	SHOWHISTO	b	Show the histogram of inimage on outimage
inimage outimage	SHOWMAP	b	Show the mapping table of inimage on outimage
inimage outimage thresh	STRETCH	b	Stretch the above thresh value range of inimage to 0 through 255 based on histogram
in1image in2image outimage	SUB	b	in1image - in2image --▷ outimage
inimage outimage	SQRTMAP	b	Adjusted square root function
inimage maskimage outimage thresh	TMASK	b	If maskimage > thresh, copy the corresponding cell of inimage --▷ outimage else do nothing
inimage outimage	USETABLE	b	Use the piecewise mapping table
outimage	VRAMP	b	Send a vertical ramp (constant columns) to outimage
inimage outimage	W>B		inimage (word) --▷ outimage (byte)

Image Editor Commands

startrow endrow startcol endcol	!WINDOW	Set the window as specified
n	+D	Move the window down n rows
n	+L	Move the window left n columns
n	+R	Move the window right n columns
n	+U	Move the window up n rows
	.WINDOW	Print the window limits: startrow: endrow, startcol: endcol
	D	Move the window down 1 row
value startrow startcol endrow endcol	DRAW	Draw a line with value from (startrow, startcol) to (endrow, endcol)
value row column	I!	Store value at (row, column)
row column	I?	Print the contents of (row, column)
row column	I@	Fetch the contents of (row, column) onto the parameter stack
	GETWINDOW	Set the window from the MAF-1 frame
	L	Move the window left 1 column
	POSITIONING	Load +D, +L, +R, +U, D, L, R, and U for use
	R	Move the window right 1 column
value	RFILL	Fill the window with value
	SHOW	Show the contents of the window
	SWIN	Use the subimage of the active image as the window
	U	Move the window up 1 row

DV-8 Commands

	ALIGN	Align on next track; allows up to 4 bands to be shown simultaneously
a b	ALTERNATE	Alternately display track a and b 10 times for 1 second each
	GETFRAME	Read the MAF-1 frame and place on the parameter stack
	LOCATE	Display last output which was written out using the active ICB
	NTK	Display next track
	PTK	Display previous track
start stop n	REPEAT	Repeat SWEEP n times
n	SEEK	Seek to channel n
start stop	SWEEP	Display tracks start through stop in turn for 2 seconds each
track	TRACK	Seek to channel 1 of track
n	TSK	Skip over n channels before beginning output
?CURSOR		Read cursor values and put them on the parameter stock.

Image Attributes

	NAMED name	Sets the filename to name
	NULL	Selects the null device
p	PRECISION	Sets the precision (p = BYTE or WORD/DWORD
	PRIMARY	Selects the active ICB as the primary ICB also
n	ROWS	Set image size to n rows
rows columns	SIZE	Set image size to the specified number of rows and columns
	SPAREBANDS	Set the number of spare bands to n
startrow endrow startcol endcol	SUBIMAGE	Set the subimage
n	SYMBANDS	Set the number of symbolic bands to n
	TAPE	Select SWING magnetic tape as the device (not implemented)
	TEMPORARY	Select the temporary device
	UNDER username	Set the current user id and the ICB user id according to username
	WHOLEIMAGE	Set the subimage to the size of the image
	RECORDER	Select Optronics film recorder as the device (output only)
	TELESPAZIO	Select TELESPAZIO tape as the device (input only)
	OLIVEN	Select Bendix M^{2}S tape as the device (input only)

Image Attributes

	12BAND	Select 12 channel tape as the device (input only)
	ALL	Select all bands (data and symbolic) for processing
	ALLDATA	Select all data bands for processing
	ALLSYM	Select all symbolic bands for processing
	BAND n	Select band n for processing
	BYTE	As in BYTE PRECISION
	CAMERA	Select camera as the device (input only)
n	COLUMNS	Set image size to n columns
	COPYOF from	Copy the ICB from to the active ICB
	CRT	Select the terminal as the device (output only)
	CSUB to	Copy subimage from active ICB to to ICB; make to active
n	DATABANDS	Set the number of data bands to n
	DISK	Select (digital) disk as the device
	DISPLAY	Select analog disk as the device (output only)
	GETSUB	Set subimage from the MAF-1 frame
	HARDCOPY	Select the printer/plotter as the device (output only)
	LANDSAT	Select LANDSAT tape as the device (input only)
	LIKE from	Copy selected items from the from ICB to the active ICB

Image Header Editor Commands

n	!ANCILLARY name	Setup current user id and name as the n-th ancillary file
value	!HASPECT	Set horizontal aspect to value
value	!HSCALE	Set horizontal scale to value
value	!LAT	Set latitude to value
value	!LONG	Set longitude to value
value	!VASPECT	Set vertical aspect to value
value	!VSCALE	Set vertical scale to value
number	?ANCILLARY	Print ancillary file name and user id of the n-th ancillary file
	?CAPTION	Print the caption
	?HASPECT	Print the horizontal aspect
	?HSCALE	Print the horizontal scale
	?LAT	Print the latitude
	?LONG	Print the longitude
	?VASPECT	Print the vertical aspect
	?VSCALE	Print the vertical scale
	CAPTIONED caption	Set the caption
	HDREDITOR	Load all of the above commands except ?CAPTION and CAPTIONED (which are normally loaded)

2. Hardware

A detailed description of the system hardware ist out of the aim of this report. Only a brief description of some unusual components appearing in fig.58 will be given, specially concerning the analog system ISI 15o.

The analog system communicates with the computer through the DV-8, which is capable of D/A-A/D conversion and video formatting of the data. This permits the digitalization of TV frames from the video disk and the storage of D/A converted and video formatted pictures in the video disk. A total of 6oo TV frames can be stored and selected for display normally with the disk controller or by a program through the DV-8. The VP-8 and AP-3 allow some very simple image manipulations to be carried out in real time (arithmetric operations, false color, equidensities, etc.) and transparencies can be read on video disk through a TV camera. A description of the very well known digital components is not necessary.

View of the image processing system.

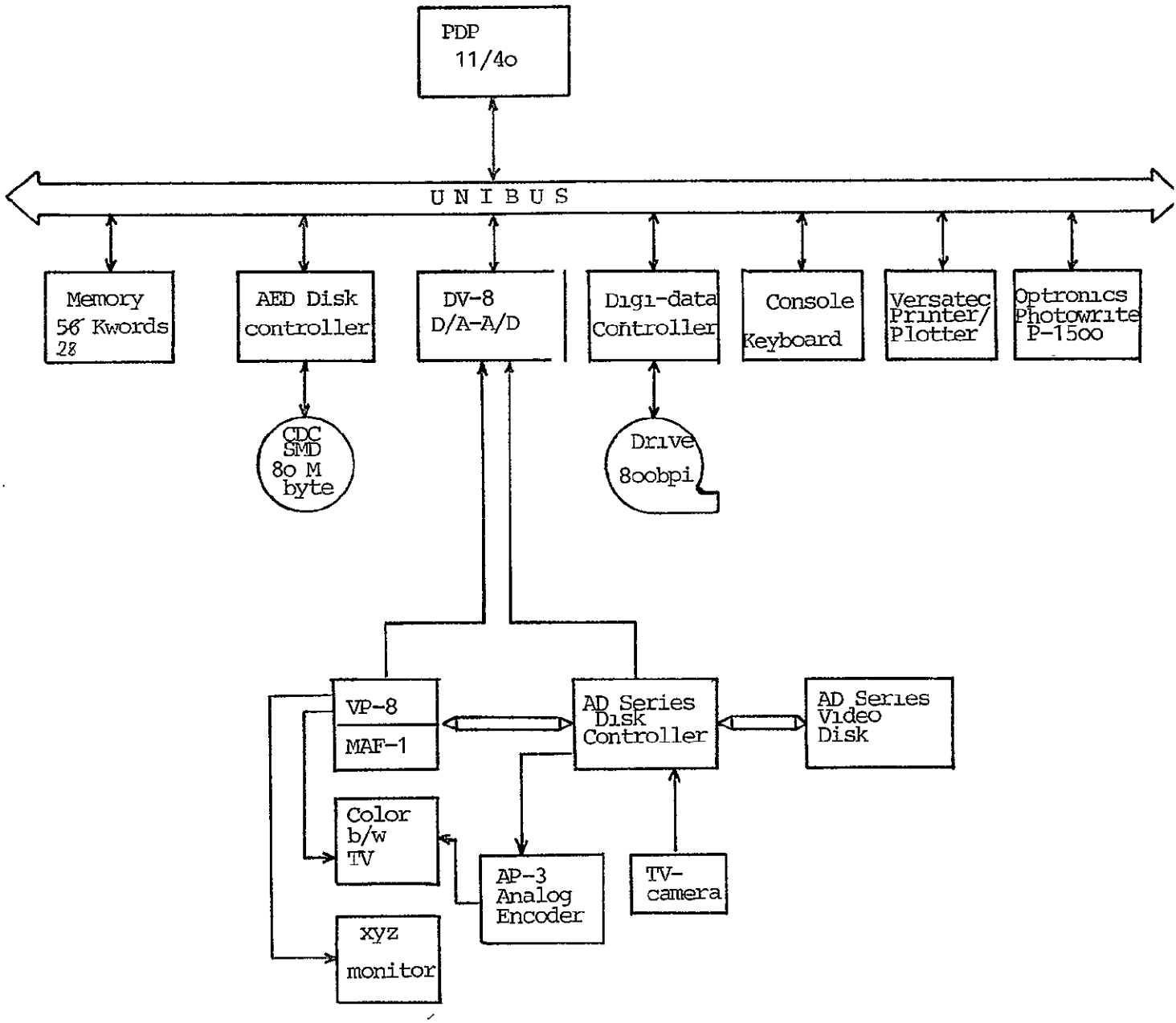

Fig. 58 : Hardware Configuration

B. The Use of the System 47o for Educational Purposes

The combinatıon of analog and dıgıtal data processing techniques - the hybrid concept - probably has dısadvantages wıth respect to the user's interactivity through the TV-dısplay whıch is optımally gıven on the basıs of a dıgıtal refresh memory.
Nevertheless, we have decıded to move towards a hybrid data processing concept, because there exist certaın advantages whıch are ındispensible with respect to the ıntroductıon and training at earth scıentısts in the use of remote sensıng data.
Durıng the last years we have experienced that there exists a tremendous communicatıon gap between technıcal oriented and scıence oriented people. The lack of communıcation becomes evident, if the earth scientist becomes ınvolved in digital processıng of data.
From the technical side a varıety of possibilitıes to process multıspectral data are offered. The operator normally ıs not able to identify the earth scıentific problem and the earth scientıst is not capable to identify the kind of processing required or even to recognize the information exhıbited by multispectral data.
Because of above mentioned problems and the sıgnificance of applying image data processing techniques we are using our hybrid system under two aspects:

1) To introduce potential users of remote sensıng methods to the data he has avaılable.

2) To help establish experıence ın handlıng the data.

In the followıng a short descrıption of above aspects ıs given.

Under normal situations the unexperienced user community is confronted to bulk data products such as black and white copies of individual bands or color composites.

This kind of data probably exhibit a trememdous amount of information identifiable immediately.
In order to fully utilize and recognize the information content, the user must be in a position to carry out some additional manipulations on the data. We have learned, the best results in terms of motivation and output were obtained if the scientist is experiencing the effects of processing on the data personally.
Under this aspect the hybrid data processing concept is optimally suited and we are using the following approach:

1) Make available of 1 or 2 CCT's exhibiting the area of interest.
2) Digital enhancement of the area of interest (histogram stretch), transfer and storage of enhanced data onto the video disc for display and analog processing purposes.
3) Introduction of analog processing system to the user. In order to fully use the analog system, a training of 1-2 hours is sufficient.
4) The user is left with the analog system where he can perform in realtime.
   - ratio processing
   - linear transformations
   - flicker operations
   - color composition of originally or analog preprocessed data
   - density slicing on original or analog preprocessed data
   - pointwise readings of densities
   - density profiles.

Normally the user spends several hours manipulating the data.

5) Discussions with the user about the earth scientific problems he wants to investigate.
The experience has shown, that after spending some hours with the analog system, the user is capable to discuss his requirements and he is able to demonstrate to the operator the phenomenon he is interested in.
In many cases he even experienced and extracted additional information

6) Digital processing of the data.
On the basis of previous discussions the operator tries to digitally enhance and display the identified phenomena in order to provide the user with a high quality film product (photo-write) for further interpretation.

Above described approach has been carried out with earth scientists representing geology, vegetation sciences, hydrology and oceanography. Of special interest is the experience that the requirements towards the application of automatic classification procedures is decreasing on the basis of increased experience in handling the data. This matter of fact is probably related to the increased ability of the user to critically explore multispectral data which has to be built up in an itterative learning process.

PART III

SUMMARY OF USER REQUIREMENTS WITH RESPECT TO OPERATIONAL SATELLITE REMOTE SENSING AND ITS IMPACT ON THE DEFINITION OF AN EUROPEAN SATELLITE SYSTEM

With respect to Landsat 1 and 2 investigations which are being carried out with users representing various desciplines, during the last years the capabilities of Landsat and additional user requirements were discussed in detail. In addition to this we participated in activities of ESA's Remote Sensing Working Group, RSWG, (Chairman J. Bodechtel), which set up multinational working parties to define user related requirements from the European standpoint.

In the following chapter a summary of our experience concerning key applications and resulting user requirements is given. The manifold discussions led to a concept of an earth resources satellite which was defined together with Messerschmitt-Bölkow-Blohm (MBB).

The basis knowledge of the earth for solving environmental problems more and more assume global proportions. The application of spaceborne and airborne remote sensing techniques has proved their potential for various scientific and economic disciplines. The evaluation of Landsat and Skylab data has shown that global and continental (european) user requirements can be met with spaceborne techniques. Imagery from satellites in relatively low earth orbits and subsequent interpretation has to be part of the efforts aimed at accomplishing these permanent future tasks in an efficient manner. The final goal will be the application of those techniques in application oriented operational satellite systems.
For the definition of tasks concerning earth observation by spaceborne remote sensing techniques, outstanding advantages are:

- synoptic view and analysis of regional conditions and interrelationships of large and medium size areas
- continuous observation and monitoring of dynamic features as well as permanent targets on the earth surface.

Multispectral and multitemporal data acquisition from satellite platforms for large scale phenomena, interrelationships and changes are approaching within the next 10 years on operational phase. Satellites will be the first order platform for global and regional tasks.

Europe defined and further has to define its own needs and a global system has to meet and include if possible all those requirements. Certain scientific and problem areas of static phenomena and dynamic processes in natural resources monitoring and management, in environmental monitoring, in monitoring changes in phenology, land use and hydrology, only to mention some tasks, have to be solved by remote sensing and equipment and programs have to be adapted to these needs.

In fulfilling the need of continuous monitoring with high repetition rate, beside Earth and Ocean monitoring-satellites, the data of weather satellites like Meteosat, will be useful for largescale correlation of fast changing phenomena.

Within a research program the more operational aspect of remote sensing has to be considered. This involved not only investigations concerning the feasibility of remote sensing as a basis, but also the definition of relevant applications and as a final goal the optimization of technical and scientific requirements.
Intensive studies on the spectral behaviour of surface features are carried out. The present investigation is mainly restricted to the visible and infrared part of the spectrum. Future basic investigations will have to concentrate more on the microwave region of the spectrum not least due to its independence of the weather.

Onefurther task is the development of automatic evaluation models based on spectral characteristics varying in illumination and seasonal changes. Those models are the basis for the indispensable automatic data evaluation for thematic cartography of different and varying earth surface features.

The latter goal will be a main requirement to keep the data output on a level which is compatible with the data evaluation capacity and capability of the user community.

1. Key Applications for an Operational System

The overall objectives can be envisaged for both regional and global tasks. Of first order are the regional tasks

- to monitor dynamic features in developed regions such as Europe, and possibly in selected areas within the developing regions;
- to provide basic resources information for developing

regions to be used within the framework of development aid programs.

Global aspects are
- to monitor the global oceans,
- to monitor the global atmosphere, in particular with respect to the climate and climate changes, and air quality measurements,
- to map global resources such as basic food supplies, soils and forests.

The involvement depends on internal Euroepan priorities. High priority must be given to the implementation of regional space systems providing data that can be applied both in Europe and within the framework of development aid programs.

It is important to consider that the interest of Europe extends beyond its political boundaries. It includes global monitoring of the oceans and atmosphere, the use of remote sensing data within the framework of development aid programs, and to monitoring global resources (e.g. food supplies and raw materials) of vital interest to a continent highly industrialized and poor on natural resources.

The main emphasis is placed on the management and conservation of known resources, rather than in the exploration and exploitation of new resources. The two main exceptions to this general rule are the continental shelf areas and Greenland. This emphasis in resource management leads to the requirements to monitor at high resolution the changing features of the European landscape.

The dynamic character of the main requirements plus near continuous cloud cover over many European regions, point to the need to develop high resolution all-weather remote sensing capabilities.

The following table lists key areas where an operational satellite system could support to solve important tasks.

Key Applications of Major European Interest

Land Use

Land use mapping and classification, ecological mapping, regional and urban planning, real time land use data-bank for dynamic parameters.

Agriculture and Forestry

Statistical information on agricultural products = crop inventory, yield prediction for key crops.
Agrometeorological monitoring
Forst inventory, monitoring of the green wave.
Soil moisture and irrigation monitoring.
Monitoring of vegetation desease and stress.

Extractive Resources

Basic studies in tectonics, lithology for mineral exploration and prospecting - thematic mapping.
Monitoring of changing secondary indicators (e.g. vegetation, soil moisture) for detecting anomalies due to subsurface geology, mineralization, thermal anomalies etc.

Inland Water Resources

Monitoring of snow coverage and snow melt,
Calculation of run off.
Areal monitoring of precipitation and soil moisture.
Monitoring of frost line and permafrost.

Oceanography and Coastal Zones

Sea currents, chlorophyll-concentration, upwelling areas, sea ice monitoring.
Continental shelf operations.
Pollution (oil) monitoring of coastal zones.
Contineous monitoring of interior (mediterranea and baltic) and marginal (northern sea and shelf) seas.

Polar Zones

Thematic mapping and monitoring of Greenland and arctic islands.
Ice surveys, perma frost.
Vegetation monitoring, sea ice monitoring.

Development Aid

Topographic and thematic mapping 1:100.000.
Mineral resources exploration.
Planning and inventories in agriculture, forestry and land use.
Disaster monitoring and damage assessement.

2. Requirements for Operational Applications

Europe's own needs and special requirements lead consequently to an own segment in a global monitoring system. The sensors configuration, orbit and repetition characteristics, spectral and resolution specifications have to fullfill Europe's specific needs and have to be comparable and where possible compatible with other mainly US systems in operational world wide satellite remote sensing.

The key problem areas for operational application, which cannot be met by existing experimental systems are

- spatial resolution
- spectral band selection and combination
- repetition rate.

For land application the main analytical sensor with high ground resolution will be for the near future in the optical field of the spectrum. To fill the gaps for the required repetition rate in an operational system and to fullfill specific tasks active microwave sensing is indispensable, also if the complete

use of this technique needs further basic investigations via SPACELAB experiments.
For sea application the combination of microwave and optical sensing with coarse and medium ground resolution and high spectral resolution in the optical field seems the ideal combination.
Fig.59 shows the existing and planned earth observation satellites, their spectral bands, sensors and ground resolution (in brackets) and where a proposed european satellite would fit in. Fig. 60 demonstrates the time frame and expectable life time of these earth observation satellites.

The requirements on spectral band location for the optical part of the spectrum (fig.61) demonstrates that in general 4 - 6 bands with varying bandwidths are required. Especially in the medium IR but also in the visible certain technology has to be developed.
Systems with flexible spatial and spectral resolution can be achieved by using modular opto-electronic multispectral scanners. This sensor should provide images in the visible and infrared spectral ranges, using the CCD technique based on the "pushbroom" process.
Generalized requirements meeting the major applications shows fig. 62.

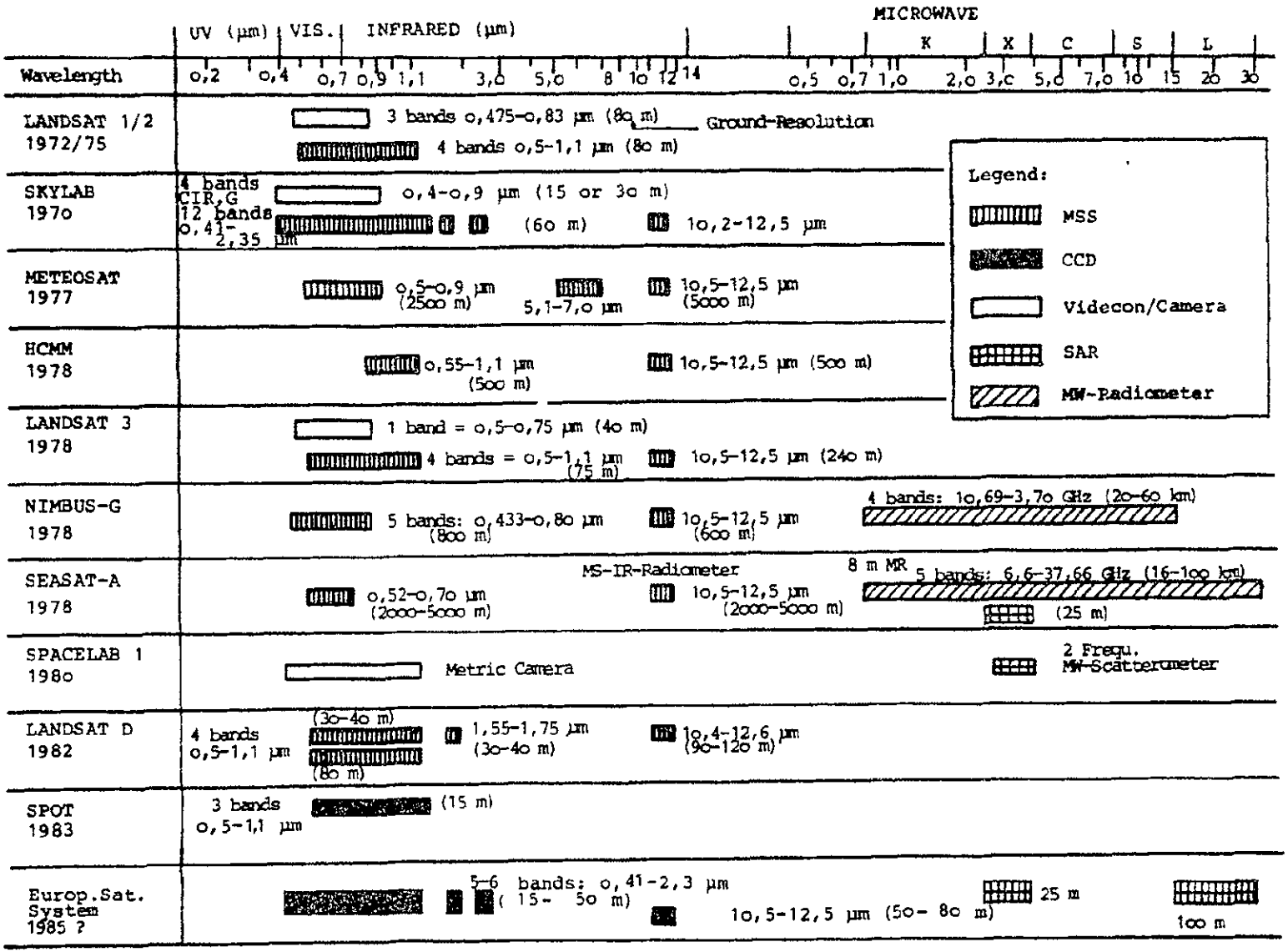

Fig.59: Imaging Systems in earth observation satellites

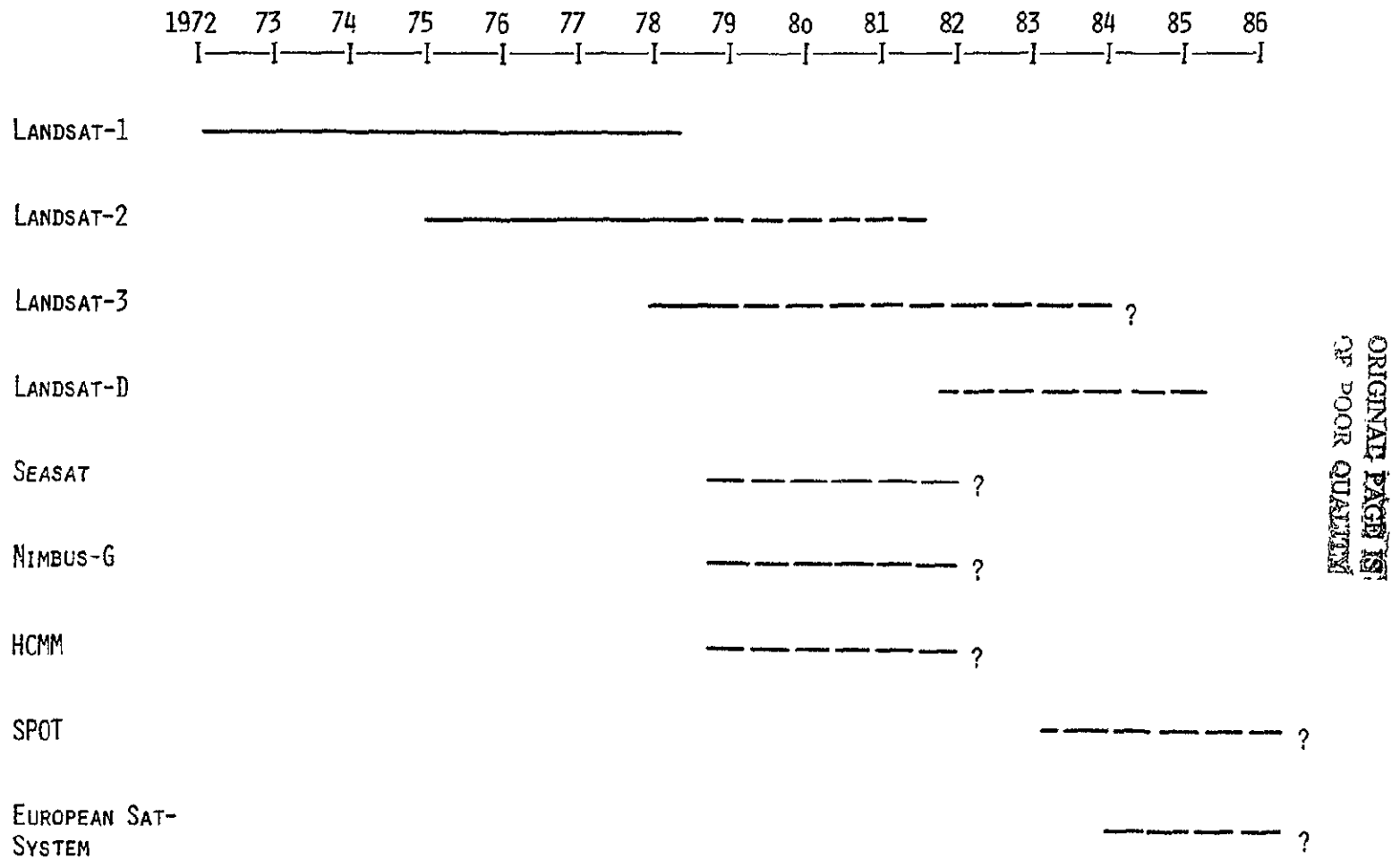

Fig. 60: Existing and projected satellite systems.

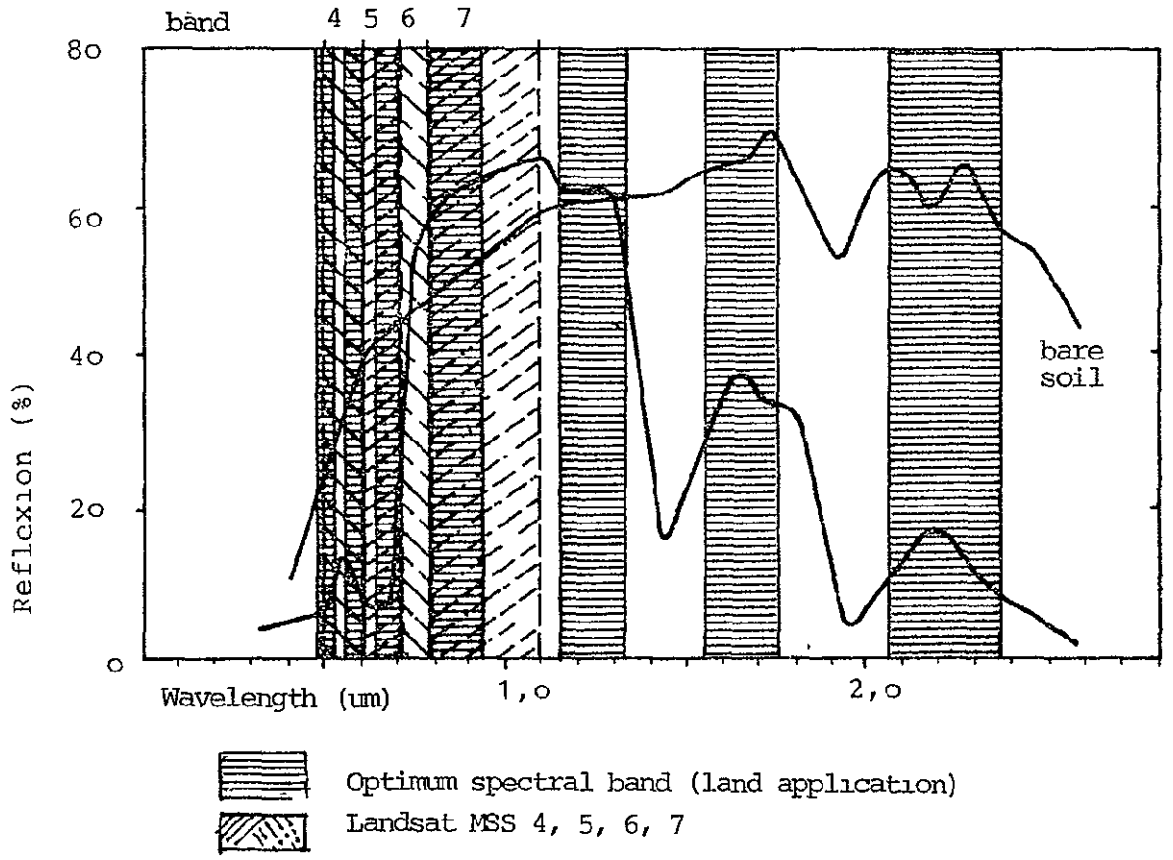

Fig. 61: Major spectral bands for land application.

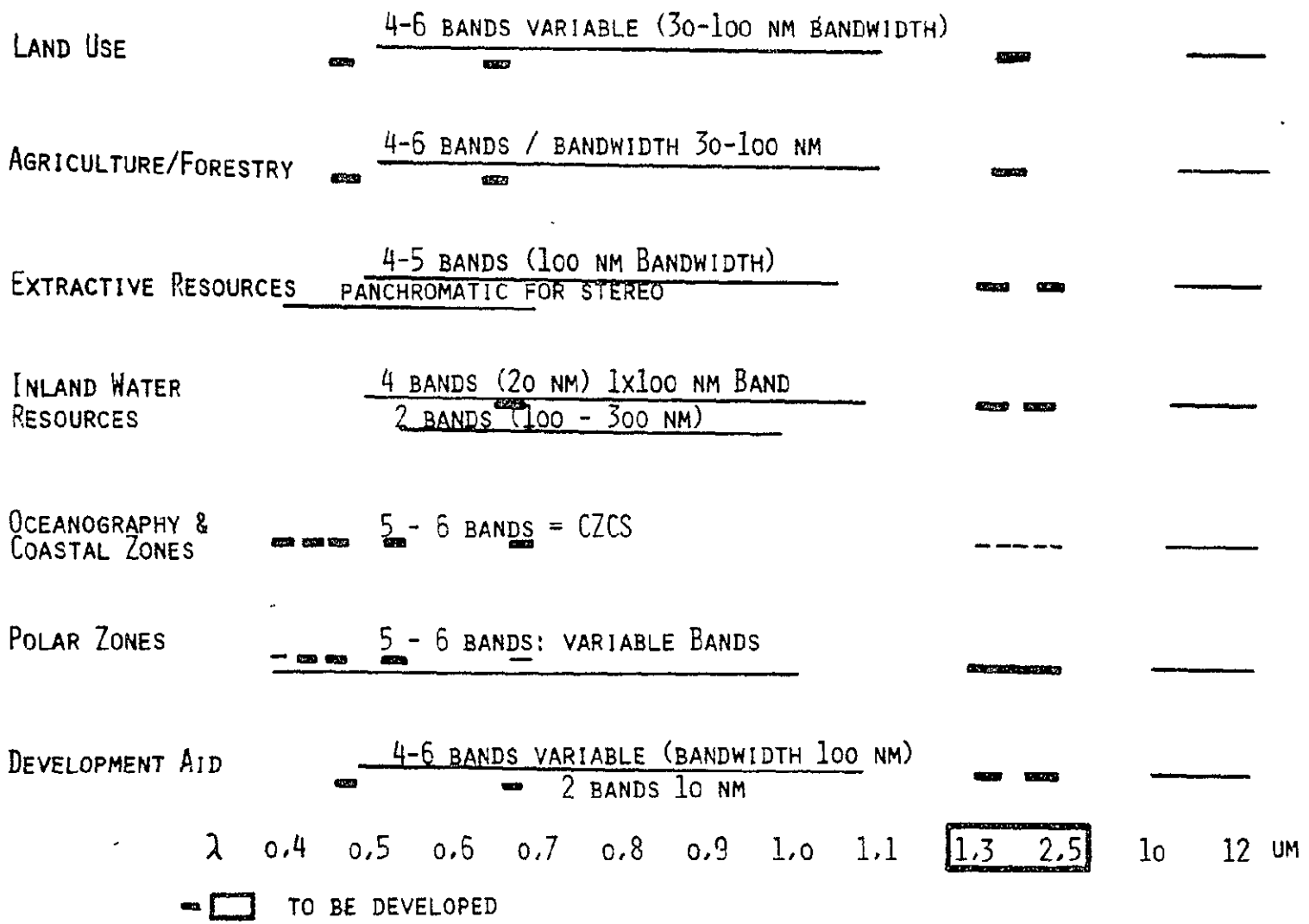

Fig. 62: Requirements of spectral band locations

The repetition rate for most monitoring tasks can be fullfilled with 7 - 9 days period. To guarantee for continuous monitoring and in the case of agriculture expecially for the growing season weather independant sensing is indispensable. As exeption are tasks in oceanography where daily repetition rate is required (fig. 63).

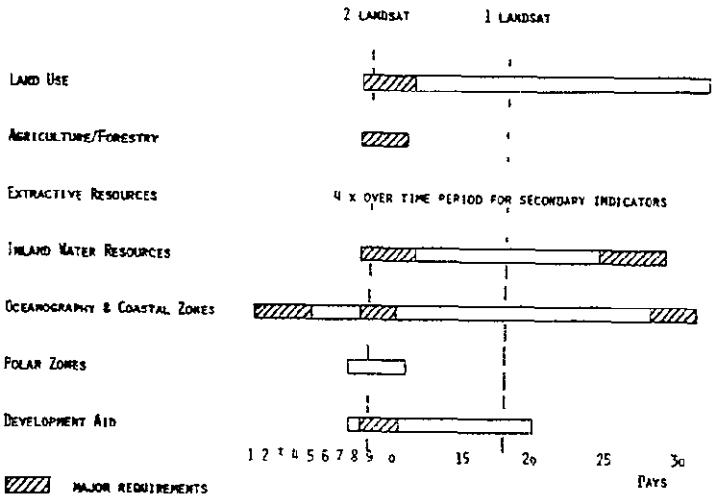

Fig. 63: Repetition rate in days.

The other driving factor for European tasks are the requirements on the ground resolution. Fig. 64 shows in the visible to medium IR and the active microwave region requirement for multispec-ral sensing around 20 m resolution. The requirements in the thermal IR and passive microwave radiometry are around 80 m, large scale oceanography requires less than 500 m with high repetition rate.
Summarizing all requirements fig. 65 shows the European needs in the different fields of earth observation in comparison

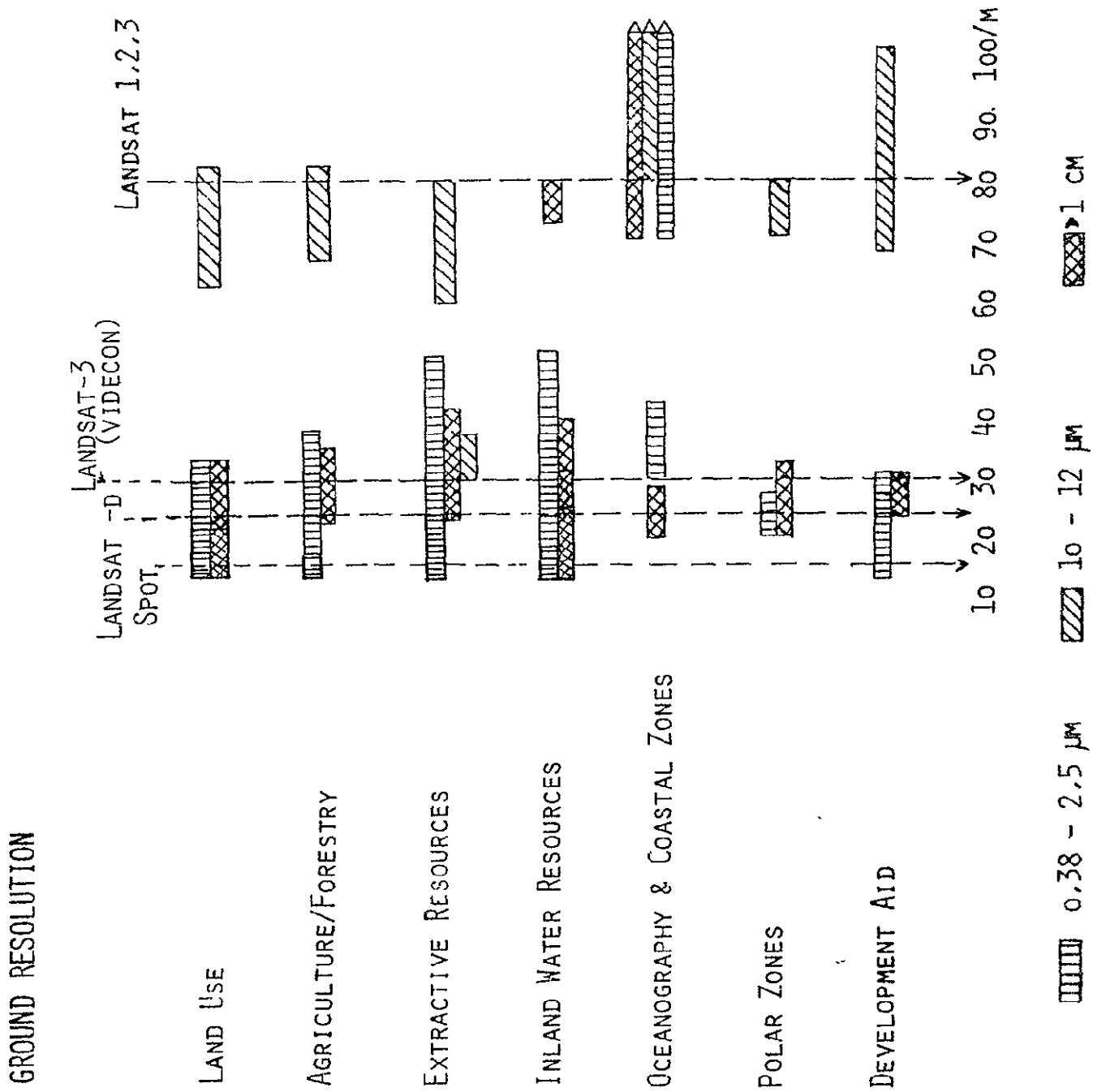

Fig. 64: Ground resolution

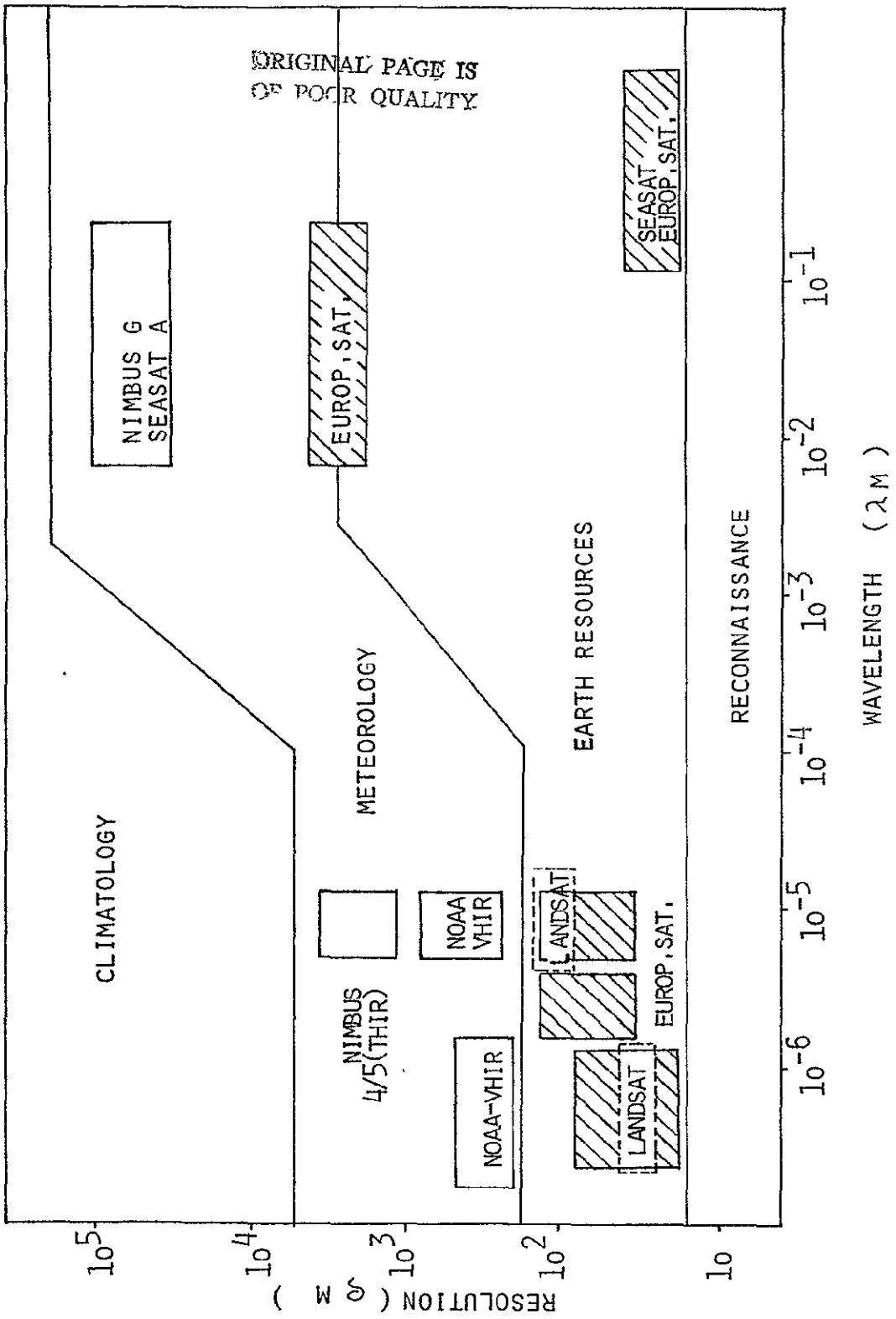

Fig. 65

with American systems in a diagram ground resolution versus wavelengths. It demonstrates the overlapping and differing areas.

In conclusion the tasks in the different applications cannot be met with one payload configuration. Three different systems are required for land application, coastal zones and water resources and oceanography and polar zones.
Driving factor for using different payload configurations are the differing requirements on optimum spectral band and ground resolution. Possibly coastal zone requirement could be met by land application payload configuration. Though at least two systems according to fig. 66 are required for major monitoring and inventory tasks.

APPLICATION	SYSTEM REQUIREMENTS
AGRICULTURE/FORESTRY LAND USE EXTRACTIVE RESOURCES DEVELOPMENT AID	OPTICAL PAYLOAD (MED. AND HIGH GROUND- RESOLUTION) TWO FREQUEN. SAR
COASTAL ZONES WATER RESOURCES	OPTICAL PAYLOAD (MED. GROUND-RESOLUTION HIGH SPECTRAL RESOLUTION) SAR + IMAG.MICR.RADIOMETER
OCEANOGRAPHY POLAR ZONES	OPTICAL PAYLOAD (COARSE GROUND-RESOL.) IMAG.MICR.RADIOMETER

Fig. 66: Typical European satellite systems

Operational earth observation satellites under European and global aspects will be either dedicated to special tasks for a limited number of applications with special orbital and sensor requirements or to a multidisciplinary approach in two possible payload configurations. In general the following parameters including European needs have to be considered:
Sun-synchroneous orbit of 570 or 980 km altitude.
A spatial resolution of the sensors in the visible and near infrared between 20 and 30 m regarding the small-scale pattern of intensive land use areas.
In a global system including non european satellites a net of two or three satellites within an orbital distance of 120^{o} latitudes to observe fast changing targets and their regional interrelationship.
Great emphasis to be given to microwave systems due to the global varying climatological conditions and for the monitoring of special phenomena.

3. Proposal for a Pre-Operational European Satellite

Within the limits of the above described applications, and requirements, an Earth-observation payload can be met in the medium term by European technology. In particular, with a view to earlier pre-operational use, preference should be given to sensor systems whose basic operational characteristics are known. On the basis of users' experience, the peculiarly European requirements for optical and passive microwave systems may already be laid down. In order to meet the operational requirements, Argus proposes the following

- A modular, opto-electronic, multispectral scanner (MOMS) with 20-m resolution in the visible and near infrared and 60-m resolution in the thermal infrared.

  Taking advantage of earlier German pre-development work, this sensor could be developed by 1980 using American components, or by 1983 with excluxively European ones.

- A passive multifrequency microwave scanner radiometer (PAMS) with a resolution of 3 to 5 km at 33 GHz, 6 to 8 km between 19 and 10.6 GHz, and about 12 km at 5,5 GHz.

These sensor systems cater for the pre-operational and experimental requirements as follows:

Pre-operational aspects

MOMS:

- The provision of high-resolution, synoptic satellite images for the various branches of environmental planning within the EEC.
- Improved classification cpability, and the provision of topographical data (stereo images) with a geometrical resolution of some 30-m for developing countries' purposes.

- Thematic mapping of geological, hydrological and vegetation phenomena in developing countries.
- Provision of thematic maps.

PAMS:

- All-weather observation of oceanographic phenomena in the Central and North European areas (coastline, coastal zones, Mediterranean and Arctic Sea areas).
- Acquisition of data on snow phenomena over extensive areas.

Experimental aspects

MOMS:

- Investigation with a view to the acquisition of relevant spectral signatures.
- Optimization of the spectral regions to be used for specific applications.

PAMS:

- Investigations of the applications potential of passive microwaves for acquiring data of hydrological phenomena over extrensive areas (soil moisture).
- Use of passive microwave processes in connection with the employment of the opto-electronic payload for atmospheric correction.

Last but not least, active microwave systems (SARs) appear to be essential for continuous operational, meteorological independent monitoring tasks. Admittedly, extensive fundamental research and costly technical development will be necessary in this area, in order to be able to set up a

multifrequency system for the quantitative automatic utilization of the data.

ARGUS, a Modular Satellite System

Argus is a modular satellite system, designed to be launched by Ariane. The design allows the progressive addition and use of purely optical payloads up to and including passive microwave scanners and active radar systems.

- The basic support module,measuring 1.8 x 1.8 x 1 m, consists of the basic structure, thermal-control system, power-conditioning arrangements and the system for transmitting, receiving and handling data. These sub-systems themselves are in turn modular, so that the respective requirements of the various configurations can easily ba met. Attached to the basic module is the solar array, which is also modular and adaptable to the various power and performance requirements.

- The optical module consists of the interchangeable camera element, whose measurements correspond to those of the basic support module. The camera element can be mounted either on the cut-away side of the module or on one of the narrow faces. In every case, the optical module has a heat-radiation system pointing away from the sun and, if required, a tape recorder for intermediate storage while contact with the ground is lost.

- The microwave module consists of a basic rectangular block measuring 1.8 x 1.8 x 4 m. An integral part of it is a 2.8 x 4 m paraboloid antenna. The latter is mounted along the diagonal of the side surface and extends some 2o cm beyond the block in either direction in the flight path. In passive operation, a linear receiver system

is mounted on the Earth-pointing side of the block, making possible phase-controlled scanning by the antenna radiation pattern at right angles to the satellite's flight path (scanning radiometer). The receiver system is designed for two frequency bands: 5.3 and 10.6 GHz. The ancillary elements required for operating the antenna are located in the block above the basic structure.

In place of the passive microwave module, an active side-looking synthetic aperture radar (SAR) can be mounted. Fig. 66 shows a 10-m long SAR antenna consisting of five planar arrays each 2.2 x 2 m. After deployment, it is swung out of the orbital plane to the required angle of sight.

In the passive operating mode, a further antenna for the 30-GHz band can also be mounted on the microwave module. It operates directly, without a reflector, on the phase-selection principle, and also allows the receiver-antenna pattern to scan at right angles to the flight path. This antenna may be inclined to the Earth at angles between 0 and 90° and can be folded against the block during launch.

3.1 Payload

Modular Opto-Electronic Multispectral Scanner (MOMS)

Based on Landsat 1 and 2 experiences optical sensor systems have to lead from experimental systems to flexible operational systems adapted to the broad variety of requirements.
A system with flexible spatial and spectral resolution can be achieved by using the modular opto-electronic multi-spectral scanner (MOMS). This sensor provides images in the

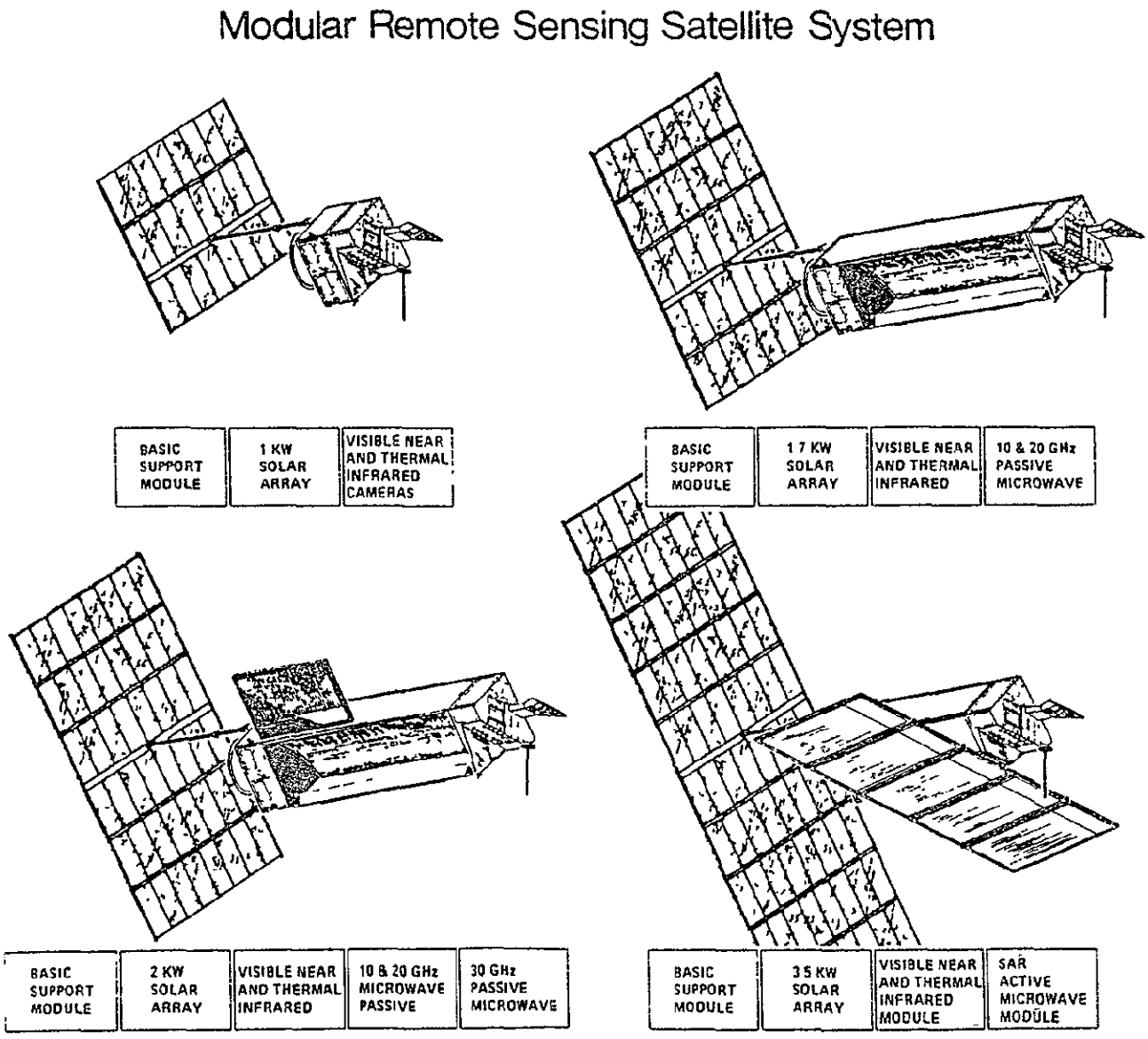

Fig.66: Argus modular multidisciplinary Earth-resources satellite system

visible and infrared spectral ranges by electronic scanning with semi-conductor detector arrays, using the CCD technique based on the "pushbroom" process.

This technique, which is specially suited to producing geometrically exact orthogonal images, represents a marked technical advance over the presently used scanners with mechanically driven scanning mirrors. In addition to its small weight and satisfactory dimensions, this system's imaging geometry is very flexible. Thus, for orbits between 600 and 900 km, the spatial resolution (maximum 20 m) and the image swath width (60 - 240 km) can be adjusted to suit the measurement tasks and the texture of the area covered. These characteristics also apply to stereo images.

A separate module with its own optical system is provided for each spectral channel and for stereo images. The basic version of the MOMS shown in fig.67 comprises six modules and a tape recorder; the latter can, when appropriate, be exchanged for a stereo module. The principles of the individual modules are shown in fig. 68 . A given image area is viewed twice through two lenses by three of the suitably adjusted elements and sensed by a detector array of six linearly arranged CCD elements each with 1700 pixels. This process enables an exact reconstruction of the image lines without distortion due to the mechanical lateral limitation of the CCD elements.

The effective length of the detector line can thus be lengthened virtually at will. By means of appropriate specifications, it can be suited to the image width and the resolving power. The process makes it possible to use CCD elements with fewer pixels (e.g. 500 instead of 1700) without loss of image. This means that the system can be developed regardless of the availability of American CCD elements.

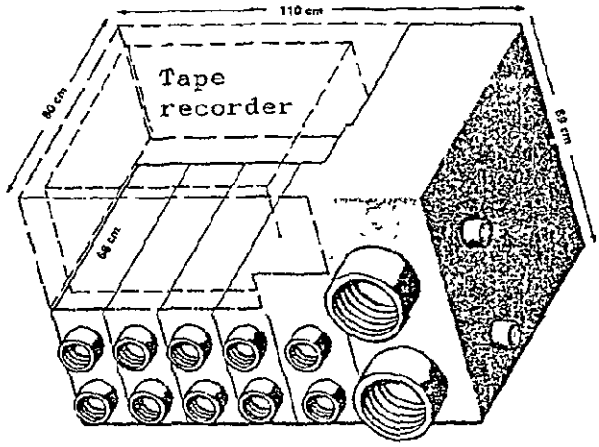

FIG. 67 Modular opto-electronic multi-spectral scanner (MOMS)

	Channels 1 - 3	channel 4	channel 5	channel 6
Spectral region (μ)	0,45 - 1,0	0.45 - 1	1.5-1.7/2.1-2.3	10.5 - 12,5
Spectral bandwidth (μ)	0.05 - 0 1	0.02	Variable	2 0
Max spatial resolution (m)	20 / 40 / 60	60 / 100	60 / 100	60 / 100
	0. 25 / 50	50 / 100	50 / 100	50 / 100
Image swath width (km)	55 / 110 / 240	110 / 240	110 / 240	110 / 240
Temperature resolution (K)				0 5 - 1.0
Number of detector chips	2 x 3 x 1728	2 x 3 x 1728	2 x 4 x 500	2 x 4 x 500
Type of detector	Si photodiodes	Si photodiodes	InSb or PbS	HgCdTe
Pixels per scanning line	- 10368	10368	4000	4000
	MOMS - Overall characteristics			
Total mass (kg)	77 (including cooling radiator and tape recorder)			
Dimensions (cm)	110 x 69 (front face) x 80			
Maximum digital data rate (Mbps)	approx 45 (forgoing maximum performance			
Development time:	approx 5 years (including Spacelab tests)			

Fig. 69: Characteristics of the scanner system

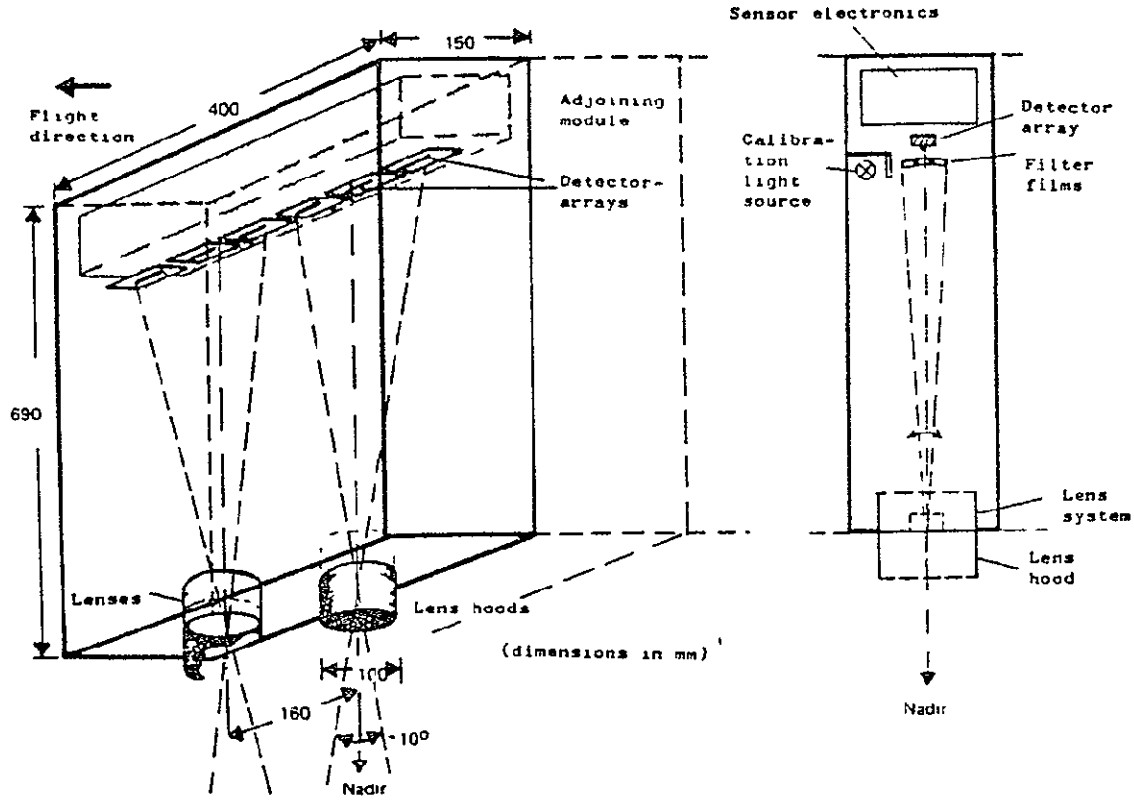

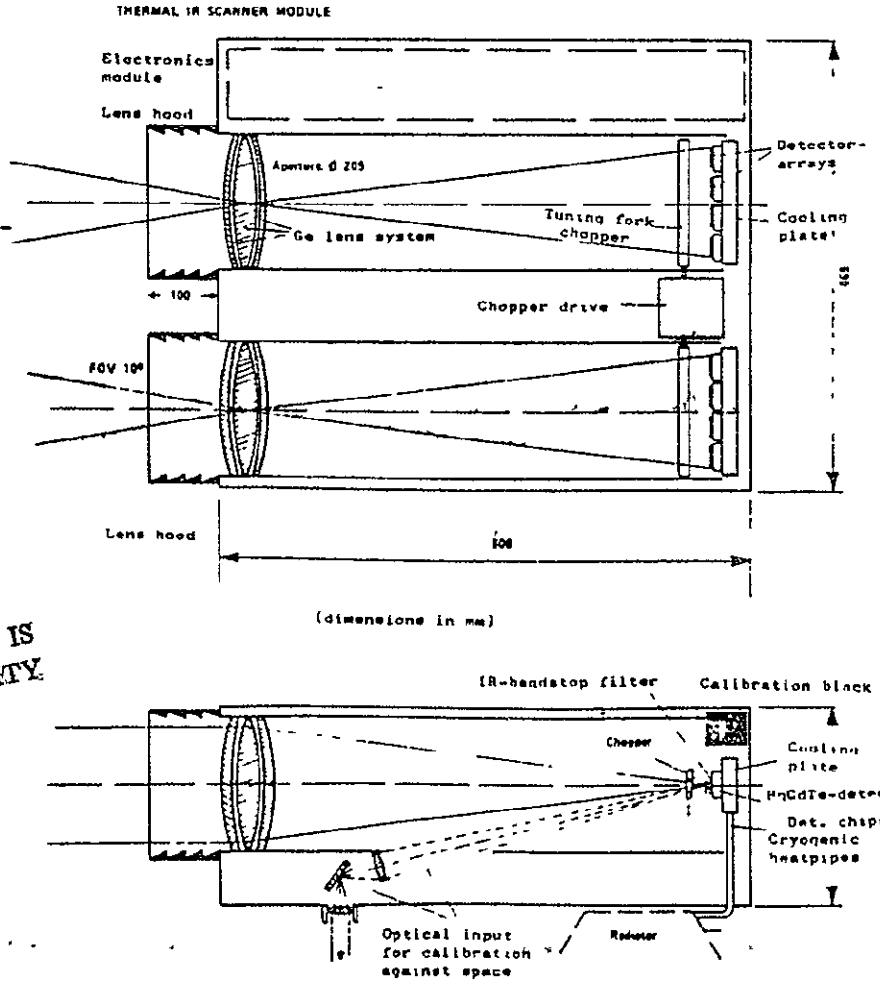

FIG. 4: Sketch of multi-sectral scanner module

Fig. 68: Principle of the multispectral scanner module for visible to near IR.

The stereo module operates on the same principle, but has two detector arrays parallel to one another, arranged symmetrically about the image central axis at a distance appropriate to the base-to-height ratio. This enables the simultaneous viewing in the flight path of a swath both in front of and behind the satellite. The resultant radiometric and geometric image quality is better than has hitherto been achieved in space: an essential feature for mapping, particularly in the developing countries.

In the visible region, standard optical systems with apertures of some 10-cm are satisfactory, and germanium lenses of some 20-cm in the infrared. The latter are available at short notice in Germany.

Such small apertures are possible because each spectral band has its own lens. In contrast, the systems that have hitherto been customary used a wide aperture together with beam dividers, which have been eliminated in the MOMS.

The spectral band covered by a module is determined by the type of detector used and by a filter located between the lens and the detector array. For the basic version, combination filters are provided with triply variable centre frequencies and bandwidths. Fig. 69 shows the various types of detector and the corresponding sensor characteristics. One of the channels also provides a high spectral resolution of 0,02 bandwidth in the 0,45 - 1,1 u band, albeit with reduced spatial resolution (60 instead of 20 m). This channel is used to cover specific absorption bands and radiation maxima. Particular phenomena can thus be selectively recognised, for example cereal diseases in the 0,62 - 0,68 u band and chlorophyll from 0,64 to 0,67 u.

The system's high measurement accuracy is ensured by careful calibration during operation. This compensates electronically for the sensitivity variation of the individual diodes of the CCD elements.

Applications	Frequencies (GHz)				
	5,3	10,6	19,35	22,25	30 – 35
Surface temperature measurement ($\Delta T_{abs} \approx$ 1 K/280 K) - Land areas	○	◉	○		○
- Water areas	◉	◉	◉		
Ice/water assessment	◉	◉			◉
Snow/ice/land assessment	◉	◉	◉	○	
Determination of snow moisture	○	○	○	○	
Determination of age of ice	○	○	○	○	
Determination of soil moisture: - total	◉	◉	○	○	○
- through vegetation cover	○	○			
- with penetration	◉	○			
Determination of type of soil	○	○	○		○
Measurement of cloud layer thickness and precipitation rates	○	◉	◉	◉	
Measurement of atmospheric moisture			◉	◉	
Spectral measurement of sea states (with variable polarisation)	○	○	○		
Salinity determination					

○ fully applicable ◉ supporting measurements recommended

Fig. 71: Typical application of a multichannel microwave scanning radiometer

	Channel 1	Channel 2	Channel 3	Channel 4
Frequency (GHz)	5.3	10.6 *	19.35 *)	33
Wavelength (cm)	5.7	2.8	1.55	0.9
Type of antenna	Cyl.-parab.	Cyl.-parab.	phased array	phased array
Antenna aperture (m)	4 x 2.6	4 x 2.6	1.8 x 1.5	1.8 x 1.5
Image swath width (km)	200 – 220	200 – 240	200 – 220	220 – 280
Spatial resolution (half beamwidth, degrees)	1.15 x 0.9	0.6 x 0.45	0.75 x 0.5	0.42 x 0.3
Spatial resolution (km)	12 x 9.5	6 x 4.7	8 x 5.7	4.4 x 3
Antenna gain (db) (after deduction of losses)	43 approx.	45 approx.	47 approx.	70 approx.
Temperature resolution (K, at instrument) - 200-MHz bandwidth	0.08	0.1	0.25	0.4
ditto - 100-MHz bandwidth	0.15	0.3	0.7	ca. 1
	PAMS – Overall characteristics			
Masses: Cylinder parab. antenna + radiometer phased-array antenna + radiometer	75 kg 115 kg			
Mean electric power requirement	120 W + 230 W			
Development time	about 5 years (including SPACELAB testing)			

*) Radioastronomy port

Fig. 72: Characteristics of the passive microwave scanning radiometer

Fig. 7o shows the first test image obtained by a flight version of an opto-electronic module.

Passive microwave scanning radiometer (PAMS)

The modular, extensible microwave scanning radiometer represents a first step towards the employment of microwave sensors, which are required for an operational satellite remote sensing system. The current operational use of passive microwave systems, e.g. in the Nimbus satellites, for meteorological and oceanographic purposes may be extended to Earth sensing even before active radar systems are available in Europe. An improvement in resolving power from some 14o-km (Nimbus) to 5-1o km enables the investigation and all-weather monitoring of important small-dimension phenomena in coastal and continental-shelf regions, as well as on land.

PAMS is designed for this task. As shown in fig.71 , it is a multi-channel system enabling the acquisition of the ground signatures of various types of phenomena at 5,3, 1o,6, 19,35, and 33 GHz. The frequency of 22,5 GHz, which is of value for determining the water-vapour content of the air, is provided as an option. At a temperature resolution of under o,5 K, the resolving power at all frequencies is better than about 1o km.

Figure 66,p. , shows the PAMS' two antenna systems. They employ electronic beam scanning based on the phased array technique. A linear phased array with a cylindrical reflector having a 4-m axial aperture is provided for the frequencies of 5,3 and 1o.6 GHz. For 19,35 and 33 GHz, a planar phased array of 1,8 m aperture is fitted. A further similar antenna for 22,25 GHz is provided as an option and can be mounted beside the planar antenna.

The development of the antenna system involves only small technical risks. The characteristics in fig.72 are based on

Fig. 7o: First test image obtained by an opto-electronic module (o,4 - 1,o u).

previous experience. The cylinder system can be developed from the Helios antenna, which has already been proven in space in order to achieve the required surface accuracy of about 1/2o of a wavelength, the reflector design is based on carbon-fibre technology; it is likewise available. The only significant new item to be developed is the phase-shift electronics for electronic beam scanning. This involves no fundamental problems, however, and the same is true of the planar system.

In order to achieve high ground and temperature resolution, it is necessary to limit the scanned image swath width, which in the case of PAMS lies between 22o and 28o km, as shown in fig. 73 . These figures take account of satellite velocity and the integration time required per image pixel. The image data from PAMS are transmitted to Earth in digital form, as for the optical system, and stored there on tape for further processing. In addition, the passive system has a data rate that is smaller by two orders of magnitude than an active system giving the same resolution, since, as in the case of optical scanning, only one signal value is assigned to each image pixel. Image recovery and evaluation on the ground can therefore be accomplished for both MOMS and PAMS using the same equipment and related software as for Landsat data, whereas extensive new development is required in connection with the processing of radar data.

3.2. Orbit Selection

The selected orbit is a compromise between the requirements for good resolution by the sensors, maximum repetition rate and lifetime. This led to the 593 km sun-synchronous orbit, of which details are given in fig. 74 . The altitude results from selecting a repetition rate of exactly 12 days, i.e. the orbital tracks of the twelfth day coincide exactly with those of the first day.

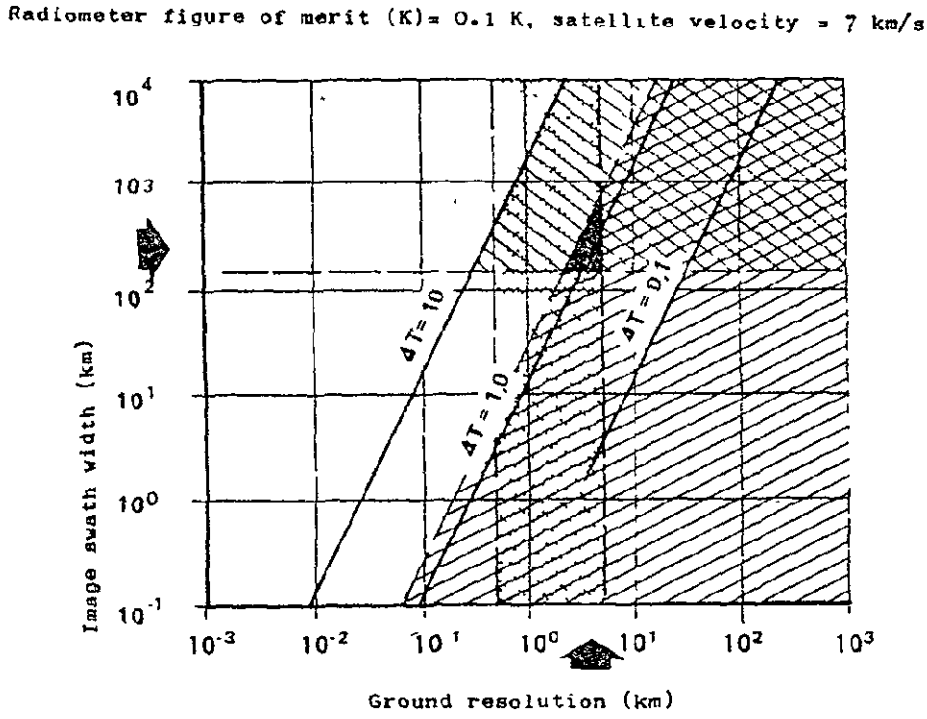

Fig.73: Spatial resolution plotted against image swath width for a passive microwave scanning radiometer

Table IV: Orbit and coverage parameters

Inclination	97.747°
Orbit altitude	593, km
Orbital period	96.536 min
Number of orbits per day	14.917
Distance at the Equator between two successive orbital tracks on the same day	24.13° (= 2687 km)
Daily drift of orbital tracks referred to the Earth	2.01° (224 km)
Repetition rate for worldwide coverage by ground tracks	12.0 days
Intersection of 1st-day image swath with corresponding swath of 2nd day (swath width 200 km)	±25.4° latitude

Fig. 74: Orbit and coverage parameters.

Earth coverage

The requirement for measurements along the ground tracks at approximately the same illumination conditions (constant local time) leads to the necessity for the inertial drift of the orbit's nodal line to be sun-synchronous. The inclination resulting from this requirement is 97.747° with respect to the equator.

Fig. 75 shows schematically the geometry of the orbit, the satellite and the direction of the sun.

The ground tracks of this orbit were determined over a period of two days and the essential coverage parameters deduced therefrom. The worldwide plot is shown in fig. 76 , while fig. 77 shows the European coverage.

The daily drift of some 224 km (measured at the equator) - resulting from the fact that there is not an exact number of orbits in 24 hours - is necessary in order to achieve a progressive, continuous coverage of the whole Earth in 12 days.

As can be seen in fig. 77 , the European region is crossed each day by three north-south ground tracks and three south-north tracks. The time difference at an intersection point between the northbound and southbound ground tracks is some ten hours. This means that if, for example, it is decided that the northbound track shall cross the equator at 1o.oo, any given area will be overflown twice a day: once in the morning and once in the evening.

Communication with Ground Stations

Fig.77 shows the areas over which the satellite is in contact with Redu and Fucino respectively. A minimum elevation of 5° above the horizon is assumed, which is sufficient for TM/TC. Contact is maintained for a maximum of some 1o minutes longer.

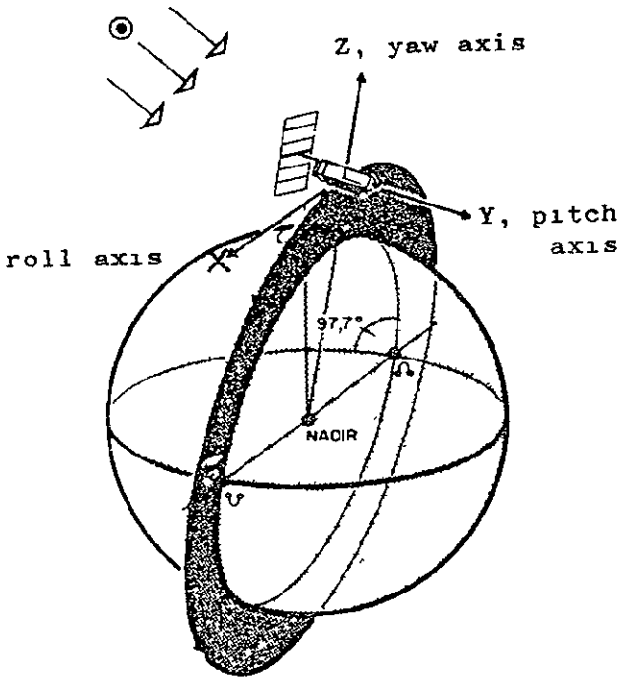

Fig.75: Sketch of satellite's orbital geometry and attitude

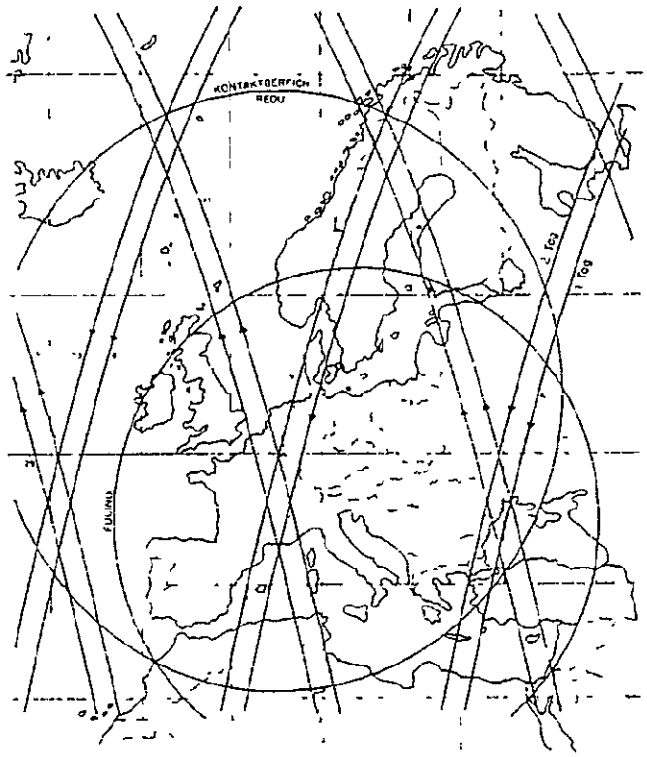

Fig.77: Ground tracks over Europe, and coverage areas of Redu and Fucino during the two days after injection

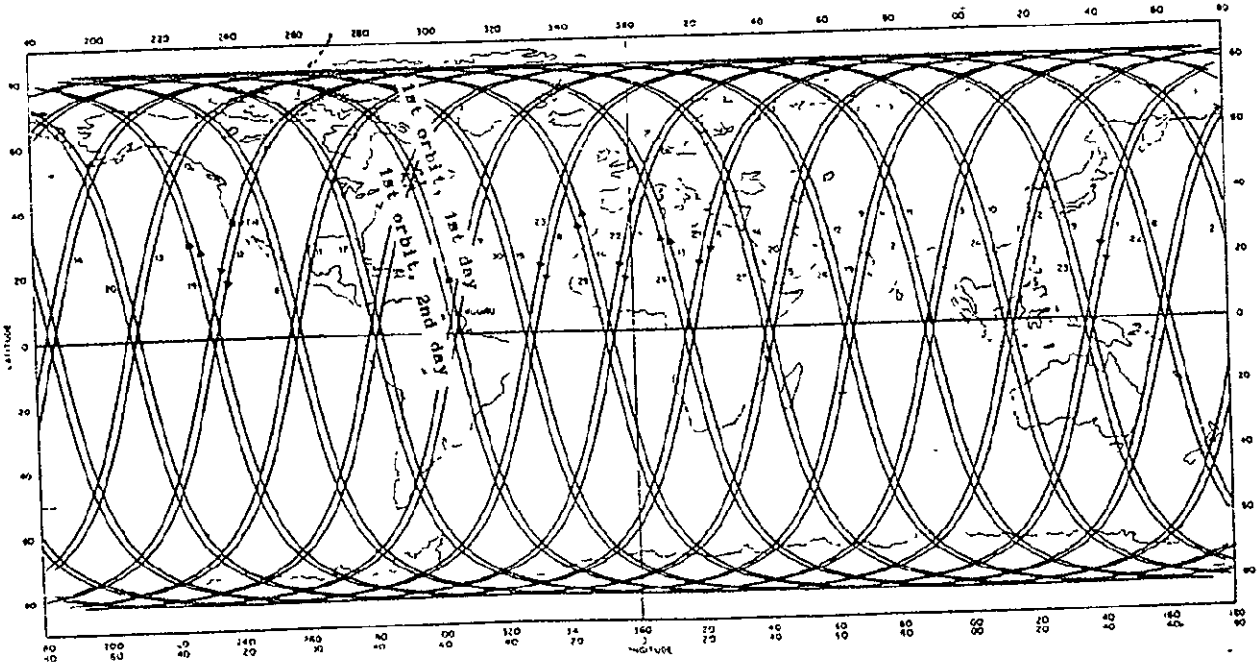

Fig. 76: Worldwide distribution of ground tracks during the two days after injection

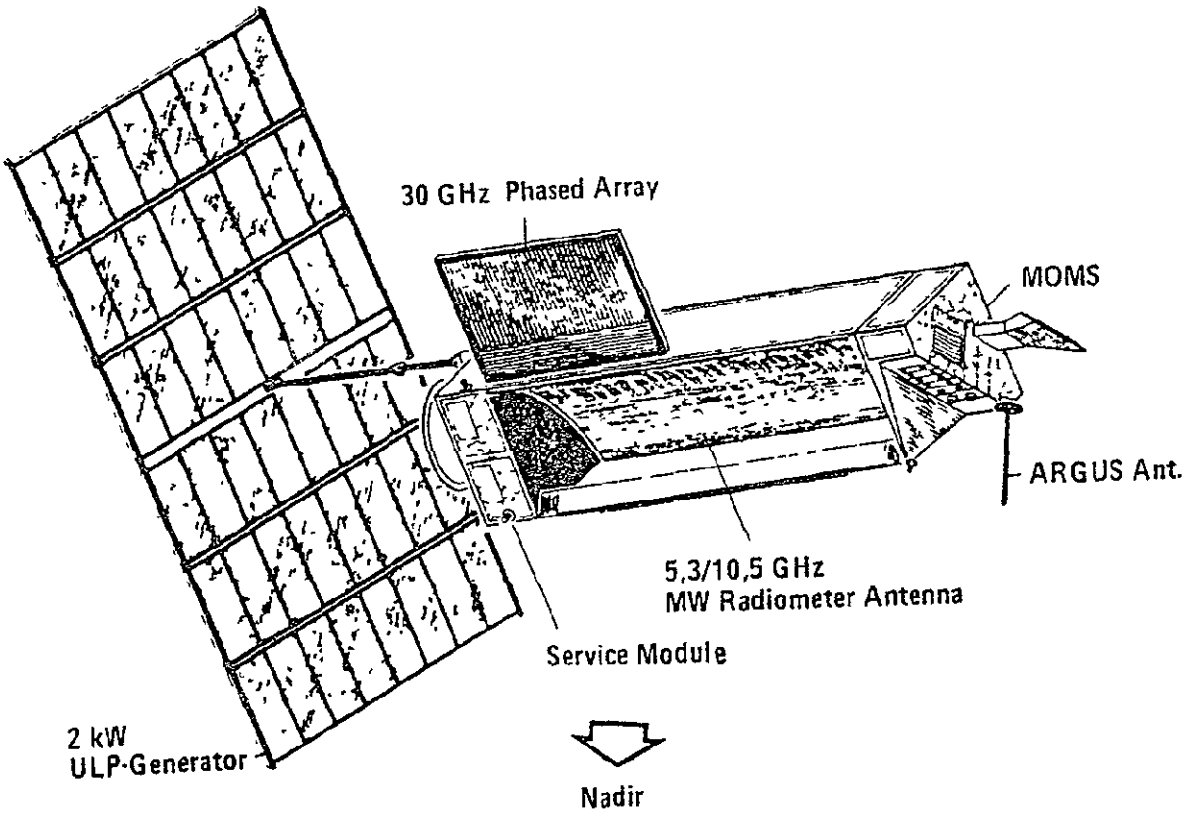

Fig.78: Flight configuration of Argus satellite with optical multispectral scanner, two passive microwave radiometers (three frequencies) and 2-kw ULP solar generators

3.3 Description of the Satellite Concept

Satellite Design

Argus is designed for launching by Ariane or Space Shuttle into sun-synchronous low Earth orbit. Its main features are as follows (see fig.78):

- Modular construction: power supply module, microwave module, optical payload module
- Three-axis stabilisation aligned on the nadir and the sun by means of momentum wheels and magnetic torquers
- System for correcting orbital inclination and altitude for a lifetime of three years.
- Steerable solar array, capable of extension up to 3.5 kW of electrical power using the MBB ULP technology (Ultra Lightweight Panels made on carbonfibre reinforced plastic).
- Full use made of the Ariane payload volume, with a rigid cylindrical paraboloid antenna for the microwave radiometer operating on 5.3 and 1o.6 GHz.
- Deployable planar antenna for a third microwave frequency of 33 GHz.

Its modular construction makes it possible to mount the SPOT payload proposed by CNES on the basic module, in addition to the payload described above, or else to mount an active radar system in place of the passive microwave radiometer.

The dimensions of the basic configuration shown in fig. 78 are based on the constraints imposed by the payload fairing in the launch configuration

The 1.8 m square cross section is suitable for the dynamically useable diameter of 2.8 m, and also gives maximum width to the cylindrical-paraboloid antenna, which stretches along a diagonal of the block.

The power-supply module consists of the cylindrical adapter of 1.2 m diameter, the adjacent sandwich box structure and the deployable solar array. The overall height of the basic module has been kept to 1 meter, so that the whole 4 meter height of the cylindrical Ariane fairing is available for the microwave antenna. Access to the interior is by removeable side panels.

The orbit-correction system is fitted in the adapter, while the other bus components such as attitude control, batteries, S-band TM/TC and solar-array drive are mounted in the square main structure.

The solar array, which in the basic design gives 1.6 kW after three years, consists of 6 ultra-lightweight (ULP) panels, secured to a side wall. The drive shaft has three joints, which are required for deploying the array and pointing the unfolded panels towards the sun. During one orbit, the satellite turns once around the array-drive axis, so that its longitudinal axis is at right angles to the orbital plane and thus forms the pitch axis.

In order to allow the IR sensor to radiate heat, the optical module is mounted on the microwave module. The cooling radiator thus faces neither the sun nor any part of the satellite. By slanting the horn and making its Earth-facing side longer, the Earth's albedo is prevented from reaching the inside of the radiator.

The paraboloid outline of the microwave antenna lies along a diagonal of the rectangular basic module, so that the radiator can be mounted on the corner in front of it. The same arrangement is used at the upper end, by means of the

advancing corner of the optical payload module. The normal of the cylindrical paraboloid points towards the nadir, and the optical module is therefore similarly cut away in the diagonal direction.

The cylindrical paraboloid and the backward-facing surfaces have to be made of very rigid carbon-fibre reinforced plastic in order to be able to carry the payload module which weighs over 130 kg, and to remain correctly pointed.

Options and Possibilities of Extension

The Argus system can cater for:

- Because of its modular construction, various payload sensors, e.g. high-resolution optical sensors in the visible and infrared, passive microwave sensors (reflector antennas and/or phased arrays), active microwave sensors (SAR or scatterometer), or combinations of optical sensors and microwave payloads.
- Various sun-synchronous orbits, e.g. orbit altitudes between 500 and 1200 km and various orbit node-line arrangements (e.g. 06.00 to 18.00, in which case between 06.00 and 13.00 Argus can remain pointed in the same direction towards the Earth).

The characteristics of the Argus system as designed for Ariane and a 600 km sun-synchronous orbit lie within the following limits:

- Payload mass	10/300/1000 kg
- Payload power requirement	1000/450/100 W
- Payload bit rate	300/100/20 Mbps
- Memory capacity	up to about 10^{11} bits
- Mission duration	4, 3, or 2 years

- Overall mass 3ooo kg
- Overall power requirement (3 years) 3,5 kW

Telecommunications System

The sensors proposed for Argus would produce the following provisional bitrates if an error-detecting code was used:

- MOMS	approx.	4o.o Mbps
- PAMS	"	4.3 Mbps
- IR-Radiometer	"	3.4 Mbps
- Housekeeping	"	o.3 Mbps
	Total:	48.o Mbps

These values are comparable to those for the optical payload proposed for the first generation of SPOT (45 Mbps).

In view of the high data rate, real-time transmission to a central ground station is envisaged, e.g. to the ESA Earthnet (Fucino and Kiruna), assuming 3 day and 3 night orbits per 24 hours, with a contact time of some 1o minutes for the European region. For extra-European regions or the northern fringes of Europe, it will be necessary to store data on board for a short time (1o, 3o or 6o minutes), with the result that the quoted telemetry rate will be increased by a factor of between 2 and 3.

If no greater quantity of data can be stored, mobile receiver stations will have to be sent to the developing countries.

Whereas the satellite platform TT & C system operates at around 2 GHz in the unified S-band (USB), which is compatible with ESA and NASA practices, the payload telemetry must

be transferred to higher frequencies, e.g. 8, 21.51 or 65 GHz, which permit greater bandwidths and hence higher bitrates. Using the 8 - 8.4 GHz band, the nominal Argus bitrate can be transmitted to the ground using 2 bands, or the higher britrate using 6 bands. The ground stations will be suitable for this kind of working; typically, 6 HDDT per day will be recorded; only the receiving antenna will have to be modified for this frequency range.

The transmitted power in the 8-GHz band should amount to about 24 W per channel for a station 600 km distant. However, in order to use the whole contact time for data transmission with approximately uniform quality, the transmitter power must be higher, e.g. 40 W per channel, and the transmitting antenna must have a shaped beam pattern with a gain at least 5 dB higher for angles greater than 60°. If a 0-dB antenna is used, four travelling wave tubes with powers of some 200 W would be needed for transmitting some 140 Mbps.

Data_management_

A modular on-board data-management (OBDM) system is provided, based on a programmed on-board computer (OBC). The OBC-controlled data-and-command bus together with the remote terminal units (RTU) enable flexible adaptation of the OBDM to a wide range of payload requirements. In this connection, a non-rigid (floating) telemetry format is recommended.

The OBC performs the following tasks:

- Data handling, i.e. data-bus and format control;
- Arrangement of the payload-specific data-recording times, spectral regions, ground resoltuion, track selection for MOMS, and quantification, i.e. data reduction is also possible;
- Data pre-processing, e.g. data redoction by means of delta modulation;

- Attitude determination tasks (Calmanfiltering) and attitude control, automatic position determination and orbit control;
- Management of the bus sub-systems, e.g. thermal control and power supply (batteries), in which connection fault monitoring and automatic switching of redundant components are important.

3.4 Availability of Major Components in Europe

- Multispectral scanner

The development of the MOMS here described is based on the following assumptions:

1) The modules for the visible to near infrared spectral region (channels 1-4 and stereo module) are directly derived from the aircraft experimental module developed by MBB under contract to the BMFT. There is no discernible risk associated with the development costs and time-schedule. Admittedly, the concept here described is based on the use of American CCD diodes, but comparable suitable detectors could equally be prdouced in Europe in less than 2 years.

2) For the module for the near-to-middle infrared region (Channel 5), suitable individual detectors exist in Europe, but as yet no linear arrays. Suitable CCD detectors indeed exist in the USA, but are currently not commercially available outside that country. The development work must therefore be undertaken in Europe. If need be, HgCdTe elements of channel 6 could be used for this region, with enlarged aperture.

3) The thermal IR module (Channel 6) is being developed from the existing French detector array using HgCdTe

elements, by increasing the number of detectors per element. Development costs and times are considerably greater than for the modules for channels 1 - 4, but there is not discernible risk.

The basic feasibility of the complete electronic multispectral scanning system using European and extensively German sensor technology has been established on the basis of an extensive market analysis and the study underlying this paper.

- Passive Microwave Radiometer

This cylindrical-paraboloid reflector is immediately available, with the present carbon-fibre/aluminium-core composite construction, as qualified for the solar arrays and paraboloid antennas of contemporary communications satellites. Carbon-fibre reinforced plastic wound skins up to 10 m long can be wound onto cores 2 m in diameter at MBB.

Microwave radiometer electronics are being developed in several institutes and firms in Europe, e.g. in the UK, Denmark, Switzerland and Germany (DFVLR) so that their use in 1983/84 seems assured.


FEB 1979
RECEIVED